

COASTLINE IMPACTS OF TROPICAL CYCLONES AND CLIMATE CHANGE ON MAURITIUS



Yanick Douce

Submitted in fulfillment of the academic requirements for the degree of
*Master of Science in Civil Engineering, College of Agriculture,
Engineering and Science,
University of KwaZulu-Natal, Durban*

November 2014

Supervisor: Prof. Derek Stretch

Co-Supervisor: Dr. Stefano Corbella

DECLARATION 1 – PLAGIARISM

I, Yanick Douce, declare that

1. The research reported in this thesis, except where otherwise indicated, is my original research.
2. This thesis has not been submitted for any degree or examination at any other university.
3. This thesis does not contain other persons' data, pictures, graphs or other information, unless specifically acknowledged as being sourced from other persons.
4. This thesis does not contain other persons' writing, unless specifically acknowledged as being sourced from other researchers. Where other written sources have been quoted, then:
 - a. Their words have been re-written but the general information attributed to them has been referenced.
 - b. Where their exact words have been used, then their writing has been placed in italics and inside quotation marks, and referenced.
5. This thesis does not contain text, graphics or tables copied and pasted from the Internet, unless specifically acknowledged, and the source being detailed in the thesis and in the References sections.

Signed _____ Date _____

Mr. Yanick Douce

As the candidate's supervisor, I agree/do not agree to the submission of this thesis.

Signed _____ Date _____

Prof. Derek Stretch

As the candidate's co-supervisor, I agree/do not agree to the submission of this thesis.

Signed _____ Date _____

Dr. Stefano Corbella

ACKNOWLEDGEMENT

I would like to express my infinite gratitude to Doctor Stefano Corbella for his priceless assistance throughout the study. Thanks to my supervisor, Professor Derek Stretch, for his support and guidance.

Thanks to the Ministry of Environment of the Republic of Mauritius and the Mauritius Meteorological Services for the wave data and the reports on the coastal studies. Thanks to my friends and ex-colleagues at GIBB (Mauritius) Ltd for providing valuable information.

Thanks to Dylan Bruce Kime and his team at DHI Group (South Africa) for their help with the MIKE 21 model.

A special thanks to my wife, Nathalie, my parents and my friends who have provided support and encouragement in completing this study.

ABSTRACT

The tourism industry has grown to become the third pillar of the Mauritian economy, due mainly to its prestigious beaches. However, Mauritius is prone to severe tropical cyclones which can have detrimental impacts on its coastal environment and ultimately its economy. It is predicted that the frequency and intensity of these tropical cyclone will increase under the influence of climate change. This may accelerate the rate of coastal erosion as a result of rising sea level, tidal waves and storm surges.

Prior to 2003, no preventive coastal management framework was available in Mauritius to address the impact of tropical cyclones. Since, various studies have recommended that wave prediction models be adopted to assess and quantify the amount of sediment transport resulting from tropical cyclones.

In this research, the relative coastal erosion due to the predicted impact of climate change on tropical storm waves at Belle Mare beach in Mauritius was studied. This was achieved by, firstly, the generation of cyclone wind fields as the primary driving mechanism for the wave model using the MIKE 21 Cyclone Wind Generation model. This required cyclone parameters such as the cyclone tracks, maximum wind speeds and maximum pressures which were extracted from the “Australian Severe Weather” centre.

Mike 21 SW model, a 2D-spectral numerical modelling software, was then used to generate cyclone-induced waves and surges. This required the creation of a regular grid defining the shoreline and bathymetry which was obtained from “NOAA data centre”.

Based on the published expected effect of climate change on cyclones, the intensity of cyclone Davina (1999) was increased by 5%, 10% and 15% respectively. The resulting wave outputs for each scenario were applied in the XBeach model to assess and quantify the coastal erosion at Belle-Mare. The outputs from XBEACH revealed that the reef surrounding Mauritius reduces the cyclone wave height before it reaches the beach by some 85%. Despite the beneficial influence of the coral reefs on storm surge, the relative volume of sediment erosion resulting from the various intensified cyclone scenarios for Davina is significantly high; 15.36m³/m for a 5% cyclone intensification, 18.16m³/m for 10% and 21.45m³/m for 15%. XBEACH was found to produce reliable results in modelling processes in the coastal zone with accuracy. The implementation of vegetated dunes was proposed as a suitable and natural coastal defense measure at Belle Mare beach for environmental, aesthetical, socio-economic and financial reasons.

CONTENTS

Contents	iv
List of Figures.....	viii
List of Tables	x
Nomenclature	xi
Chapter 1: Introduction	1
1.1 Effects of cyclone wave on coastline	1
1.2 Problem definition (Motivation, aim, objective).....	1
1.2.1 Research question.....	1
1.2.2 Motivation.....	2
1.2.3 Aim & Objectives	3
1.3 Approach.....	3
1.3.1 Belle Mare Public Beach.....	3
1.4 Structure of Dissertation	5
Chapter 2: Literature Review	6
2.1 Introduction	6
2.2 Waves and Tropical cyclones.....	6
2.3 Climate change and tropical cyclones	8
2.3.1 Predicted effect of climate change on tropical cyclone.....	9
2.3.2 Discussion:	11
2.4 Cyclone Potential Intensity increase for Case Study	13
2.5 Global sea level trend.....	13
2.5.1 Sea level rise	13
2.6 Tides.....	14
2.7 Storm surge	14
2.8 Sources of coastal sediment	14

2.9	Resulting effect of climate change on coastlines on predicted surge and erosion	15
2.10	Numerical modelling.....	15
2.10.1	MIKE 21 Cyclone Wind Generation.....	15
2.10.2	MIKE 21 Spectral Wave (SW) module.....	20
2.10.3	XBEACH	23
2.11	Shoreline defence and preservation	25
2.11.1	Hard protection measures.....	26
2.11.2	Soft protection measures	26
2.11.3	Preservation of the coral reefs.....	27
2.12	Literature review conclusion.....	28
Chapter 3: Case Study: Data for Tropical Cyclones in the INdian Ocean		29
3.1	Classification of cyclones	29
3.2	Cyclone trend in the Indian Ocean.....	29
3.2.1	Improved Cyclone Data	30
3.3	Modelled tropical cyclones	33
3.3.1	Calibration and Validation	33
3.3.2	Quantification of predicted erosion.....	33
3.4	Summary	34
Chapter 4: Case Study: General Description		35
4.1	Coastal Livelihoods and degradation	35
4.2	Previous coastal studies in Mauritius	36
4.2.1	Extent of coastal studies.....	36
4.3	The coastal geology of Mauritius.....	37
4.4	The wave climate of Mauritius	38
4.5	Recorded wave data	39
4.6	Tide regime	39
4.7	Sea Level Rise.....	39

4.8	Cyclone Return Period	40
4.9	Coastal Vulnerability and Selection of Pilot site	43
4.10	Coastal features of Belle Mare beach.....	45
4.11	COSMOS model output.....	46
4.12	Coral reef degradation.....	47
4.13	Proposed mitigation for erosion at Belle Mare	48
4.14	Limitations and Constraints	48
4.15	Summary	49
 Chapter 5: Model Data and Methods.....		50
5.1	Mike 21: Model Setup, Calibration and Validation	50
5.1.1	Model extent, bathymetry and mesh grid.....	50
5.1.2	MIKE 21 Cyclone Wind Generation.....	52
5.1.3	Spectral Wave (SW) module.....	52
5.1.4	Calibration and Validation	53
5.2	XBEACH: Application and Model Setup	56
5.2.1	Application.....	56
5.2.2	Model bathymetry	56
5.2.3	Model setup.....	57
5.3	Summary	59
 Chapter 6: Results and Discussion		60
6.1	Introduction.....	60
6.2	MIKE 21 SW	60
6.3	XBEACH	68
6.3.1	Predicted Erosion	68
6.3.2	Wave energy dissipation	69
6.4	Discussion of results	74

Chapter 7: Shoreline Defence	76
7.1 Assessment of various coastal defences for Belle Mare	76
7.1.1 Alternative 1: “Do-Nothing”	76
7.1.2 Alternative 2: Vegetated dunes	77
7.1.3 Alternative 3: GSCs with vegetated dunes.....	77
7.1.4 Alternative 4: Beach nourishment.....	77
7.1.5 Alternative 5: Hard measures.....	77
7.2 Selection of coastal defence alternative	78
Chapter 8: Conclusion	79
8.1 Recommendations for future work.....	81
References	82
Appendix A Cyclone Data From The Australian Severe Weather Between 1997 And 2011	App A - 1
Appendix B XBEACH set-up file for Belle Mare: Scenario 1	App B - 1

LIST OF FIGURES

Figure 1-1	Map of Mauritius showing Belle Mare Beach	4
Figure 3-1	Cyclone activity in the South Indian Ocean (longitude 15°E to 135°E) between 1945 and 2011	30
Figure 3-2	Graphical representation for the classification of the total number of cyclones and frequency between 1997 and 2011 in the SIO	31
Figure 3.3	Annual most severe TC between 1997 and 2011 in the SIO based on Pressure (hPa)	32
Figure 3-4	Annual most severe TC between 1997 and 2011 in the SIO based on Maximum wind speed (m/s)	33
Figure 3-5	Trajectory of Tropical cyclone Davina (1999)	34
Figure 4-1	The estimated percentage of coastal types and land usage for Mauritius	37
Figure 4-2	Geographical location of Mauritius	39
Figure 4-3	Interannual variation in sea level since 1990	40
Figure 4-4	Geographical representation showing vulnerability of beaches listed in Table 4-2	44
Figure 4-5	Location site Map of Belle Mare	45
Figure 5-1	Map of study area showing the bathymetry	50
Figure 5-2	Model mesh grid showing different scales for the model domain	51
Figure 5-3	Measured and predicted significant wave heights for cyclone Darius (2003)	54
Figure 5-4	Cyclone Darius track (2003) from the Australian Severe Weather website	55
Figure 5-5	Measured and predicted significant wave heights for cyclone Hennie (2005)	55
Figure 5-6	Location of surveyed alignment along Belle Mare beach	56

Figure 5-7	Beach Profile along Belle Mare beach shown in different scales	57
Figure 6-1 (a to d)	Cyclone Davina (1999) trajectory on 09 March 2014	61
Figure 6-2	Trajectory of cyclone Davina (1999) from the Australian Severe Weather website	63
Figure 6-3	Significant wave heights for scenario 1 to 4 at latitude 20.09°S and longitude 57.47°E at Belle Mare for cyclone Davina (1999) using MIKE 21 SW (outside lagoon).....	64
Figure 6-4	Wave rose diagrams (in metres) for scenario 1 to 4 for cyclone Davina (1999) at at latitude 20.09°S and longitude 57.47°E (offshore of Belle Mare beach)	65
Figure 6-5	Measured beach profiles and surveyed bathymetry at Belle Mare before and after Cyclone Davina shown in different scales	68
Figure 6-6	XBEACH wave decay for cyclone Davina at time step “0000-01-01 03:00:00” at Belle Mare	71
Figure 6-7 (a to d)	Wave run-up and extent of erosion for Scenarios 1 to 4 from XBEACH for cyclone Davina at Belle Mare	72
Figure 6-8	Relation between erosion (m ³ /m) and Hm0 (m) for various cyclone intensities (%) for cyclone Davina	75

LIST OF TABLES

Table 2-1	Summary of the resulting effect of climate change on the main parameters that affects the formation of tropical cyclones	11
Table 2-2	Effect of climate change on the intensity of tropical cyclones as predicted by various studies	12
Table 3-1	Classification of tropical cyclones in the Indian Ocean based on pressure (hPa) and wind speed (km/h)	29
Table 3-2	The improved cyclone track information w the maximum wind speed and minimum pressure from 1997 to 2011 in the SIO	31
Table 4-1	Design wave conditions in Mauritius as determined by Baird [2003]	41
Table 4-2	Summary of the degree of vulnerability of public beaches in Mauritius with regards to erosion as identified by Baird [2003] and JICA [2013]	43
Table 4-3	Lateral Retreat and Eroded Volume for a Range of Cyclones at Belle Mare [Baird, 2003]	46
Table 5-1	Spectral Wave (SW) input parameters used for wave simulations	52
Table 5-2	XBEACH input parameters used for sediment transport	58
Table 6-1	XBEACH predicted erosion (m ³ /m) for scenarios 1 to 4 for cyclone Davina at Belle Mare beach	69
Table 6-2	Comparison between the significant wave heights offshore (MIKE 21) and inside the lagoon (XBEACH) for cyclone Davina	70
Table 6-3	XBEACH output results for surge (m) and wave run-up (m) for cyclone Davina	71

NOMENCLATURE

Acronyms

1D	One dimension
2D	Two dimension
CD	cyclone Davina
DHI	Danish Hydraulic Institute
GEBCO	General Bathymetric Chart of the Oceans
GHG	greenhouse gases
GDP	Gross domestic product
GLM	Generalized Lagrangian Mean
GoM	Government of Mauritius
GSC	geotextile sand filled containers
HAT	highest astronomical tide
LAT	lowest astronomical tide
MoE	Ministry of Environment
MMS	Mauritius Meteorological Services
N/A	Not Applicable
NCEP	National Centers for Environmental Prediction
NOAA	National Oceanic and Atmospheric Administration
RH	relative humidity
SE	South East
SH	Southern Hemisphere
SIO	South Indian Ocean
SST	Sea Surface Temperature
SW	Spectral Wave
TC	Tropical Cyclone
USD	US Dollar

Greek Symbols

ζ	Low level relative vorticity
φ	angle between the radial arm and the line of maximum winds
ρ_A	air density
δ_{fm}	correction factor
θ_{max}	angle measured relative to the cyclone movement direction
$\bar{\sigma}$	mean relative frequency

γ	free breaking parameter
θ_m	Mean wave direction

Roman Symbols

B	Shape Parameter
C_f	Dissipation Coefficient
C_d	Drag Coefficient
D_h	Sediment Diffusion Coefficient
$\overline{D_w}$	Directionally Integrated Total Wave Energy Dissipation due to Wave Breaking
E	Ocean Thermal Energy
E_{tot}	Total Wave Energy
E^u	Eulerian Mean Velocity
f	Coriolis Parameter
f_p	Wave Frequency
h	Local Water Depth
H_m	Maximum Wave Height
H_{rms}	Root Mean Square Height of wave
H_s / H_{m0}	Significant Wave Height
m	Bed Slope
\bar{k}	Mean Wave Number
k_N	Nikuradse Roughness
m_0	Zeroth Moment of the spectra
N	Wave Action Density Spectrum
P	Pressure
P_c	Central Pressure
P_n	Neutral Pressure
Q_b	Fraction Of Breaking Waves
R_m	Radius to Maximum Winds
s	Specific Weight of the Sediment
S	Source Term for Energy Balance Equation
S_{bot}	Bottom-Friction Parameter
S_{ds}	White-Capping Parameter
S_{in}	Wave Growth by Wind Action
S_{nl}	Wave Energy Transfer due to Non-Linear Wave-Wave Interaction
S_{surf}	Depth-Induced Wave Breaking Parameter

S_z	Vertical Shear
T_p	Peak Wave Period
t	Time
T_0	Mean Wave Period
T_s	Adaptation Time For Entrainment of the Sediment
U_{cr}	Minimum Water Velocity at which sediment sets in motion
V	Total Wind Speed
V_{10}	Surface Wind
V_f	Forward Speed
V_{fm}	Forward Cyclone Speed
$V_g(r)$	Gradient Wind
V_{max}	Maximum Wind Speed
\bar{v}	Propagation Velocity of a wave group in the Four-Dimensional Phase
∇	Four-Dimensional Differential Operator
w_s	Sediment Fall Velocity

CHAPTER 1

INTRODUCTION

1.1 Effects of cyclone wave on coastline

Extreme natural phenomena such as cyclones and storm surges greatly affect the socio-economic activities of Mauritius [JICA, 2013]. Although these natural catastrophic events occur over a short temporal cycle, their impacts can be detrimental. Coastal erosion, one of the adverse effects of tropical cyclones, has contributed significantly to the deterioration of the coastal environment of Mauritius. The extent of coastal erosion produced by cyclones depends on several influential factors such as the frequency, intensity, duration and the trajectory.

Climate change, a consequence of natural and anthropogenic forcings, may amplify the intensity of tropical cyclones (refer to Chapter 2). Furthermore, a rise in the sea level has been observed over the last decades which has been attributed to climate change [IPCC, 2013]. The combined effect of these two products of climate change is believed to increase the reach of bigger storm surges which will accelerate coastal erosion.

It is therefore advisable to quantify the possible impacts of cyclone intensities on coastal vulnerability in Mauritius for planning purposes.

1.2 Problem definition (Motivation, aim, objective)

The repeated actions of cyclones on the coastal zone can be disastrous. It is vital to re-create these phenomena with the aid of models in order to accurately predict, quantify and mitigate their impacts.

1.2.1 Research question

What is the coastal erosion associated with tropical cyclones under the influence of climate change for the Island of Mauritius?

Tropical cyclones generally approach Mauritius from an Easterly direction and hence have a bigger influence on this part of the Island. The Belle Mare public beach has been selected as a case study for this research since it is situated on the east coast of Mauritius. Belle Mare also comprises numerous luxurious hotels along the coast. Therefore the research question may be posed more specifically as what is the coastal erosion associated with tropical cyclones under the influence of climate change for the Belle Mare public beach.

1.2.2 Motivation

The tourism industry has experienced considerable growth in Mauritius since 2007, becoming an important pillar of its economy [JICA, 2013]. This growth is mainly due to the attractive coastal landscape which has led to extensive development along the shoreline. Over the past decades, this coastline has been subject to increasing stress as a result of anthropogenic and natural forcings. Tropical cyclones in the Indian Ocean, one of the most significant natural forcings, generally occur during the summer season, between the months of November and April.

The average number of cyclones recorded in the Indian Ocean from 1997 to 2011 is 22 per year, with an average of 10 per year having direct effects on the Island of Mauritius (refer to Chapter 3). These cyclones vary in intensity and therefore have different degrees of coastal impact. Severe tropical cyclones have proven to be of real concern to the coastal zone, social-economic development and human life. This being said, the only evidence pertaining to extreme coastal erosion in Mauritius was recorded and reported in 1960 which was caused by severe tropical cyclone Carol [Baird, 2003]. Its impacts were reported in the form of surveyed beach profile transformation both pre and post-cyclonic activity. Cyclone Carol was responsible for the destruction of coastal infrastructure and serious beach degradation. Notwithstanding the above, little information relating to the characteristics of cyclone Carol and its wave climate is readily available. Furthermore, no proper record of subsequent severe cyclones was available until 1979. Meanwhile, the disastrous effects of tropical cyclones have been experienced in Mauritius [Baird, 2003; JICA, 2013]. Today, various mitigating measures to combat erosion can be observed around Mauritius but very few, if any, are based on design wave characteristics factors. In addition, climate change and sea level rise are undisputed factors that affect the impacts of cyclones. Consequently, reliable engineering models need to be developed to replicate these events to understand and design appropriate mitigating measures. This research aims at quantifying the risks associated solely to the effects of tropical cyclones and climate change and adopting appropriate protective measures.

1.2.3 Aim & Objectives

1.2.3.1 Aim

The aim of this dissertation is to estimate the vulnerability of Mauritius to tropical cyclones under the influence of climate change and recommend appropriate coastal defence(s).

1.2.3.2 Objectives

- To use the available cyclone data to calibrate and validate deep water waves using MIKE 21 by DHI.
- To generate, through a return period calculation for tropical cyclones, a trend for the occurrence of severe coastal storms in the region.
- To simulate a tropical cyclone with different intensities, based on the predicted effect of climate change, using the MIKE 21 model
- To use the generated data to create an XBEACH model [Deltares & TUDelft] and simulate the erosion impacts of the different cyclone intensities.
- To estimate the predicted relative potential erosion for the return period
- To propose a suitable shoreline protection defence based on prevailing conditions

1.3 Approach

1.3.1 Belle Mare Public Beach

Belle Mare, one of the popular beaches along the east coast of Mauritius, stretches from the north of Trou D'Eau Douce (southern part) to Pointe de Flacq (northern part), see Figure 1-1. This represents a length of about 10km over which more than a dozen luxury hotels such as Lux Belle Mare, Le Prince Maurice, One & Only Le Saint Geran, La Residence, etc. are found. Belle Mare is a good representation of the reef-lagoon-beach system surrounding the Island. The coastline is mainly comprised of sand spanning approximately 30m wide from the vegetated dune inland to the mean sea level. The reef extends over 500m offshore which, in general, offers a good dampening effect to extreme storm surges. Nevertheless high erosion has been observed over the years, especially during cyclone Carol [Baird, 2003].

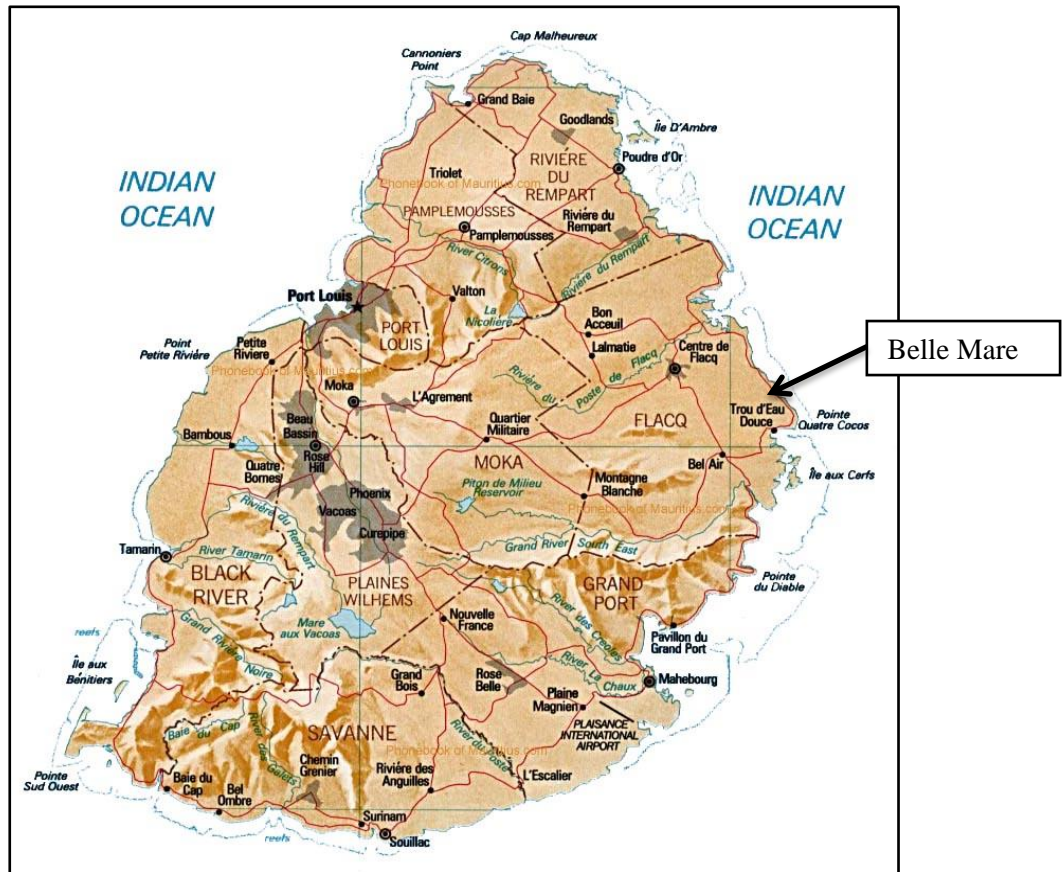


Figure 1-1: Map of Mauritius showing Belle Mare Beach
(Source of imagery: Google Earth, 2014)

Historical cyclone wave data and beach profiles are very limited in Mauritius. Owing to the lack of information, the Government of Mauritius has recognized the need to address the coastal degradation and, through the Ministry of Environment, has initiated various studies to identify the causes and to propose mitigating measures to preserve its resources. Studies conducted by Baird [2003] and JICA [2013] categorize vulnerable locations around the island of Mauritius based on limited information. Both reports have identified the Belle Mare public beach as a medium to high priority zone for potential erosion.

Historical cyclones from 1998 to 2011 with sufficient data were extracted from the global database for the entire Indian Ocean region. The MIKE 21 SW [DHI] model was used to calibrate and validate the wave output against available recorded wave data. Thereafter, the intensity of the most influential cyclone identified from the historic record, Davina, was increased by 5%, 10% and 15% increments based on published expected climate change effect on cyclones. A 1-D XBEACH model [Deltares & TUDelft] was used to assess and quantify the relative coastal erosion at Belle-Mare beach.

1.4 Structure of Dissertation

The following chapters cover the influence of climate change on tropical cyclones and its related impacts on the coastline of Mauritius as a case study. A brief recommendation on the suitability of various coastal defences is also presented.

- Chapter 2: contains basic information about the parameters that affect the formation of cyclones (cyclo-genesis) and the predicted effect of climate change on cyclo-genesis. It also contains an overview of the numerical software used for modelling: (i) the propagation of tropical cyclones using MIKE 21 Cyclone Wind Generation [DHI], (ii) the growth, decay and transformation of offshore cyclone waves using MIKE 21 Spectral Wave module and (iii) the computation of nearshore processes, especially for sandy coastlines using XBEACH. The chapter also presents the various coastal protection measures available.
- Chapter 3: provides information about the trends in occurrence of tropical cyclones in the Indian Ocean. The chapter also provides information on the methodological approach used to conduct the research project.
- Chapter 4: provides information on the wave climate of Mauritius and the coastal vulnerability of various beaches around Mauritius as predicted by previous studies undertaken by the Government of Mauritius. The physical characteristics of the Belle Mare beach (as the case study) are presented, as well as the findings on the predicted rate of erosion at Belle Mare by the previous studies.
- Chapter 5: provides information about the methods used to conduct the research project. The chapter also provides information on MIKE 21 Cyclone Wind Generation, MIKE 21 Spectral Wave module and XBEACH used to model the relative rate of coastal erosion by tropical cyclones under the influence of climate change for the case study.
- Chapter 6: presents the output results obtained from MIKE 21 Spectral Wave module and XBEACH simulation analysis for the case study. It also analyses the results and highlights possible shortcomings of the simulation and mentions future considerations.
- Chapter 7: discusses the merits for a suitable erosion control based on a theoretical approach only.
- Chapter 8: is a summary and conclusion on the research topic.

CHAPTER 2

LITERATURE REVIEW

2.1 Introduction

This section presents the background information pertaining to the various contributing factors of this dissertation namely the mechanisms related to wind-generated waves, climate change, trends in sea level rise and trends in the evolution of tropical cyclones in the Indian Ocean. This background is required for the prognosis of the wave climate and its effect on the coastal erosion faced on the Island of Mauritius.

2.2 Waves and Tropical cyclones

The theory of wind-generated waves is well documented [Goda, 2008]. Waves are characterized by a random and irregular surface undulance. However, short parameterized wave records (i.e. varying wave heights, periods and wavelengths over a timescale of typically 20 minutes) passing a stationary point in space have been found to approximate a sinusoidal variation. Some important wave parameters associated with short-term statistical analyses of waves are:

- Significant wave height, H_s defined as the average of the highest one-third of the waves
- Mean wave period, T_0 defined as the mean of all the wave periods.

Wind-generated waves are a major supplier of energy to the coastal system [Bosboom & Stive, 2012] that continuously affects the coastal morphology through sediment transport. Wind waves are a function of the wind speed, the duration of the wind and the distance over the water over which the wind blows [Baird, 2003]. These factors are significantly amplified in the case of a tropical cyclone. Therefore, although of short duration and seasonal, a tropical cyclone may have devastating effects on the coastal environment.

Tropical cyclones are low-pressure systems that form over tropical oceans as a result of various complex factors. Gray [1968] defines tropical storms as warm-core cyclonically rotating wind systems in which the maximum sustained winds are 35 knots (64.82 km/hour) or more. These formations have been observed in the latitude belts of 5 to 15° [Gray, 1975]. To this day, the early stages in the formation of tropical cyclone are not fully understood and cyclo-genesis is beyond the scope of this dissertation. However, an understanding of the causative factors of their formation is necessary to get an appreciation of the forthcoming sections.

The formation of tropical cyclones is dependent on the combination of the following six factors, amongst others [e.g. Gray 1968, 1975, 1998]:

i. Low level relative vorticity (C):

A continuous low level import of mass, momentum and water vapour is necessary for the formation of tropical cyclones [Gray, 1975]. These are thought to be related to the strength of the Ekman-type of frictional wind veering. These low pressure areas occur when the atmospheric pressure at sea level is below the surrounding regions which are caused by wind divergence at the upper levels of the troposphere.

ii. Coriolis parameter (f):

Gray [1975] states that cyclones do not form within 4 to 5° of the equator and therefore the influence of the earth's rotation appear to be of primary importance in the formation of cyclones. Furthermore, Gray [1975] states that winds on the equator are very weak and assumes that cyclone genesis cannot proceed if Boundary Layer velocities cannot be maintained. Significant Coriolis force allows the developing vortex to achieve gradient wind balance which allows latent heat to concentrate near the storm core. This results in the maintenance or intensification of the vortex.

iii. The inverse of the vertical shear of the horizontal wind between the lower and upper troposphere ($1/S_z$):

Minimum vertical shear of the horizontal wind between the lower and upper troposphere is required for the formation of tropical cyclones [Gray, 1975]. This means that tropical cyclones are fuelled by the temperature gradient between the warm tropical ocean and the colder upper atmosphere. The absence of ventilation coupled with an enthalpy gain at the upper levels of the troposphere plays an important role in the formation of tropical cyclones.

iv. Ocean thermal energy or sea temperature above 26°C to a depth of 60m (E):

Tropical cyclones require warm waters of at least 26°C to form and maintain the warm core that fuels tropical systems. Gray [1975] makes reference to various researches that have shown that storms consume a significant amount of calories per day. This energy consumption is associated with an oceanic upwelling within and around the storm's centre causing a reduced air pressure at this position.

- v. Vertical gradient of potential temperature between the surface and 500mb ($\partial\Theta_e/\partial p$):
Vertical coupling of lower and upper tropospheric flow pattern produced by deep cumulus convection favours the development of cyclones. In this atmospheric instability, a lifted parcel of air will be warmer than the surrounding air at altitude. Since it is warmer, the air is less dense and is prone to further ascent. This vertical motion is associated with the formation of weather systems and their severities.
- vi. Middle troposphere relative humidity (RH) :
High middle tropospheric humidity is essential for the formation of tropical cyclones [Wu et al., 2012]. High humidity encourages deep cumulus convection and precipitation which influences the enthalpy change [Gray 1975].

Gray [1975] further states that the product of the above parameters influences directly the cyclone genesis frequency as follows:

$$Seasonal\ Genesis\ Frequency \propto \left(\underbrace{\zeta \times f \times \frac{1}{S_z}}_{\text{Dynamic potential}} \times E \times \underbrace{\frac{\partial\theta_e}{\partial p} \times RH}_{\text{Thermal Potential}} \right)$$

2.3 Climate change and tropical cyclones

Global consensus regarding climate change has been established from historic records and continuous monitoring [IPCC, 2013]. Climate change is the result of an increase in the emission of greenhouse gases (GHG) such as carbon dioxide, methane and nitrous oxide through both natural and anthropogenic processes. The IPCC [2013] reports, with high confidence, that these increases in GHGs have been associated with changes in atmospheric and surface (ocean and land) temperature, water vapour, sea level, ocean acidification and climate extremes. Human activities are responsible for a 40% increase in the emission of carbon dioxide into the atmosphere between 1750 and 2011.

Climate change greatly affects the oceanic environment and influences the occurrence and intensity of natural processes that form over the ocean such as tropical cyclones. Consequently, these intensified processes impact significantly on the coastal environment. Notwithstanding the above, the direct effect of climate change on the frequency and intensity of tropical cyclones is still a controversial topic since the formation of tropical cyclone itself is not fully understood (as mentioned in the previous section). Numerous researchers [Henderson-

Sellers et al., 1998; Knutson et al., 2004, 2010; Webster et al., 2005; Emanuel, 2005; Bengtsson et al., 1996, 2007] have monitored the trend in the frequency and intensity of tropical cyclones since the emergence of the focus on climate change and have attempted to relate these two phenomena. However, the lack of reliable cyclone data, especially before the satellite era in 1970, does not give great confidence in this relationship.

It is obvious that the impact of climatic changes on one or a combination of the causative factors in the formation of tropical cyclone may alter its physical characteristics. One must consider this in the holistic planning and design of coastal developments in a dynamic coastal environment. The topic of climate change is not explicitly dealt with in this research but its potential effect on tropical cyclones is a key theme.

The previous section laid the foundation associated with the formation of tropical cyclones. The next section looks at the predicted effects of climate change on parameters associated with the formation of tropical cyclones.

2.3.1 Predicted effect of climate change on tropical cyclone

Coastal engineers, scientists and government bodies have recognized the importance of understanding wave climate to adequately predict, plan and mitigate its effects on the coastline as well as coastal developments, especially under extreme conditions such as tropical cyclones/storms.

The influence of climate change on each of the causative parameters is presented below. It is important to note that Bengtsson et al. [2005] and Caron & Jones [2007] report a discrepancy across the various genesis regions.

i. Low level relative vorticity (ζ):

Elevated low-level relative vorticity is required, amongst other factors, for the formation of tropical cyclones [Gray 1968, 1975, 1997; Tory et al., 2013]. Bengtsson [1996] predicts a decrease in the low-level relative vorticity with an increase in CO₂ level. Bengtsson [1996] associates this effect with a reduction in the frequency of tropical cyclones.

ii. Coriolis parameter (f):

The coriolis parameter is a function of the earth's angular velocity and is dependent on the latitudinal position [Elsner et al., 2009]. Therefore, no change is expected under the influence of climate change.

- iii. The inverse of the vertical shear in the horizontal wind between the lower and upper troposphere ($1/S_z$):
Thatcher and Pu [2011] and Knutson et al. [2004] report that high vertical wind shear (above 10s^{-1}) has a negative effect on the intensity of tropical cyclone and vice-versa. Knutson et al. [2004] and Vecchi & Soden [2007] also report an observed increase in vertical wind shear under the influence of high CO_2 levels. Emanuel [2006] suggests that a 10% increase in wind shear would decrease the TC intensity by 12%.
- iv. Ocean thermal energy or sea temperature above 26°C to a depth of 60m (E):
Recent climate changes are associated with a global increase in the sea surface temperature (SST). IPCC [2013] attributes this temperature increase in part to anthropogenic forcing. IPCC [2013] also reports a global SST increase ranging between 0.5°C to 1.3°C over the period of 1951 to 2010. Many studies [Emanuel, 1987; Evans, 1993; DeMaria and Kaplan, 1993; Walsh and Pittock, 1998; Knutson, 2004; Webster et al., 2005; Emanuel, 2006; Vitart et al., 2007; Bengtsson et al., 2007; Yu and Wang, 2009; Yamada et al., 2010; Knutson et al., 2010] have linked the increase in SST to the potential increase in intensity of tropical cyclones. Furthermore, Emanuel [2006] predicts that a 10% increase in water temperature would increase TC intensity by 65%.
- v. Vertical gradient of potential temperature between the surface and 500mb ($\partial\Theta_e/\partial p$):
Li et al. [2010] states that climate change is responsible for a larger increase in air temperature in the upper troposphere than in the lower troposphere over the lower latitudes. This results in the stabilization of the atmospheric temperature and pressure between these two regions and, is associated with the decrease in the frequency of tropical cyclones in some basins. Whilst the troposphere is warming up, cooling of the stratosphere is observed under climate change [Held, 1978; Bengtsson et al., 1995; Rind et al., 2005; Sherwood et al., 2010; Akperov and Mokhov, 2013]. This causes the warm air to rise poleward and cold air to sink as it moves equatorward. Hence energy is transported towards the poles through the process of baroclinic instability resulting in a poleward shift of the storms.
- vi. Middle troposphere relative humidity (RH) :
The effect of climate change on relative humidity is said to be minimal according to various researchers [Emanuel, 1987; Paltridge et al., 2009; Held and Shell, 2012; IPCC, 2013]. This is explained by the fact that water vapour, which is the primary GHG in the atmosphere [Gettelman et al., 2006] has increased. This increase is associated with an increase in the hydrological cycle and the weakening of the large-scale atmospheric circulation [Bengtsson, 2007]. The net effect is said to result in a constant relative humidity.

Table 2-1 summarizes the predicted effect of climate change on the causative parameters for cyclo-genesis.

Table 2-1: Summary of the resulting effect of climate change on the main parameters that affects the formation of tropical cyclones.

Primary Parameters	Magnitude required for development of tropical cyclone	Effect of Climate Change on Magnitude	Result on tropical cyclone
Relative vorticity (ζ)	High	↓	Decrease in frequency
Coriolis parameter (f)	Low	→	N/A
Vertical wind shear ($1/S_z$)	Low	↑	Decrease in intensity
Sea temperature (E)	High	↑	Increase in intensity
Temperature gradient ($\partial\Theta_e/\partial p$)	High	↓	Decrease in frequency
Relative humidity (RH)	High	→	Nil

‘↓’ = predicted decrease; ‘↑’ = predicted increase; ‘→’ = no predicted change

2.3.2 Discussion:

The influences of climate change on the various parameters necessary for cyclo-genesis have been reviewed. Although detailed consensus does not exist within the climatology community, a summary on the impacts of climate change on cyclo-genesis is given in Table 2-1.

The net combined effect of the above causative parameters necessary for cyclo-genesis, under the influence of climate change, is believed to yield the following:

- A potential increase in intensity,
- A potential decrease in frequency in the tropics.

Table 2-2 summarizes the predictions of climate change on tropical cyclones by various studies. A potential increase ranging from 3% to 20% is widely predicted with lower confidence over this range.

Table 2-2: Effect of climate change on the intensity of tropical cyclones
as predicted by various studies.

No.	Paper	Year	Authors	Intensity Prediction
1	The dependence of hurricane intensity on climate	1987	K. Emanuel	40% to 50% increase
2	Tropical cyclones and global climate change: A post-IPCC assessment	1998	A Henderson-Sellers, H Zhang, G Berz, K Emanuel, ...	10% to 20% increase
3	Impact of CO ₂ -induced warming on simulated hurricane intensity and precipitation	2004	T. Knutson, et al.	5 to 7% increase
4	Increasing destructiveness of tropical cyclones over the past 30 years	2005	K. Emanuel	10% increase
5	Changes in tropical cyclone number, duration, and intensity in a warming environment	2005	P Webster, G Holland, J Curry, H Chang	Increases
6	Tropical cyclone climatology in a global-warming climate as simulated in a 20km-mesh global atmospheric model: frequency and wind intensity analyses	2006	K. Oouchi, J Yoshimura, H Yoshimura, R Mizuta, S Kusunoki, A Noda	Increases
7	Impact of greenhouse gas concentrations on tropical storms in coupled seasonal forecasts	2007	F. Vitart, F. Doblas-Reyes	3 to 6% increase
8	How may tropical cyclones change in a warmer climate?	2007	L. Bengtsson, et al.	6 to 8% increase
9	On tropical cyclone intensity in the Southern Hemisphere: Trends and the ENSO connection	2007	Y Kuleshov, L Qi, R Farcett, D Jones	Increases
10	Response of tropical cyclone potential intensity over the north Indian Ocean to global warming	2009	J Yu, Y Wang	2.9 to 6.3% increase
11	Response of tropical cyclone potential intensity to a global warming scenario in the IPCC AR4 CGCMs	2009	J Yu, Y Wang, K Hamilton	Increases

Table 2-2 continues

Table 2-2: Effect of climate change on the intensity of tropical cyclones
as predicted by various studies (contd)

No.	Paper	Year	Authors	Intensity Prediction
12	Tropical cyclones and climate change	2010	T. Knutson, et al.	2 to 11% increase
13	Projection of changes in tropical cyclone activity and cloud due to greenhouse warming: global cloud-system-resolving approach	2010	Y Yamada, K Oouchi, M Satoh, etc	Increases
14	Tropical cyclone intensification trends during satellite era	2012	C Kishtawal, N Jaiswal	30% increase

2.4 Cyclone Potential Intensity increase for Case Study

Based on the predicted increases in the intensity of tropical cyclones shown in Table 2.2, this research investigates the coastal vulnerability when the intensity of a tropical cyclone (Section 3.3.2) is increased by 5%, 10% and 15%.

2.5 Global sea level trend

The fluctuation of the sea level plays an important role in coastal engineering and coastal management. The water level at any particular location is dependent on various global and local factors such as oceanic conditions, atmospheric forcing, storm surge, waves, tides, land subsidence or uplift, wind, warming or cooling of the ocean, continents and ice sheets, and river flow [Ewing, 2010]. It is evident how variations in sea level coupled with an intensified tropical cyclone can influence coastal conditions.

2.5.1 Sea level rise

Various tide gauges installed across the Northern and Southern hemispheres have recorded global average rate of increase in sea level of 1.7mm yr^{-1} between 1901 and 2010 [IPCC, 2013]. This translates to a rise in sea level of 0.19m in 110 years. Since the introduction of high-precision satellite altimetry record, an accelerated mean rate in sea level rise of 3.2mm yr^{-1} between 1993 and 2010 has been reported [IPCC, 2013]. The projections of IPCC [2013], based on a 95% probability model, show a global mean sea level rise of 0.72m between 1990 and 2100. Ewing [2010] uses the Bruun's rule to predict that, for gently sloping beaches, for every meter of sea level rise 50 to 100m of beach width is lost.

2.6 Tides

Tides are generated by the gravitational forces of the earth-moon and the earth-sun. The frequency of tides follows a diurnal and semi-diurnal trend due to the interaction between the earth, moon and sun. Bosboom and Stive [2012] state that the sun contributes to about 30% of the tidal amplitudes with the moon accounting for the remaining 70%. The daily variations in water level affect the coastal morphology through constant sediment transport. Due to the difference in the rotating axes between these 3 solar systems, daily inequalities occur i.e. the high and low tides are not equal in amplitude. The largest inequality occurs at a cycle of 18.3 years.

The coastal environment is affected the most during high tides and the impacts are greater in the event of storms. Moreover, the effect of sea level rise will cause the water during high tide to move further inland and this migration may extend the reach of storms.

2.7 Storm surge

Storm surge are sudden, short-term fluctuations in the water surface caused by high winds which are generated by a storm field. These fluctuations can be significant in the case of severe storms. As discussed in the previous section, storm surges occurring during high tides can be disastrous to the coastal system.

2.8 Sources of coastal sediment

Fine sediments (i.e. sand) deposited along the coast come primarily from the continent. These emanates from weathered rock which consist of quartz and feldspar [Bosboom and Stive, 2012]. Rivers determine the availability of sediments to the coastal system. The other source of sand to the coast is carbonate sediments. These come from fragment of shells and/or remains of marine life [Bosboom and Stive, 2012]. Prior to the 2000's, sand was used to make concrete in Mauritius. Due to the depletion of the sand along the beach and degradation thereof, this practice was banned. Also, beach sediment recovery following erosion may be hampered by the action of dams which retain the sediments. This dissertation does not investigate the availability of sediments to the coastal system of Mauritius.

Longshore sediment transport is the movement of sediments across the shoreline. The sediments are displaced parallel to the shoreline and to the depth contour lines [Bosboom and Stive, 2012]. Cross-shore sediment transport is the movement of sediments along the beach profile, i.e. between the upper and lower shoreface, as a result of wave action.

In Mauritius, in general, the coastal morphology is dominated by longshore sediments transport [Baird, 2003].

2.9 Resulting effect of climate change on coastlines on predicted surge and erosion

The coastal environment is subjected to perpetual changes through anthropogenic and/or natural forcing of which erosion is one of the major concerns in coastal degradation. In this dissertation, the rate of erosion caused by a potential intensified tropical cyclone resulting from climate change is addressed. As mentioned in the previous section, it is obvious that a potential increase in the intensity of the tropical cyclone coupled with a sea level rise may have devastating impacts on the coastal morphology.

2.10 Numerical modelling

The dynamics associated with coastal processes are very complex and the development of various modelling software has aided in simulating, to a high degree of accuracy, these dynamics. As such, the aims and objectives of this dissertation were achieved through the use of numerical modelling tools namely the MIKE 21 suite developed by the Danish Hydraulic Institute (DHI) and the XBEACH software by UNESCO-IHE, Deltares (Delft Hydraulics), Delft University of Technology and the University of Miami. Descriptions of the numerical models used are given in Section 2.10.1 to 2.10.3 and these literatures are available in the MIKE 21 Toolbox [DHI, 2011], the Mike 21 SW Scientific Documentation [DHI, 2011] and the XBEACH Model Description and Manual [Unesco-IHE Institute for Water Education, Deltares and Delft University of Technology, 2010].

2.10.1 MIKE 21 Cyclone Wind Generation

The wind and pressure fields generated by a travelling cyclone can often be described through a few parameters as cyclones are normally nearly circular. By obtaining these parameters from meteorological publications (or extracting them from synoptic weather charts), MIKE 21 Cyclone Wind Generation generates the space and time varying pressure and wind field within a model area for later use in a hydrodynamic or offshore wave simulation. In this way cyclonic surges or waves can readily be computed using MIKE 21 Spectral Wave (SW) module.

2.10.1.1 Parametric Models

Mike 21 Cyclone Wind Generation consists of various parametric models which can be chosen, depending on the available cyclone parameters. Several parameters are common for these parametric models. These parametric models are as follows:

- A.1 Young & Sobey [1981]
- A.2 Holland [1980] [Holland, 1980]
- A.3 Holland – double vortex [Holland, 1980; Thompson and Cardone, 1996]
- A.4 Rankine [Wood & White, 2013]

A.1 Young & Sobey parametric model

➤ Wind field parameters

The parameters required to simulate the wind fields are as follows:

- Radius to maximum winds, R_{mw}
- Maximum wind speed, V_{max}
- Cyclone track
- Forward speed, V_f and
- direction

The wind field consists of a rotational and a translational component. At a distance, R , from the centre of the cyclone, the rotational wind speed, V_r , is given as

$$V_r = V_{max} \times \left(\frac{R}{R_{mw}}\right)^7 \times e^{[7(1-R/R_{mw})]} ; \quad \text{for } R < R_{mw}$$

and

$$V_r = V_{max} \times e^{[(0.0025R_{mw} + 0.05)(1-R/R_{mw})]} ; \quad \text{for } R \geq R_{mw}$$

where R and R_{mw} are given in km.

The translational component, V_t , is given by

$$V_t = -0.5 \times V_f \times (-\cos \varphi)$$

where φ is the angle between the radial arm and the line of maximum winds.

The total wind speed, V , is the sum of translational and rotational components

$$V = V_r + V_t$$

➤ Pressure field parameters

The pressure, P , at a particular location is given as

$$P = P_c + (P_n - P_c) \times e^{(-R_{mw}/R)}$$

where the pressure field is comprised of:

- Central pressure, P_c
- Neutral pressure, P_n

A.2 Holland parametric model

➤ Pressure field parameters

Holland defines the pressure, P as follows

$$P = P_c + (P_n - P_c) \times e^{(-R_{mw}/r)^B}$$

where B is a shape parameter to match different kind storm pressure profiles, and is referred to as the Holland parameter or profile “peakedness”. The magnitude of B varies between 1 and 2.5 and can be obtained from:

$$B = 2.0 - \left(\frac{P_c - 900}{160} \right)$$

➤ Wind field parameters

The wind, as defined by Holland, can be obtained as follows

$$V_g(r) = \sqrt{(P_n - P_c) \times \frac{B}{\rho_A} \times \left(\frac{R_{mw}}{r} \right)^B \times e^{(-\frac{R_{mw}}{r})^B} + \left(\frac{r \times f}{2} \right)^2} - \frac{r|f|}{2}$$

where ρ_A is the air density and f the Coriolis parameter.

Neglecting the Coriolis effect, it follows that

$$V_{max} = \sqrt{(P_n - P_c) \times \left(\frac{B \times e}{\rho_A} \right)}$$

If the maximum wind speed (V_{max}) is known, an alternative method to determine B is given by

$$B = \frac{\rho_A \times e \times V_{max}^2}{(P_n - P_c)}$$

A.3 Holland – double vortex parametric model

- Pressure field parameters

The Holland – double vortex model includes a secondary vortex as follows

$$P = P_c + \left[\Delta p_1 \times e^{\left(-R_{mw1}/r\right)^{B_1}} \right] + \left[\Delta p_2 \times e^{\left(-R_{mw2}/r\right)^{B_2}} \right]$$

where $\Delta p_1 + \Delta p_2 = P_n - P_c = \Delta p$

- Wind field parameters

The gradient wind is given by

$$V_g(r) = \left\{ \sqrt{\begin{aligned} &\left[\left(\frac{R_{mw1}}{r} \right)^{B_1} \times \left(\frac{B_1 \times \Delta p_1}{\rho_A} \right) \times e^{\left(-\frac{R_{mw1}}{r} \right)^{B_1}} \right] + \\ &\left[\left(\frac{R_{mw2}}{r} \right)^{B_2} \times \left(\frac{B_2 \times \Delta p_2}{\rho_A} \right) \times e^{\left(-\frac{R_{mw2}}{r} \right)^{B_2}} \right] \\ &+ \left[\left(\frac{r \times f}{2} \right)^2 \right] \end{aligned}} \right\} - \frac{r|f|}{2}$$

A.4 Rankine parametric model

The modified Rankine vortex model uses the following velocity distribution:

$$V_g(r) = \begin{cases} V_{max} \times \left(\frac{r}{R_{mw}} \right) & , \quad \text{for } 0 \leq r < R_{mw} \\ V_{max} \times \left(\frac{R_{mw}}{r} \right)^X & , \quad \text{for } r < R_{mw} \end{cases}$$

where X ranges between 0.4 and 0.6

2.10.1.2 Wind Correction

B.1 Geostrophic correction

MIKE 21 Cyclone Wind Generation allows for a boundary layer wind speed correction to be applied to the gradient wind to obtain surface winds. This surface wind, V_{10} , is given by

$$V_{10}(r) = K_m \times V_g(r)$$

where the K_m parameter can be obtained from

$$K_m = \begin{cases} 0.81 & , \quad \text{for } V_g < 6 \text{ m/s} \\ 0.81 - [(2.86 \times 10^{-3}) \times (V_g - 6)] & , \quad \text{for } 6 \leq V_g < 19.5 \\ 0.77 - [(4.31 \times 10^{-3}) \times (V_g - 19.5)] & , \quad \text{for } 19.5 \leq V_g < 45 \\ 0.66 & , \quad \text{for } V_g > 45 \text{ m/s} \end{cases}$$

B.2 Forward motion asymmetry

Cyclonic winds circulate in a clockwise direction in the Southern Hemisphere. The wind field is asymmetric and this results in the winds being typically stronger to the left of the cyclone track and lower to the right.

Hence the forward motion at surface level is given by

$$V_{10}(r, \theta) = [K_m \times V_g(r)] + [\delta_{fm} \times V_{fm} \times \cos(\theta_{max} - \theta)]$$

where;

- δ_{fm} is the correction factor used to adjust the added forward cyclone speed, V_{fm} and typical value of δ_{fm} is 0.5 or 1.
- θ_{max} is the angle measured relative to the cyclone movement direction.

The cyclone movement direction and speed are computed based on the position of the centre of the storm given in the Best Track Data table in MIKE 21 Cyclone Wind Generation.

B.3 Wind inflow angle

Frictional effects cause the inflow of winds towards the centre of the storm. The inflow angle, β is typically 25° and decreases towards the storm centre. This wind inflow is implemented as follows in MIKE 21 Cyclone Wind Generation

$$K_m = \begin{cases} 10 \frac{r}{R_{mw}} & , \quad \text{for } 0 \leq r < R_{mw} \\ 10 + 75 \left(\frac{r}{R_{mw}} - 1 \right) & , \quad \text{for } R_{mw} \leq r < 1.2R_{mw} \\ 25 & , \quad \text{for } r \geq 1.2R_{mw} \end{cases}$$

2.10.2 MIKE 21 Spectral Wave (SW) module

The MIKE 21 SW model, developed by DHI, simulates the growth, decay and transformation of offshore cyclone waves in offshore and coastal areas. MIKE 21 SW uses a fully spectral formulation and a directional decoupled parametric formulation.

2.10.2.1 Fully spectral formulation

The fully spectral formulation is based on the wave action conservation equation whereby the wave field is represented by the wave action density spectrum, $N(\sigma, \theta)$. The wave phase parameters have been chosen as the relative (intrinsic) angular frequency, $\sigma = 2\pi f$ and the direction of the wave propagation, θ .

The wave action density spectrum, N , is related to the energy density spectrum as follows

$$N(\sigma, \theta) = \frac{E(\sigma, \theta)}{\sigma}$$

In this dissertation, the wave action conservation spectrum is formulated in horizontal Cartesian co-ordinate and the conservation equation for wave action is as follows

$$\frac{\partial N}{\partial t} + [\nabla \times (\bar{v}N)] = \frac{S}{\sigma}$$

where;

- $N(\bar{x}, \sigma, \theta, t)$ is the action density
- t is the time
- $\bar{x} = (x, y)$ is the Cartesian co-ordinates
- $\bar{v} = (c_x, c_y, c_\sigma, c_\theta)$ is the propagation velocity of a wave group in the four-dimensional phase space \bar{x}, σ and θ
- S is the source term for energy balance equation
- ∇ is the four-dimensional differential operator in the \bar{x}, σ and θ -space

The energy source term (S) represents the superposition of source functions which describe the following phenomena:

- wave growth by wind action (S_{in})
 - wave energy transfer due to non-linear wave-wave interaction (S_{nl})
 - dissipation due to;
 - white-capping (S_{ds})
 - bottom-friction (S_{bot})
 - depth-induced wave breaking (S_{surf})
- } calibration parameters

The relationship for these phenomena is given by

$$S = S_{in} + S_{nl} + S_{ds} + S_{bot} + S_{surf}$$

Calibration Parameters:

➤ White-capping

Energy dissipation due to white-capping is the result of the steepness-induced wave-breaking which occurs in deeper water when the wave height becomes too large compared to its wavelength. The source function was adjusted in MIKE 21 SW to obtain a proper balance between wind input and dissipation at higher frequencies. This is given as follows

$$S_{ds}(\sigma, \theta) = -C_{ds}(\bar{k}^2 m_0)^2 \left\{ (1 - \delta) \frac{k}{k} + \delta \left(\frac{k}{k} \right)^2 \right\} \bar{\sigma} N(\sigma, \theta)$$

where;

- C_{ds} and σ are calibration parameters (The values used for these parameters are given in Section 5.1.3)
- δ, \bar{k} and m_0 represent the dissipation coefficient, the mean wave number and the zeroth moment of the spectra respectively

➤ Bottom-friction

As the term suggests, energy dissipations due to bottom-friction occurs when waves propagate into shallow water and are affected by the friction due to the wave-bottom interaction. This source function is as follows

$$S_{bot}(\sigma, \theta) = -C_f \frac{k}{\sinh 2kh} E(\sigma, \theta)$$

where C_f is a dissipation coefficient.

For this dissertation, the bottom friction is described by the Nikuradse roughness (k_N) and the optimum value is given in Section 5.2.2.

➤ Depth-induced wave breaking

Depth-induced wave breaking occurs when waves propagate into shallow areas and the wave height can no longer be supported by the water depth. The source term is as follows

$$S_{surf}(\sigma, \theta) = -\frac{\alpha Q_b \bar{\sigma} H_m^2 E(\sigma, \theta)}{8\pi E_{tot}}$$

where;

- $\alpha \approx 1.0$ is a calibration constant
- Q_b is the fraction of breaking waves
- $\bar{\sigma}$ is the mean relative frequency
- E_{tot} is the total wave energy
- H_m is the maximum wave height given by γd with γ being the free breaking parameter (default values vary from 0.5 to 1.0). The adopted value is specified in Section 5.2.2.

Lowe et al. [2005], amongst others, states that the presence of coral reefs further contributes to the dissipation of the surface wave energy through wave breaking and bottom friction. This fact was considered in the present case study, as highlighted in Section 4.9.

2.10.2.2 Directional decoupled parametric formulation

The directional decoupled parametric formulation is suitable for the near shore conditions and uses the zeroth and first moment of the action spectrum.

2.10.2.3 Model Output

Similar to other models, this module of MIKE 21 requires the user to set up a mesh using bathymetry data which contains geographical information. Boundary conditions, representing the wind-generating body, are then assigned to the mesh which will enable the software to generate and propagate the waves within the defined grid. MIKE 21 SW uses a time and space varying approach which generates output data at any specified time interval for any given point within the domain.

The following wave output data, amongst others, are obtained from MIKE 21 SW at any particular point within the domain:

- Significant wave height, H_s , which is the average of the highest one-third of waves. The significant wave height is inferred from the zero-moment of a wave spectrum and is approximately equal to $3.8\sqrt{m_0}$, where m_0 is the area under the spectrum.

- Peak wave period, T_p , which is the peak wave with the highest energy given by

$$T_p = \frac{1}{f_p}$$

where f_p is the peak wave frequency

- Mean wave direction, θ_m given by

$$\theta_m = 270 - \tan^{-1}(b/a)$$

where;

- $a = \frac{1}{m_0} \int_0^{2\pi} \int_0^{\infty} \cos(\theta - 270) E(f, \theta) df d\theta$
- $b = \frac{1}{m_0} \int_0^{2\pi} \int_0^{\infty} \sin(\theta - 270) E(f, \theta) df d\theta$

2.10.3 XBEACH

XBEACH is one of various numerical models that have been used for the computation of nearshore processes, especially for sandy coastlines [Corbella & Stretch, 2013a; Roelvink et al., 2009]. The XBEACH model comprises the following:

- Short wave (wind and swell) action balance
- Roller energy equations
- Non-stationary shallow water equations of mass and momentum
- Sediment transport and
- Bed update.

The short wave transformations are achieved using a wave action balance in 2D space, time and direction. A roller energy balance is used to parameterise complex wave breaking processes in shallow water and also represents momentum stored in surface rollers which leads to a shoreward shift in wave forcing. Using these formulations, directionally-spread infragravity waves and time-varying currents can be generated.

The directionally integrated total wave energy dissipation due to wave breaking, $\overline{D_w}$, is given as

$$\overline{D_w} = 2 \frac{\alpha}{T_{rep}} Q_b E_w$$

where;

- $Q_b = 1 - e^{\left\{-\left(\frac{H_{rms}}{H_{max}}\right)^n\right\}}$ is the fraction of breaking waves
- $H = \sqrt{\frac{8E_w}{\rho g}}$

- $H_{max} = \frac{\gamma \tanh kh}{k}$; γ represents the breaker parameter given by (H/h)
- $E_w(x, y, t) = \int_0^{2\pi} S_w(x, y, t, \theta) d\theta$ is the directional wave energy over one wave period

Based on the wave group varying mass influx associated with the short waves and rollers, XBEACH uses the Generalized Lagrangian Mean (GLM) approach to represent the depth-averaged undertow.

During the swash and collision regime, the mass flux carried by the waves and rollers returns offshore as return flow. The offshore directed flows keep the erosion process going by removing sand from the slumping dune face. In the collision regime, the transport of sediment from dry dune face to wet swash (i.e. slumping or avalanching) is modelled with an avalanching model accounting for the fact that saturated sand moves more easily than dry sand, by introducing both a critical wet slope and dry slope. Through the advection-diffusion equation, XBEACH computes the bed level changes.

The sediment transport is modelled with a depth-averaged advection diffusion equation, namely

$$\frac{\partial hC}{\partial t} + \frac{\partial hCu^E}{\partial x} + \frac{\partial hCv^E}{\partial y} + \frac{\partial}{\partial x} \left[D_h h \frac{\partial C}{\partial x} \right] + \frac{\partial}{\partial y} \left[D_h h \frac{\partial C}{\partial y} \right] = \frac{hC_{eq} - hC}{T_s}$$

Where;

- C is the depth-averaged sediment concentration which varies on the wave-group time scale
- D_h is the sediment diffusion coefficient

The entrainment of the sediment is represented by an adaptation time, T_s given by

$$T_s = \max \left(0.05 \frac{h}{w_s}, 0.2 \right) s$$

where;

- h is the local water depth
- w_s is the sediment fall velocity
- s is the specific weight of the sediment, ρ_{sed}/ρ_{wat}

Entrainment or deposition is determined by the mismatch between the actual sediment concentration, C , and the equilibrium concentration, C_{eq} , thus representing the source term in the sediment transport equation. The equilibrium sediment concentration formulation is given by

$$C_{eq} = \frac{A_{sb} + A_{ss}}{h} \left[\left(|u^E|^2 + 0.018 \frac{u_{rms}^2}{C_d} \right)^{0.5} - u_{cr} \right]^{2.4} (1 - \alpha_b m)$$

where;

- $u_{rms} = \frac{\pi H_{rms}}{T_{rep} \sqrt{2} \sinh(kh + \delta H_{rms})}$ is the near bed short wave orbital velocity
- C_d is the drag coefficient due to the flow velocity only
- A_{sb} and A_{ss} are the bed load coefficients
- E^u is the Eulerian mean velocity
- U_{cr} is the minimum water velocity at which sediment sets in motion
- m is the bed slope and α_b the calibration factor

Typical input parameters are: significant wave heights, wave direction and period, near shore bathymetry, particle size, sea bed composition (i.e. hard layers).

2.11 Shoreline defence and preservation

Bosboom and Stive [2012] discuss the management strategies with regards to coastal erosion by identifying three methods namely:

1. Retreat; a do-nothing option which tolerates beach retreat
2. Accommodate; which ensures that the coastal infrastructures are able to resist any potential threat.
3. Protect; which looks at counteracting the effect of erosion and flooding.

Although this thesis does not focus in great detail on shoreline defence systems, the common systems are summarized in the next section. Each system has its benefits and its effectiveness. The two main types of coastal protection under which these systems fall are categorized as follows:

- ‘hard’ measures which involve permanent man-made structures and
- ‘soft’ measures whereby natural measures are used.

2.11.1 Hard protection measures

‘Hard’ measures consist of the construction of groynes, breakwaters, seawalls, revetment [Corbella and Stretch, 2012b]. These prevent sediment erosion by restraining the transport of sediments. Below are a few types of ‘hard’ measures’.

- Groynes; also extend perpendicularly into the surf zone and are spaced at relatively short intervals along the beach [Bosboom and Stive, 2012]. This results in the reduction of longshore sediment transport since the sediment is trapped between groynes.
- Detached breakwaters; are built at some distance away and parallel to the coast. These can be submerged structures or can emerge above the MSL. Emerged breakwaters are generally more effective in the reduction of longshore sand transport. On the other hand, submerged systems are preferred for aesthetic reasons, although in some instances, submerged breakwaters that were constructed relatively close to the shore have had adverse effect on coastal erosion.
- Seawalls; are vertical walls constructed along the shore which shelters the erodible materials. However, if not properly designed, the reflective actions of the waves by the wall may generate strong turbulences which may expose the wall foundation, hence resulting in the failure of the system.
- Revetments; are also constructed parallel to the shore. This system has a much gentler slope in comparison to the seawall. The level of the upper end of the wall usually coincides with the highest anticipated storm surge level.
- Sea-dikes; are characterized by the absence of a beach and therefore coastal sediment. In this instance, flooding of the hinterland is prevented by the construction of an earth structure.

2.11.2 Soft protection measures

Nowadays, more emphasis is put on the concept of environmentally friendly construction practices and as a result, ‘soft’ measures are preferred such as beach nourishment and geotextile sand filled containers (GSC).

- Beach nourishment has to do with the (continuous) replacement of the eroded sediment. This system implies that the coast is allowed to erode. Sediment replacement is achieved by dredging.

- Geotextile sand filled containers (GSC), as the name suggests, involves the filling of geotextile bags with sand. Although not classified as a completely “soft” measure, GSC is an effective countermeasure for coastal erosions. These sand bags are placed in the form of dunes and are then covered with vegetation. GSCs have become the preferred coastal defence in Durban in South Africa since 2007 as they offer an environmentally acceptable measure [Corbella & Stretch, 2013c]. A typical failure of this system is the loss of sand either through improper filling, vandalism or degradation of the sand bags which cause the wall to become unstable, especially for high walls [Corbella & Stretch, 2013c].

2.11.3 Preservation of the coral reefs

Coral reefs are important to the coastal ecosystem in that they protect the shoreline from the effects of wave storms and also provide shelter to the living creatures of the sea. The rise in the Sea Surface Temperature (SSTs) as a result of climate change has greatly affected the coral reefs which cannot sustain this increase in temperature resulting in coral bleaching [ASCLME, 2012; IPCC, 2013].

The discharge of untreated effluent in the ocean sometimes causes the algae to bloom which lead to the destruction of the coral reefs [Baird, 2003; JICA, 2013]. Sedimentation caused by erosion of the coast also affects the coral reefs.

Anthropogenic impacts on the coral reefs must be minimized through the treatment of effluent before being discharged in the sea and a proper management of the coastal erosion.

2.12 Literature review conclusion

In summary, this chapter provided an insight on the various parameters that affects the intensification of tropical cyclones, as well as the background information on the tools and models (i.e. MIKE 21 and XBEACH) used to achieve the outcomes of this dissertation.

Tropical cyclones can cause severe damage to the coastal environment affecting a country's economy and/or may cause fatalities. Although not fully comprehended, the formation of these natural phenomena is believed to be influenced by natural factors as well as anthropogenic forcing through climate change.

These influences are still debated in the engineering community but the vast majority of researchers tend to agree on the potential effects of climate change on the occurrence of tropical cyclones. Sea level rise is a widely accepted concept and has been proven through historical record. The combined effect of intensified tropical cyclones and sea level rise may further affect the coastal degradation, namely erosion of sediment. As such, it is imperative to assess and quantify the effect of these combined phenomena to accurately predict and mitigate their impacts.

A continuous pattern in the occurrence of tropical cyclones must be monitored to confidently produce the trend. The statistical analysis of the occurrence in tropical cyclones based on the limited data available seems to show a potential increase in intensity. Numerical modelling software that uses the spectral wave principle has been recognized to produce accurate forecast of wind-generated waves (MIKE 21) as well as their resulting effects on the coastline (XBEACH).

The coastal environment and ecosystem face an increasing stress due to adverse natural phenomena and the uncontrolled infrastructural development. Prompt protection management is imperative if the coastal environment is to be preserved. Various methods of controlling shoreline sediment transport exist and each one has its merits when properly designed and applied.

CHAPTER 3

CASE STUDY: DATA FOR TROPICAL CYCLONES IN THE INDIAN OCEAN

This chapter discusses the cyclonic activities in the Indian Ocean and the cyclone data used for the purpose of this research. Details about the data collected and the predicted intensification of an existing cyclone due to climate change which was used to achieve the outcomes are provided.

3.1 Classification of cyclones

Cyclones in the Indian Ocean are classified according to their wind speeds as indicated in Table 3-1.

Table 3-1: Classification of tropical cyclones in the Indian Ocean based on pressure (hPa) and wind speed (km/h)

Storm Type	Category	Pressure (hPa)	Max Gust (km/h)
Tropical Low	-	≥ 996	
Category 1 Tropical Cyclone	1	986 - 995	< 125
Category 2 Tropical Cyclone	2	971 - 985	125 - 164
Category 3 Tropical Cyclone	3	956 - 970	165 - 224
Category 4 Tropical Cyclone	4	930 - 955	225 - 279
Category 5 Tropical Cyclone	5	≤ 929	> 280

3.2 Cyclone trend in the Indian Ocean

For this study, the cyclone data for the South Indian Ocean was obtained and analysed from the Regional Specialized Meteorological Centre (RSMC) and the Australian Severe Weather Centre. Although the data from both sources were similar, the information from Australian Severe Weather Centre was adopted as it is easily readable.

Cyclone data from 1945 to 2011 was extracted from Australian Severe Weather Centre (<http://www.australiasevereweather.com/cyclones/index.php>) for the South Indian Ocean (SIO) 15°E - 135°E. Full record regarding the tropical cyclones prior to 1997 is not available other than the cyclone tracks and duration. The occurrence of tropical cyclones in the SIO is tabulated in Figure 3-1. The analysis shows a positive trend in the number of cyclones from 1945 to 2011.

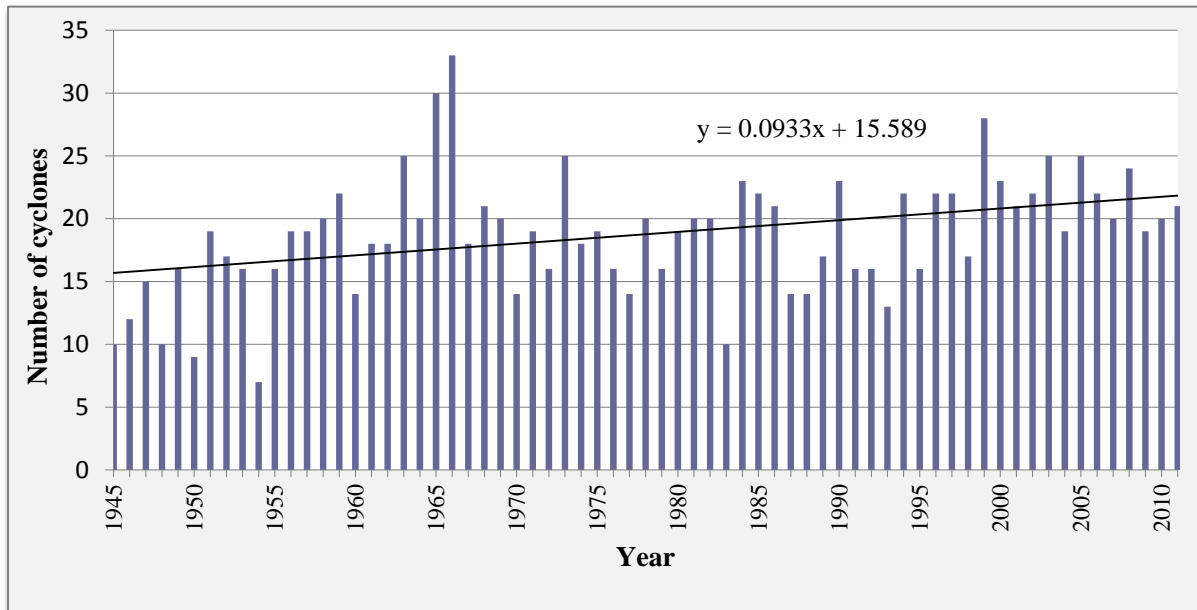


Figure 3-1: Cyclone activity in the South Indian Ocean (longitude 15°E to 135°E) between 1945 and 2011. The best fit line indicates a positive trend in the number of tropical cyclone from 1945 to 2011.

3.2.1 Improved Cyclone Data

Since 1997, better cyclone data containing minimum pressure, maximum wind speed and cyclone category is available from Australian Severe Weather Centre (<http://www.australiasevereweather.com/cyclones/index.php>). A better insight is gained on the cyclone trend in the Indian Ocean which appears to be relatively constant. This is shown in Table 3-2 and Figure 3-2.

Table 3-2: The improved cyclone track information with the maximum wind speed and minimum pressure from 1997 to 2011 in the SIO

Period	Tropical cyclone Category						Total
	Tropical Low	1	2	3	4	5	
Dec 1997 to Apr 1998	3	5	4	3	2	0	17
Jul 1998 to Apr 1999	11	5	5	2	1	4	28
Dec 1999 to Apr 2000	3	5	7	1	3	4	23
Aug 2000 to Apr 2001	9	2	4	3	3	0	21
Oct 2001 to Jun 2002	8	1	4	3	3	3	22
Sep 2002 to May 2003	8	2	5	5	3	2	25
Sep 2003 to May 2004	2	3	5	3	4	2	19
Sep 2004 to Apr 2005	7	7	5	2	1	3	25
Oct 2005 to Mar 2006	9	3	2	2	3	3	22
Oct 2006 to Apr 2007	5	3	2	3	6	1	20
Jul 2007 to Apr 2008	5	5	7	2	4	1	24
Oct 2008 to Apr 2009	2	5	8	0	4	0	19
Aug 2009 to May 2010	4	3	6	3	1	3	20
Oct 2010 to Apr 2011	10	2	3	3	2	1	21

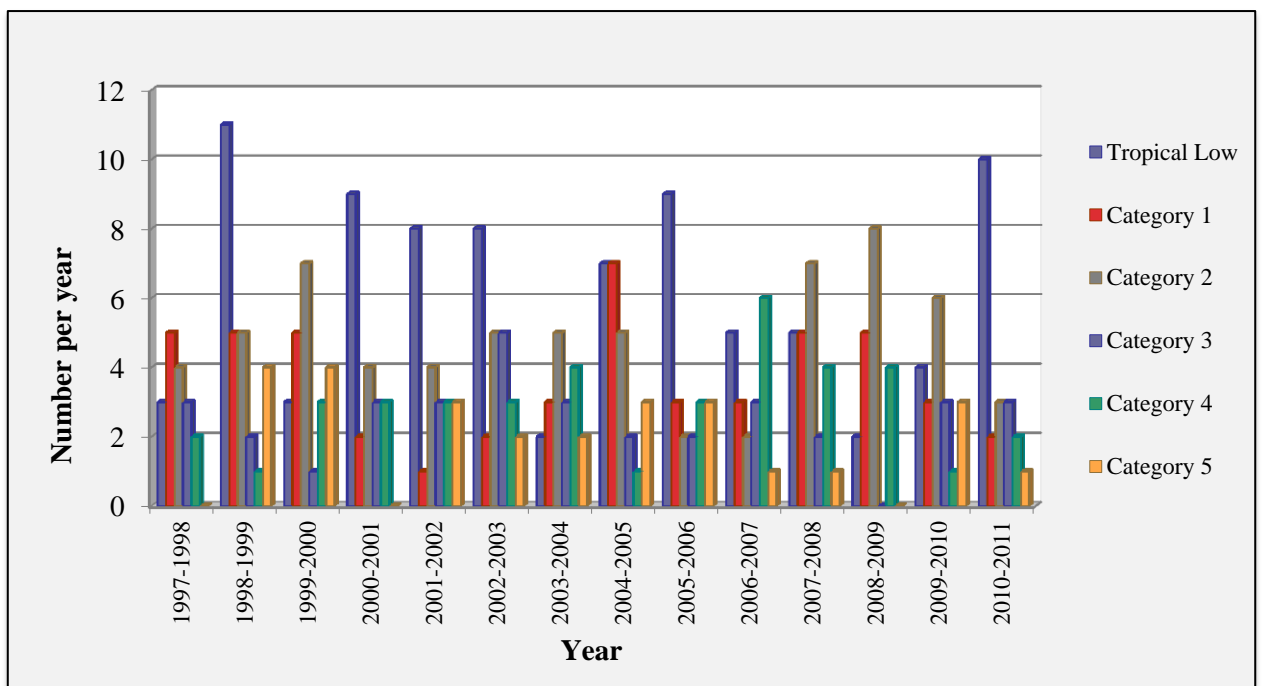


Figure 3-2: Graphical representation for the classification of the total number of cyclones and frequency between 1997 and 2011 in the SIO.

Further analyses of this improved information on the tropical cyclones in terms of their minimum pressures and maximum wind speeds are shown by Figures 3-3 and 3-4 respectively. The information generally depicts a fairly constant trend in the intensity of tropical cyclone which is not in accordance with the predicted potential increase in intensity by various researchers as mentioned in Section 2.3.1. However, it may be premature to make such comparison in the trend due to the relatively short timescale of the improved cyclone data. Indeed a proper comparison requires decades of cyclone data to allow the formulation in the trend of tropical cyclone with a high level of confidence.

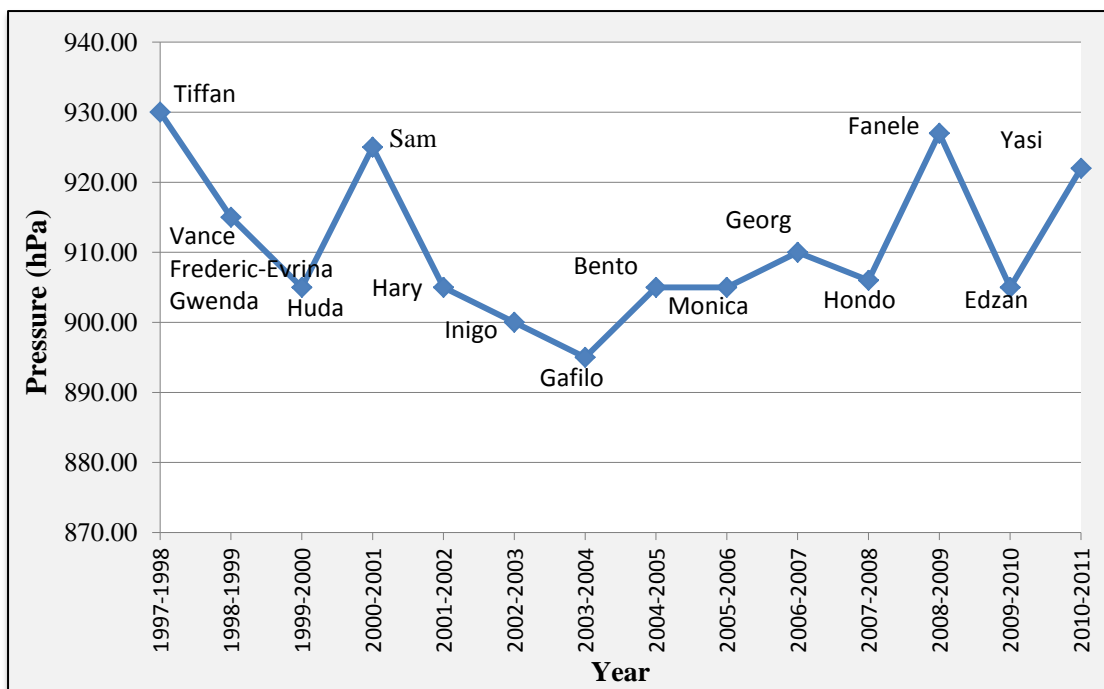


Figure 3-3: Annual most severe TC between 1997 and 2011 in the SIO based on Pressure (hPa).

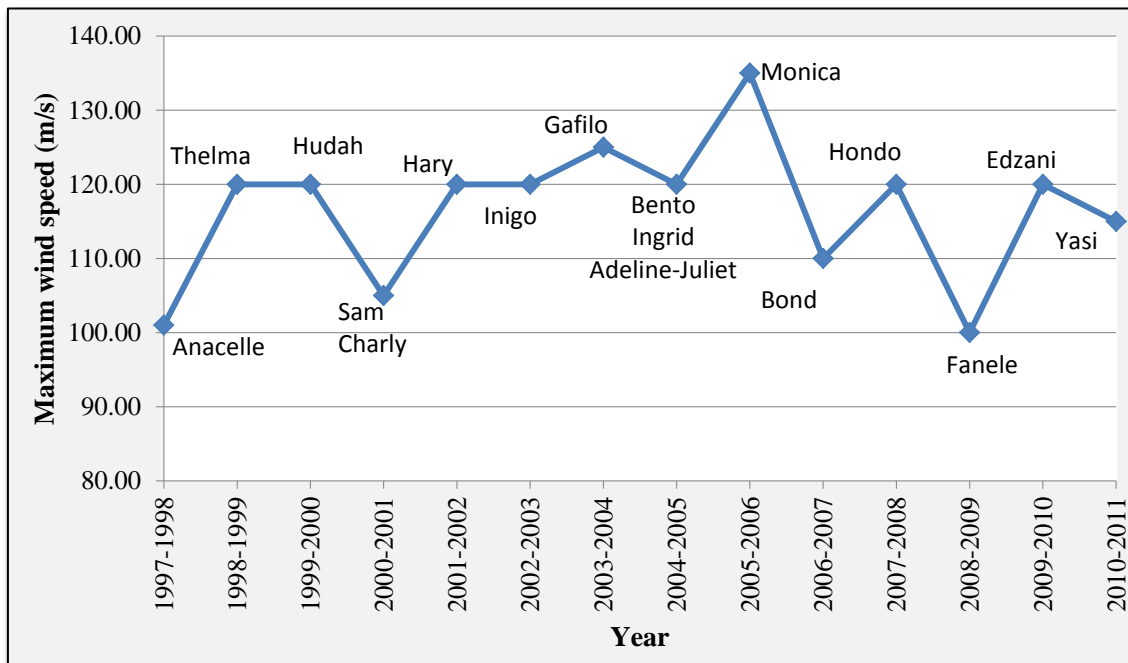


Figure 3-4: Annual most severe TC between 1997 and 2011 in the SIO based on Maximum wind speed (m/s).

3.3 Modelled tropical cyclones

3.3.1 Calibration and Validation

The Mauritius Meteorological Services (MMS) only provides cost-free monthly data to research students for a period not exceeding 5 years. The only two tropical cyclones recorded by the MMS between the requested period (2002 and 2006) are:

- Darius in 2003/2004 (cyclone category 2) and
- Hennie in 2005 (cyclone category 2).

These cyclones were used to calibrate and validate the MIKE 21 SW model respectively. The results are presented in Chapter 5.

3.3.2 Quantification of predicted erosion

The latest most influential tropical cyclone that affected Mauritius was Davina (cyclone category 4) in 1999. Davina passed within 100km of Mauritius and the maximum recorded wind speed was greater than 185km/hr. The trajectory of cyclone Davina is shown in Figure 3-5.

Cyclone Davina was used in this research to determine the sediment erosion at a particular site in Mauritius (Scenario 1). The intensity of this cyclone was then increased incrementally, based on the predicted effect of climate change on tropical cyclones as mentioned in Section 2.4, as follows:

- i. 5% intensity increase (Scenario 2)
- ii. 10% intensity increase (Scenario 3)
- iii. 15% intensity increase (Scenario 4)

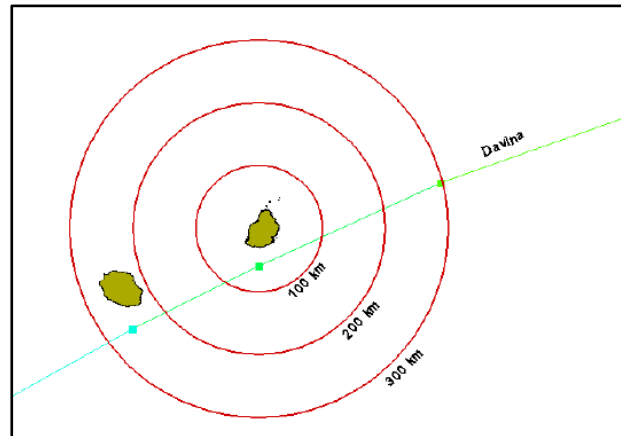


Figure 3-5: Trajectory of Tropical cyclone Davina (1999).
(Reproduced from Baird, 2003)

3.4 Summary

This chapter discusses the information used to achieve the aims and objective of the research. Limitations due to the lack of detailed historic cyclone data required to assess the trend in cyclonic activities in the SIO were mentioned. The outcomes for the calibration and the validation of the MIKE 21 SW model, as well as the predicted rate of erosion by the XBEACH model for the various scenarios are presented in Chapter 6.

CHAPTER 4

CASE STUDY: GENERAL DESCRIPTION

To achieve the aims and objective of this dissertation, a case study was required for the application of the modelling tools to assess the impacts of tropical cyclones, under the influence of climate change, on the coastal environment. This chapter presents the reasons for the selection of Belle Mare beach, in Mauritius, as the case study site for this research.

4.1 Coastal Livelihoods and degradation

Mauritius has become one of the travellers' most sought-after tropical holiday destinations in the Indian Ocean due to its climate, attractive sandy beach, calm lagoon and coral reefs. Tourism and other recreational coastal activities, such as snorkelling, etc., have blossomed in the last decades, becoming the third (3rd) major sector of its economy. JICA [2013] reported that the tourism has grown at an average rate of 3.5% between 2002 and 2011. This boom also led to an increase in the number of hotels throughout the island. In the last five (5) years, the contribution by the tourism sector to the GDP was approximately 8%. The gross earnings from tourism in 2011 were some USD 15 million based on the current exchange rate.

This rapid development was not accompanied by a detailed coastal management plan and this has led to the lack of maintenance of the coastal resources and the eco-system. As a consequence, the erosion of the shoreline and the deterioration of the coral reef have occurred at various locations. In an attempt to mitigate this beach degradation, several hard measures were constructed. However, these have proved to be ineffective. Coral bleaching has been reported by Baird [2003] and JICA [2013] as a result of the rise in the Sea Surface Temperature. The discharge of effluent into the sea has also contributed to the degradation of the coral reefs.

A great emphasis is now placed on the implementation of a proper coastal management framework for the preservation of the shoreline to sustain the growth in the tourism sector.

4.2 Previous coastal studies in Mauritius

The Ministry of Environment, under the tutelage of the Government of Mauritius (GoM), has commissioned various studies to address this coastal degradation by the following parties:

- Baird and Associates Coastal Engineers Limited, in association with Reef Watch Consultancy Ltd, in 2003, referred to as “Baird” in this dissertation.
- Japan International Cooperation Agency (referred to as “JICA”)

Several parameters and materials were extracted from these studies for this dissertation.

4.2.1 Extent of coastal studies

4.2.1.1 Baird [2003]

The study conducted by Baird in 2003 comprised the following:

- a. A comprehensive investigation of the marine biology, the reef ecology, sediment grade and water quality at various sites.
- b. The assessment of the extent of coastal erosion at several sites as identified by the GoM
- c. Identification of critical sites
- d. The investigation of the root causes for coastal erosion
- e. The assessment of the efficiency of the existing protection works
- f. The recommendation of suitable erosion countermeasures and reef preservation for inclusion in the Integrated Coastal Zone Management plan.

In his study, Baird [2003] produced a statistical return period model using historical cyclone data to predict the volume of erosion at various sites along Mauritius such as Belle Mare. The WAVAD model was used to derive the offshore wave conditions and the COSMOS model was adopted to quantify the nearshore wave transformations. The results from these models are given in sections 4.8 and 4.11.

4.2.1.2 JICA [2013]

A visual identification of the sites affected by coastal erosion was done by JICA [2013] which included a basic investigation of the coastal features. This formed the basis for the compilation of a priority list for the critical sites. No qualitative analysis for erosion was conducted. The report by JICA [2013] also addressed the suitability of the existing coastal protection measures and made recommendations for the implementation of a “Coastal Conservation Plan”.

4.3 The coastal geology of Mauritius

Mauritius has a total land area of 1,865km² and a coastline of approximately 320km long. The main island is surrounded by fringing coral reefs enclosing a lagoon, with passes (gaps) along the coral reefs. The passes are generally found at mouth of rivers and estuaries.

The coastline of Mauritius is mostly characterized by the reef-lagoon-beach system. Figure 4-1 indicates the percentage of the types of shores around Mauritius which is generally composed of sand, rock, cliff and silt/mud [JICA, 2013].

The land usage for the coastal zone of Mauritius is also shown in Figure 4-1. This coastal land usage has been divided into developed and ‘green’ zones. Developed zone refers to the areas where infrastructures are present and ‘green’ areas refer to cultivated land, public beach or farm land. The land usage for each type of shores could not be determined.

The coastline of Mauritius comprises of approximately 48% of sandy coast and 52% of rocky, cliff and silt. Presently, 56% of the coastland is undeveloped.

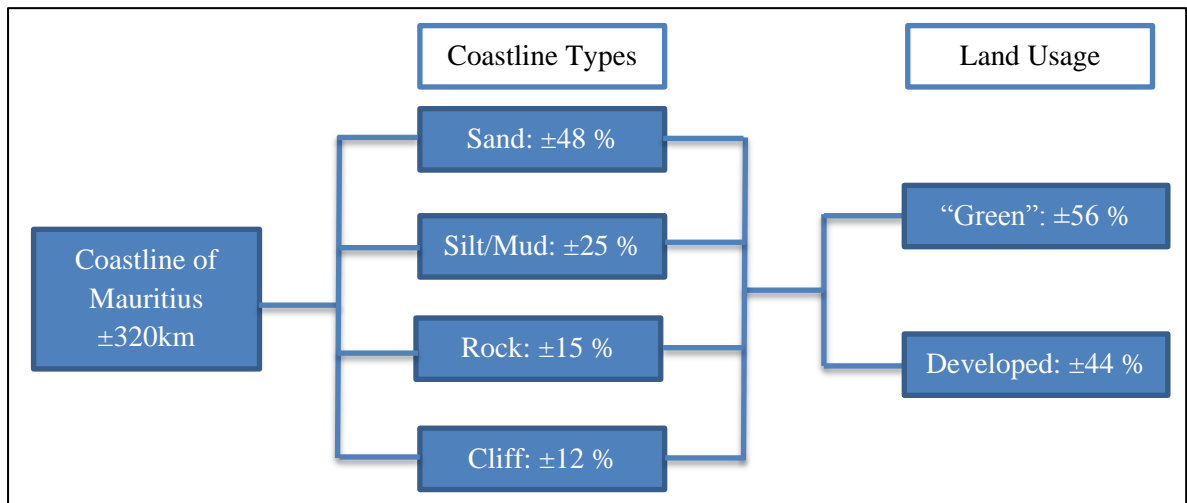


Figure 4-1: The estimated percentage of coastal types and land usage for Mauritius

4.4 The wave climate of Mauritius

The Island of Mauritius is situated in the Indian Ocean between latitudes 19°50' and 20°32'South, and longitudes 57°18' and 57°46' East (refer to Figure 4-2). Owing to its geographical location, Mauritius experiences a tropical maritime climate and its wave climate is determined by three dominant weather systems, namely:

- The South East (SE) Trade Winds which generate local waves of different magnitude and frequency all year round.
- Southern Hemisphere (SH) Swells resulting from distant storms
- Tropical cyclones which develop in the South West Indian Ocean between November and May and generally approach the island from the North East.

Long term coastal erosion results from continuous wave actions by the SE Trade winds and the SH swells. The typical wind waves vary between 0.5m and 3m in height with a period ranging between 3 to 11 seconds. In the case of swells, these waves generally range between 3 to 5m high and have a period of 12 to 20 seconds [JICA, 2013].

Tropical cyclones (TCs), on the other hand, are responsible for the short term coastal erosion. The waves generated depend on the intensity of the tropical cyclones and have been reported to be in excess of 10m in the case of severe TCs. These systems generate vast amount of energy susceptible of causing extensive damage to the coastal geology. There is limited information with regards to the relation between the intensity of tropical cyclones and the associated coastal erosion for Mauritius. For the proper management and planning of the coastal environment, it is imperative to assess the contribution of short term erosion as a function of the global erosion.

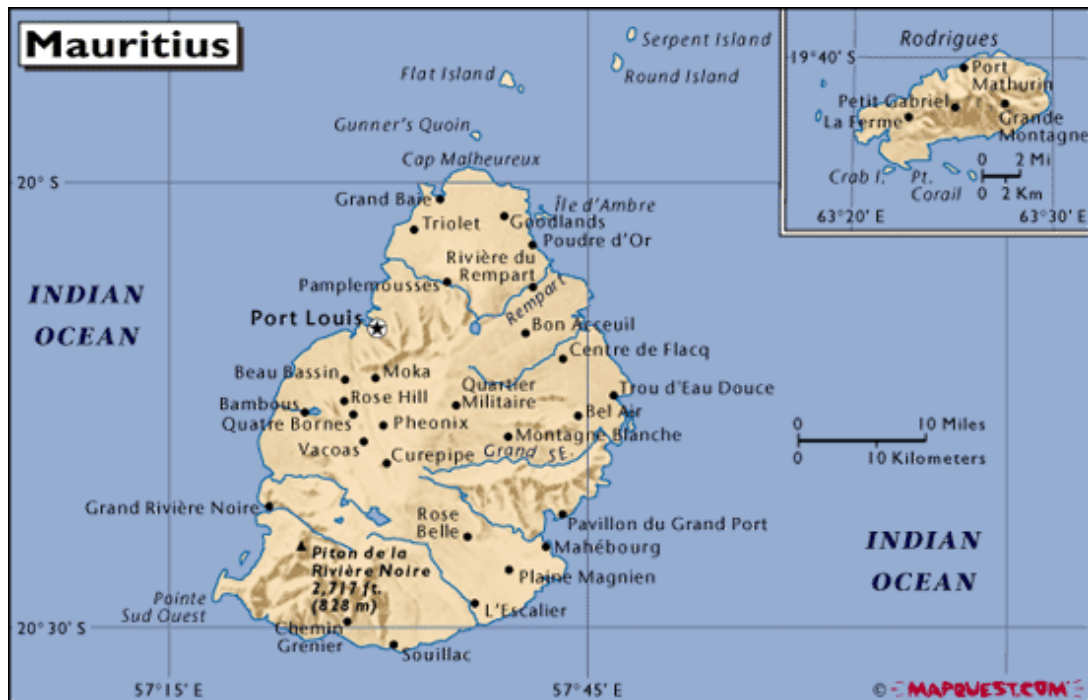


Figure 4-2: Geographical location of Mauritius
(Source of imagery: Google Earth, 2014)

4.5 Recorded wave data

A wave rider buoy was installed, in May 1996, at latitude 20.27°S and longitude 57.42°E at approximately 1km off the coast of Blue-Bay in the South East of Mauritius at a depth of 56m. The wave data, obtained from the Mauritius Meteorological Services, for the most intense tropical cyclone experienced since was compared with MIKE 21 SW model for the software validation. This is presented in Chapter 5.

4.6 Tide regime

Tides for Mauritius are semi-diurnal with a spring tidal range of 0.5m and a neap range of 0.3m. The range between the highest and lowest astronomical tide (HAT & LAT) has been recorded to be 0.8m.

4.7 Sea Level Rise

Sea gauges were installed at Port Louis in 1986 and continuous data has since been available. A decrease of 0.10 mm/year in the sea level was observed between 1990 and 2003. However, in recent years, a rise in sea level ranging between 1.2 and 3mm/year has been recorded by the National Oceanic and Atmospheric Administration (NOAA). These are depicted in Figure 4-3.

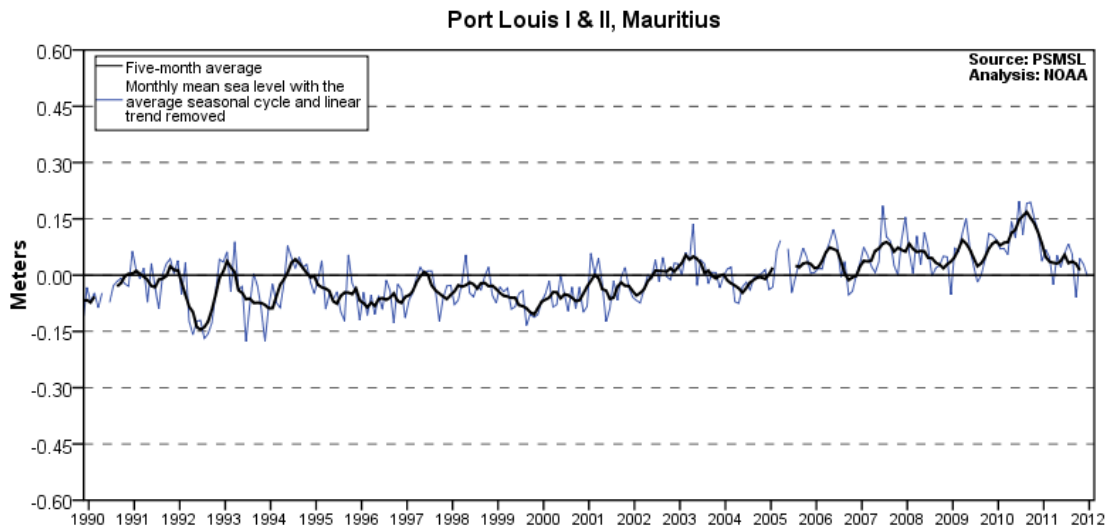


Figure 4-3: Interannual variation in sea level since 1990

(Source: NOAA)

Keeping the above average rate of increase at 3mm/year for the next 100 years, a sea level rise of $\pm 0.3\text{m}$ is predicted. This is synonymous with a potential increase in erosion.

4.8 Cyclone Return Period

When designing any structure, engineers and planners must consider all natural events that may directly affect the structural integrity of the structure over its designed lifetime. Unfortunately, the occurrence of some natural events may not always be accurately predicted. Moreover, these natural events have different degree of severity.

A conservative approach may be to design the structure for the worst known case of a particular natural event. However, this may result in the structure being overdesigned if the occurrence of the natural event exceeds the intended lifetime of the structure. Although some degree of safety is obtained by over-designing a structure, this approach is not sustainable. Therefore, a statistical analysis of the historical trend for the natural events is required to depict an acceptable probability of occurrence and this is termed the return period.

To supplement the return period analysis, a flood risk analysis is also recommended to provide grounds for a rational decision making. Prinos and Galiatsatou [2010] states that in this risk analysis, three (3) indicators that are assessed to define an acceptable flooding probabilities. These indicators are as follows:

- i. The cost-benefit analysis in which a decision is deemed acceptable if the benefits exceed the cost of protection. The cost and benefits are expressed in monetary values.
- ii. The utility analysis reflects the preferences of the society.
- iii. The life quality analysis which is related to the utility analysis and evaluates the life expectancy and the gross domestic product per capita.

The risk analysis approach requires reliable record data for its implementation. Since detailed historical cyclone data is not readily available, it was not possible to formulate a return period and/or risk analysis for the purpose of this dissertation.

Baird [2003] has devised a cyclone return period chart based on extreme value analysis of the maximum wave heights which were obtained from the simulation of twenty-five cyclones between 1979 and 2002 using the WAVAD model. Only cyclones that have affected Mauritius within a radial distance between 100 and 300 km were considered by Baird [2003]. From these simulations, the hourly wave conditions were recorded along the East, South and West shorelines of Mauritius. The characteristics defining the return periods as formulated by Baird [2003] are presented in Table 4-1.

Table 4-1: Design wave conditions in Mauritius as determined by Baird [2003]

Return Period (Years)	Surge (m)	West		South		East	
		Hm0 (m)	Tp (s)	Hm0 (m)	Tp (s)	Hm0 (m)	Tp (s)
5	0.16	12.3	14	11.2	14	11.9	14
10	0.24	14.7	16	14.4	16	13.6	15
25	0.33	17.7	18	18.6	15	15.3	16
50	0.43	20.0	20	21.9	20	17.4	18
100	0.54	22.2	20	25.1	20	18.9	18

(Reproduced from Baird, 2003)

Baird [2003] estimates the return period for cyclone Davina to be between 3.6 and 4 years. This is compared with the results as presented in Chapter 5.

Baird's [2003] approach in determining the cyclone return period is based on the extrapolation of historical records and the statistical analysis of these modelled wave height data. Nott and Jagger [2013] present a distinct method for determining more reliable cyclone return periods based on the assessment of the sediment deposited, throughout the Holocene period, over the beach ridges from inundations caused by tropical cyclones. Nott and Jagger [2013] state that beach ridges go through transformation under the influence of each successive marine flood. Each of these extreme events causes the ridge to grow in height through the transport and deposition of sediments until no further growth is achievable. In the same manner, a new ridge is formed to the seaward side by the next significant inundation and over several millennia this pattern develops into a series of ridges. Each ridge holds the details of the most extreme inundation event which can be dated using Optically Stimulated Luminescence (OSL). Nott and Jagger [2013] then apply a Generalized Extreme Value (GEV) and a Bayesian analysis approach to generate a return period chart.

Although the approach proposed by Nott and Jagger [2013] give a more sensible method of determining the cyclone return period, this method cannot be applied to this study since these data are not available. In contrast, the use of deterministic models to generate a reliable return period chart requires the assessment and simulation of over 100 years of historical data. This was not undertaken in this study due to the unavailability of historical cyclone data and/or time constraint. Therefore, the chart devised by Baird [2003] was used as a guideline.

4.9 Coastal Vulnerability and Selection of Pilot site

The Government of Mauritius (GoM) has recognized the need to address the coastal degradation and, through the Ministry of Environment (MoE), has initiated various studies to assess the root causes and to propose mitigating measures to preserve its resources. As part of these studies, various vulnerable sites around the Island have been identified by the MoE. Due to the severity of the degradation at various locations around the island, the GoM has already initiated immediate remedial measures.

Table 4-2 is a list of the sites considered in the two studies done by Baird [2003] and JICA [2013].

Table 4-2: Summary of the degree of vulnerability of public beaches in Mauritius with regards to erosion as identified by Baird [2003] and JICA [2013].

No.	Beach	Vulnerability	
		By Baird [2003]: 20No.	By JICA [2013]: 10No.
1	Pointe D'esny	Medium	High
2	Le Morne	Medium	Medium
3	Flic en Flac	High	High
4	Albion	Low	High
5	Grand Baie	High	N/A
6	Riambel	Medium	N/A
7	Pomponnette	Medium	N/A
8	Riviere des galets	High	N/A
9	Trou d'Eau Douce	Low	N/A
10*	Belle Mare	High	See Quatres Coco
11	Palmar	High	N/A
12	Baie du Cap	Medium	N/A
13	Poudre D'Or	Low	N/A
14	Cap malheureux	Medium	N/A
15	Pointe aux Piments	Low	N/A
16	Pereybere	Low	N/A
17	Bain boeuf	Medium	N/A
18	Bambous virieux	Medium	N/A
19	Quatre Soeurs	Medium	N/A
20	Petit Sable	Medium	N/A
21	Pointe aux cannoniers	N/A	Medium
22	Mon choisy	N/A	High
23*	Quatres coco	See Belle Mare	Medium
24	Ile aux cerf	N/A	Medium
25	Bel Ombre	N/A	Medium
26	Pointe aux Sables	N/A	Medium

The locations of the beaches listed in Table 4-2 are represented graphically in Figure 4-4. For the common sites identified by the two reports, the most severe vulnerable site is depicted.

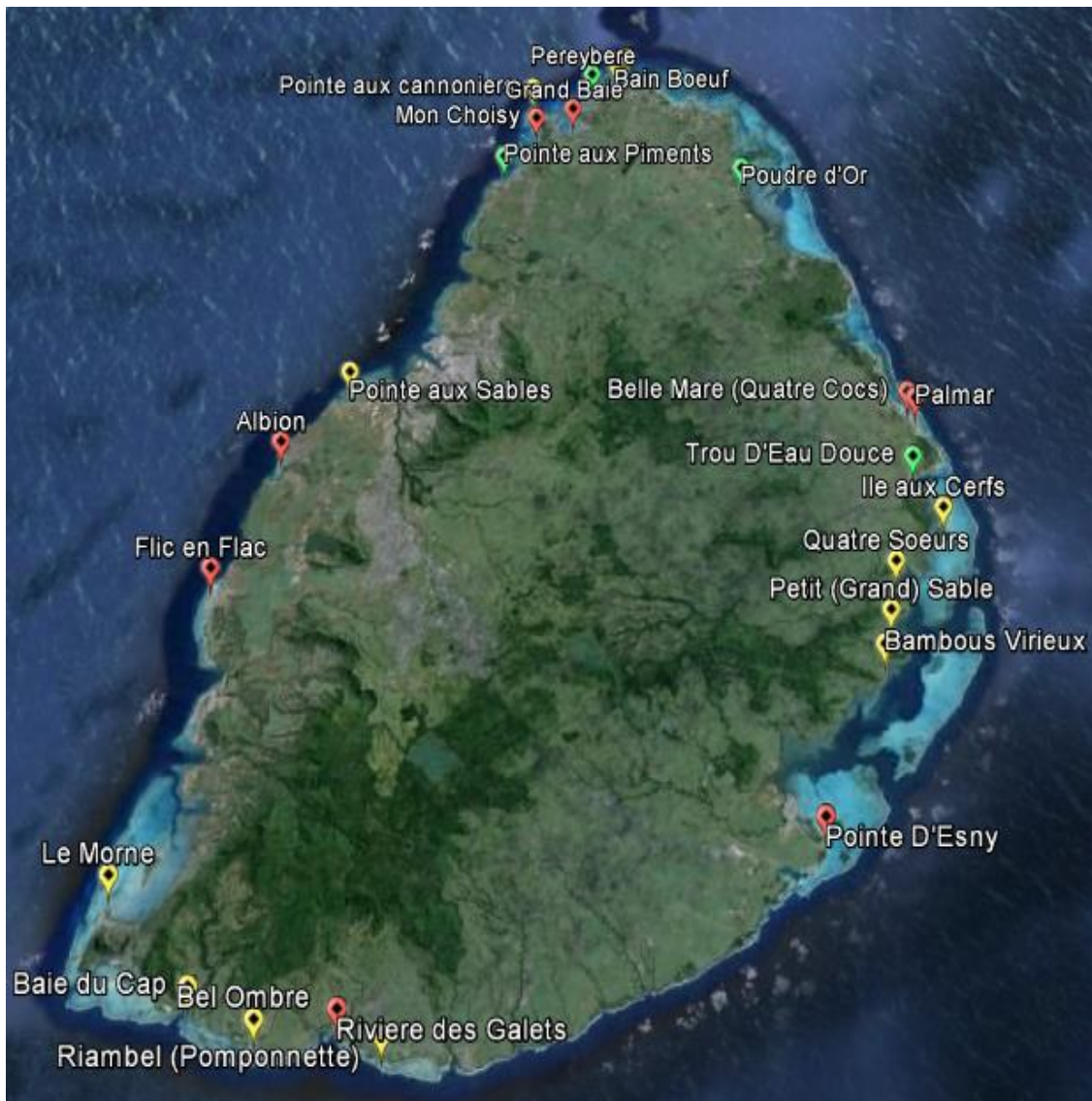


Figure 4-4: Geographical representation showing vulnerability of beaches listed in Table 4-2.

[Red tag represents High vulnerability; Yellow tag represents Medium vulnerability; Green tag represents Low vulnerability]

(Source: Google Imagery 2014).

Although Flic en Flac was identified as the most vulnerable site in both studies, Belle Mare beach was chosen for this dissertation for the following reasons:

- Belle Mare was classified as a medium to high vulnerability site
- The reef-lagoon-beach system is a typical representation of the coastal physiognomy surrounding the Island
- Belle Mare beach is highly frequented by locals and tourists
- 12 luxurious hotels are present along this stretch of the Island
- Adequate bathymetry, extracted from Baird [2003], is available for nearshore modelling using XBEACH
- Baird [2003] highlights the importance of assessing the extent of erosion during different cyclone intensities.

4.10 Coastal features of Belle Mare beach

The public beach of Belle Mare has the following features [Baird, 2003; JICA, 2013]:

- Beach with width of 30m generally, with presence of Filao (casuarinas) trees some 25m inland at places
- Beach slope is approximately 1 in 10
- Length of beach is approximately 1900m
- Well graded sediment distribution, with 50% passing for fine to medium sand generally (i.e. 0.4mm)
- Reef ranging between 450m to 900m offshore, with “passes”
- Presence of gabions and groins
- Local degradation of coral reef

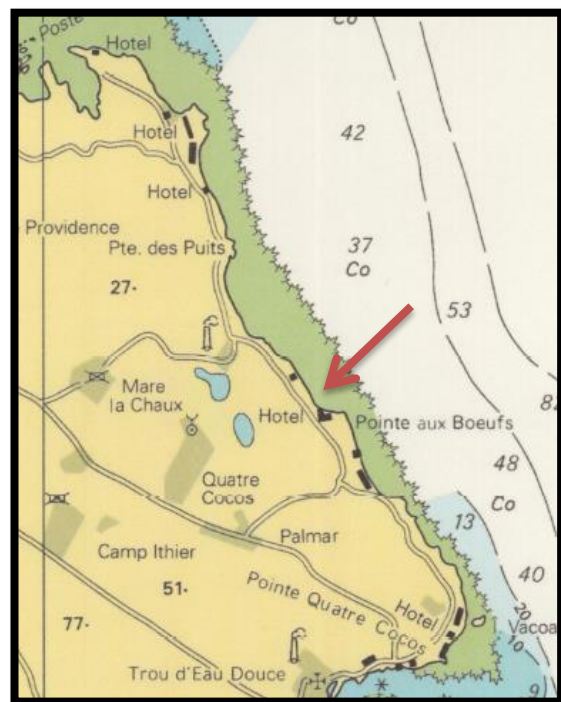


Figure 4-5: Location site Map of Belle Mare

4.11 COSMOS model output

The COSMOS model simulates the nearshore wave transformations and sediment transport [Southgate and Nairn, 1993]. The following physical processes are executed by the COSMOS model, which is similar to the XBEACH model (See Section 2.10.3):

- Wave transformation by refraction, shoaling, Doppler shifting, bottom friction and wave breaking.
- Wave set-up determined from the gradient of wave radiation stress.
- Driving forces for longshore wave-induced currents determined directly from the spatial rate of wave energy dissipation.
- Longshore currents from pressure-driven tidal forces and wave-induced forces, and the interaction between the two types of current.
- Cross-shore undertow velocities using a three-layer model of the vertical distribution of cross-shore currents.
- Transition zone effects (the transition zone is the distance between where a wave starts to break and where turbulence becomes fully developed).
- Cross-shore and longshore sediment transport rates based on the dissipation of wave and current energy, as opposed to an excess shear-stress approach.
- Lakebed level changes due to cross-shore sediment transport using a Lax-Wendroff scheme.
- Downcutting of a cohesive profile and cohesive bluff erosion due to wave action and abrasion by a covering layer of sand.

In their report, Baird [2003] presented the nearshore output results for various return periods for cyclones at Belle Mare using the COSMOS numerical model. These results are presented in Table 4-3.

Table 4-3: Lateral Retreat and Eroded Volume for a Range of Cyclones
at Belle Mare [Baird, 2003]

Return Period (years)	Greatest Retreat (m)	Erosion Volume (m ³ /m)
5	2.5 – 4	11.5 – 17
10	3 – 5	14 – 22
25	3 – 6	18 – 29
50	5 – 14	20 – 30
100	8 - 20	25.5 – 36

(Reproduced from Baird, 2003)

Despite the relatively high predicted erosion as reported above, the COSMOS model shows a considerable attenuation of the significant wave height due to the presence of coral reefs. For instance, in the case of a 5-year return cyclone, Baird [2003] states that the wave height was reduced from 12m to 1.0m when traveling over the reefs. This represents a drop of 90% which indicates that reefs play a major role in the dissipation of the wave energy.

A comparison of the predicted erosion by the COSMOS model and the results from XBEACH is presented in Section 6.3.1, Chapter 6.

4.12 Coral reef degradation

As mentioned in the previous section, coral reefs contribute significantly in the reduction of the wave energy from storm surges. When traveling over the reef, the potential energy of the wave setup is converted to kinetic energy and the movement of water is resisted by the friction on the rough surface of the reef, dissipating the energy and decreasing the water level. This protects the coastline from severe erosion.

JICA [2013] reports the reduction of coral reefs around Mauritius due to the following causes, amongst others:

- a) Coral bleaching which is believed to be associated with global warming
- b) Siltation in the lagoon
- c) Eutrophication caused by excess inflow of nutrients from fertilizers, effluent, etc which leads to algal bloom. Algal bloom reduces the oxygen level in water and this has adverse effects on the living corals.
- d) Overgrowth of seaweed as a competitor of corals
- e) Local extinction of some coral species

Belle Mare is subject to the rapid growth of algae and the considerable inflow of effluent from the hinterland affecting the water quality.

4.13 Proposed mitigation for erosion at Belle Mare

Despite the paucity of reliable data, Baird [2003] proposes the following measures, as part of the coastal zone management, to help reduce the rate of erosion generally:

- Establish a dynamic beach setback that will prevent any development
- Avoid constructing coastal structures in the dynamic beach zone
- Implement a beach erosion monitoring program
- Create awareness to reduce pedestrian and beach access
- Remove all Filao trees and replace these with plant native coastal vegetation. Baird believes that trees are not apt to retain sand. Instead, the Filao tree creates shade which does not promote the growth of sand-holding grasses, vines and shrubs.

4.14 Limitations and Constraints

Coastal science is a relatively new field of engineering which has considerably boomed in the last decades due to the growing awareness of coastal degradation/preservation. Coastal processes and dynamics is a rather complex topic and although substantial advances have been made in recent years, much remains to be done to fully comprehend this field.

In order to confidently understand and address coastal erosion, historical behaviours and trends is imperative to formulating adequate measures. This lack of information is the biggest challenge of Mauritius.

The following limitations and constraints may have resulted in the lack of accuracy in the outcome of the modelled data:

- Limited historical cyclone wave record which prevents the statistical analysis of extreme events
- Only one wave-rider is operational around the Island
- Lack of regular survey of beach profiles which would provide insight for relation between cyclone and coastal changes
- Lack of bathymetry data for hindcast and forecast modelling
- Lack of measurement of wave transformation over the reefs
- No existing coastal defence structure was modelled

4.15 Summary

This chapter highlighted the selection of the case study used to achieve the aims and objective of the research. The limitations and uncertainties due to the unavailability of reliable data on the coastal system required to run the simulations were mentioned. All the information mentioned in section 4.12 was relevant to the study. Consequently, the accuracy of the results, which were produced and presented in Chapter 6, may not be utterly reliable due to the constraints described in the previous section.

CHAPTER 5

MODEL DATA AND METHODS

This chapter describes the methods used to predict the relative sediment erosion resulting from cyclone. To achieve the above, the following modelling tools were used:

1. MIKE 21 Cyclone Wind Generation
2. MIKE 21 Spectral Wave (SW) module
3. XBEACH model

5.1 Mike 21: Model Setup, Calibration and Validation

5.1.1 Model extent, bathymetry and mesh grid

The model domain adopted for the Cyclone Wind Generation and the Spectral Wave module covers the Indian Ocean region between latitude 0° to 30°S and longitude 35°E to 90°E, as shown in Figure 5-1.

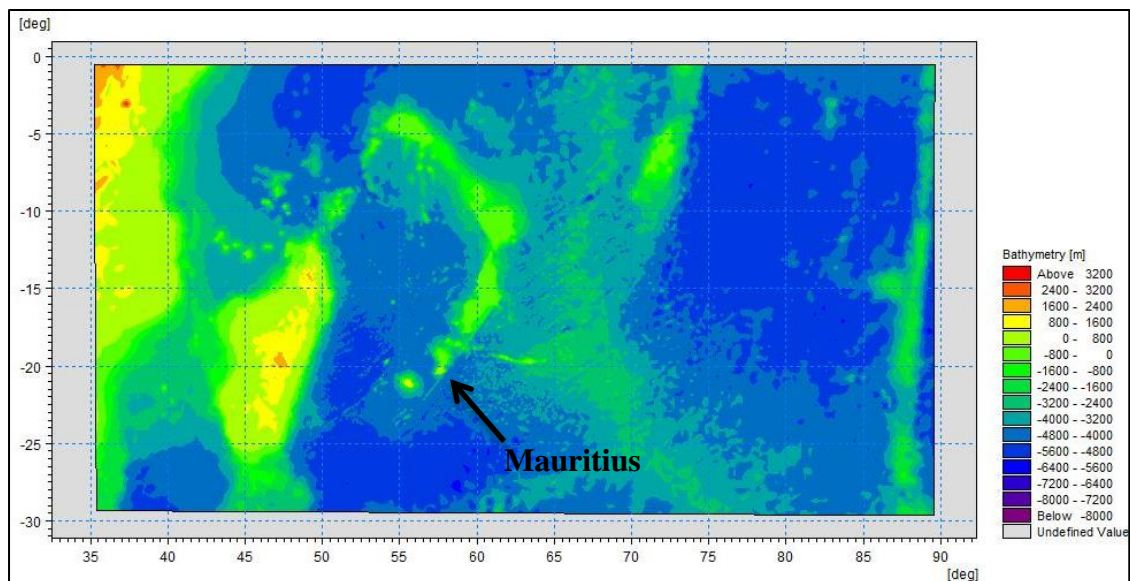


Figure 5-1: Map of study area showing the bathymetry

The extent of this domain is such that it covers a sufficiently large grid to allow for the generation and transformation of the offshore cyclone wind-wave. The bathymetry was obtained from the ‘General Bathymetric Chart of the Oceans’ [GEBCO, 2008] and is relatively coarse for nearshore application. The precision of the wave data is governed by the resolution of the bathymetry especially around the area of interest. Thus, due to the size of the domain, a coarse resolution of the mesh grid was applied at the outskirts of the domain and this was gradually refined, with the finest resolution around the Island of Mauritius.

The model grid has the following resolutions:

- Outermost area (Resolution 1): 0.1 deg^2
- 2nd outermost area (Resolution 2): 0.05 deg^2
- 3rd outermost area (Resolution 3): 0.01 deg^2
- Innermost area (Resolution 4): 0.005 deg^2

Figure 5-2 shows the different resolutions adopted based on the flexible mesh system.

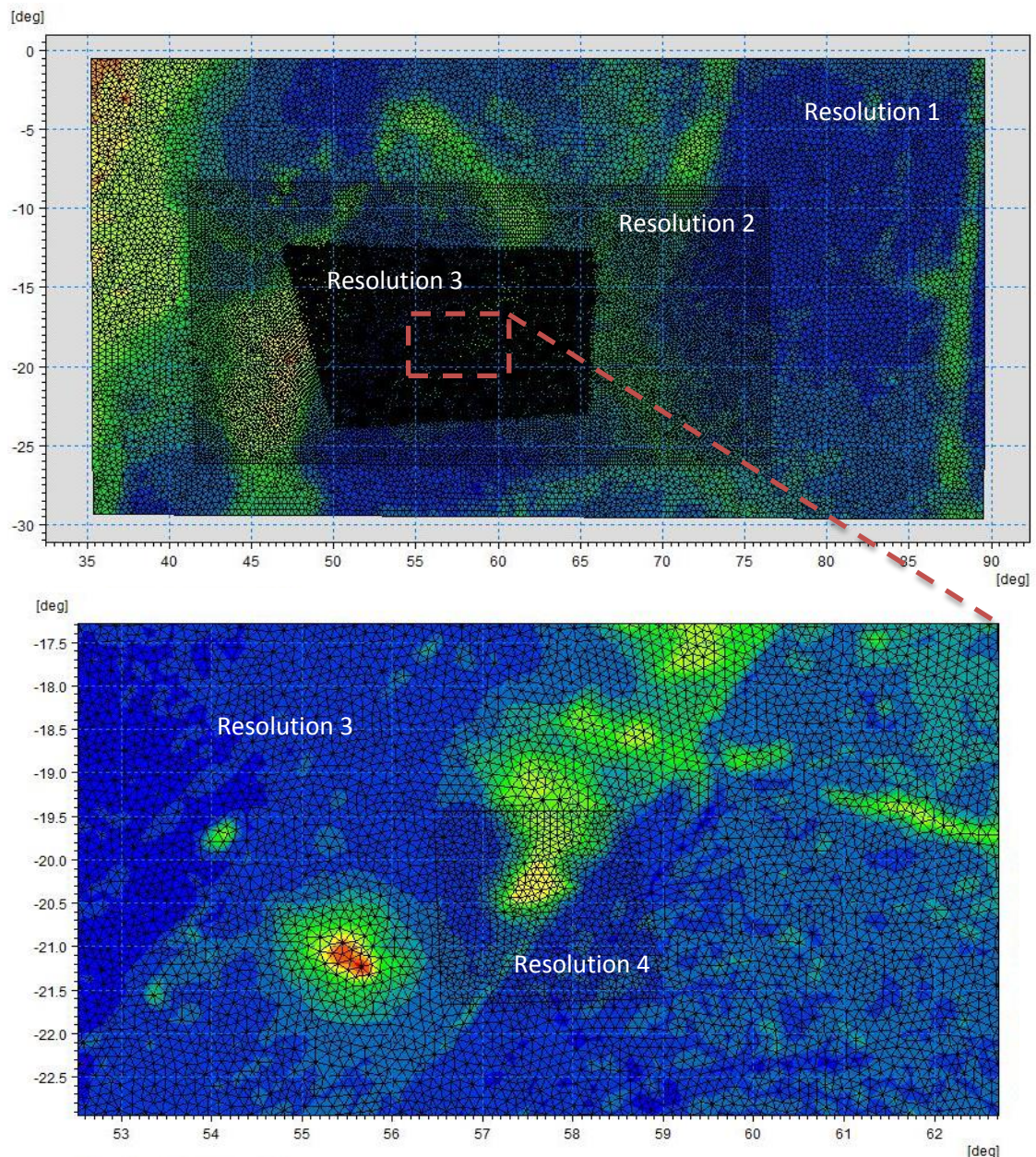


Figure 5-2: Model mesh grid showing different scales for the model domain. Fine grids are used around the Island of Mauritius.

5.1.2 MIKE 21 Cyclone Wind Generation

The Cyclone Wind Generation (refer to Section 2.10.1) was used to produce space and time varying wind and pressure fields resulting from cyclones. The ‘Young & Sobey’ parametric model was chosen to simulate the cyclonic forcings based on the readily available model set-up parameters which were obtained from the Australian Severe Weather (<http://www.australiasevereweather.com/cyclones/index.php>). These are as follows:

- Cyclone start time and time interval (in hours)
- Longitude and latitude of the cyclone centre for each time step (in degrees)
- Radius to maximum wind speed, R_{max} (in km)
- Maximum wind speed, V_{max} (in m/s)
- Central pressure, P_c (in hPa)
- Neutral pressure, P_n (in hPa)

The above data was used as set-up parameters to produce wind data, varying over time and domain. These outputs are imported into the MIKE 21 SW module for hindcast (calibration/validation) and forecast (prediction) modelling.

Appendix A contains the cyclone data extracted from the Australian Severe Weather between 1997 and 2011.

5.1.3 Spectral Wave (SW) module

The optimum values used for the model parameters are presented in Table 5-1.

Table 5-1: Spectral Wave (SW) input parameters used for wave simulations

No.	Model parameters	Component	Unit	Value
1.	Wind forcing (varying in time and space)	-	-	The output from MIKE 21 Cyclone Wind Generation was used.
2.	Spectral discretization parameters	Number of frequency	-	25
		Minimum frequency	Hz	0.04
		Frequency factor	-	1.1
		Number of directions	-	32

Table 5-1 continues

Table 5-1: Spectral Wave (SW) input parameters used for wave
 simulations (contd)

No.	Model parameters	Component	Unit	Value
3.	Solution technique	Minimum time step	sec	0.01
		Maximum time step	sec	30
4.	Wave breaking		-	0.5
5.	Bottom friction	Nikuradse roughness k_N	m	0.02
6.	White capping	C_{ds}	-	2.0
		σ	-	0.5
7.	Initial Conditions: the JONSWAP fetch growth expression was specified	Maximum fetch length	km	100
		Maximum peak frequency	Hz	0.4
		Maximum Philips constant	-	0.0081
		Shape parameter, σ_a	-	0.07
		Shape parameter, σ_b	-	0.09
		Peakness parameter	-	3.3
8.	Boundary conditions	-	-	A closed boundary condition was adopted with the assumption that no waves entered the model domain and that all outgoing waves were absorbed for the 1D model at Belle Mare.

5.1.4 Calibration and Validation

Hindcast models were simulated with the MIKE 21 SW module to reproduce past events and the results were compared with in-situ data as part of the calibration and validation processes. The nearshore in-situ data consisted of daily significant wave height, period and wave direction recorded by the wave-rider buoy at Blue-Bay.

5.1.4.1 Calibration

During the calibration process, various parameters were adjusted until an acceptable level of accuracy was obtained between the measured and hindcast wave data.

Cyclone Darius (2003) was used to calibrate the SW module and the following parameter values were selected:

- Wave breaking parameter, $\gamma = 0.5$
- Bottom friction, $K_N = 0.02m$
- Capping coefficient, $C_{dis} = 2.0$

The model predicted and observed significant wave heights at Blue Bay for cyclone Darius are shown in Figure 5-3. The maximum significant wave height occurred on 2 January 2004 in both cases. The predicted model significant wave height (red line) was found to be 4.15m high and 3.81m for the measured data (blue line). This represents a 9% difference which is a relatively good match except for the initial lag. This discrepancy in the early stage was eliminated when the NCEP global wind data was added to the SW model (green line) which indicates the presence of wind-wave forcing in addition to the cyclone induced winds. The NCEP data did not include the cyclone winds. The synoptic chart will determine whether a cyclone is the only weather system at that period. If not, wave data from other sources, such as NCEP, must be included.

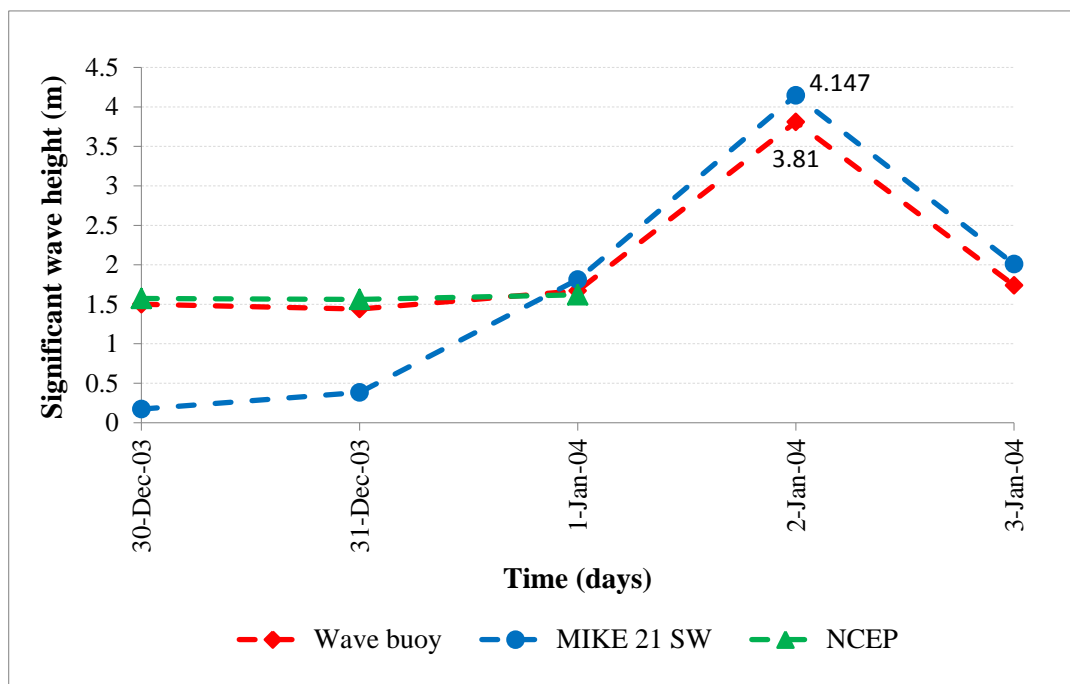


Figure 5-3: Measured and predicted significant wave heights for cyclone Darius (2003). Data points are joined by dotted lines for clarity.

Figure 5-4 shows the cyclone track of Darius which was obtained from the Australian Severe Weather website.



Figure 5-4: Cyclone Darius track (2003) from the Australian Severe Weather website.

5.1.4.2 Validation

The above optimum parameters were used for cyclone Hennie (2005) to validate the MIKE 21 SW model. Figure 5-5 shows a fairly good agreement between the predicted hindcast model and the observed significant wave heights at Blue Bay. The model slightly underestimated the peak in the significant wave height (by approximately 14%) but the overall trend was well correlated with the measured data. NCEP data was not required.

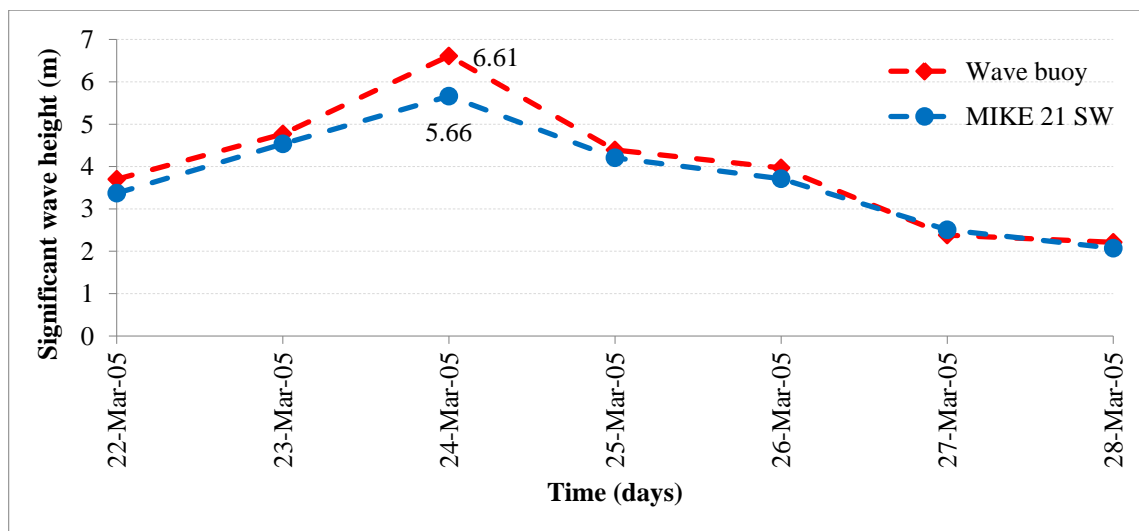


Figure 5-5: Measured and predicted significant wave heights for cyclone Hennie (2005). Data points are joined by dotted lines for clarity.

5.2 XBEACH: Application and Model Setup

5.2.1 Application

No calibration and/or validation were done for the XBEACH model due to the unavailability of surveyed beach profiles for both pre- and post-cyclone events as mentioned in Section 4.12. Therefore, the XBEACH model could not be used for hindcast modelling but was instead applied to predict the relative changes in sediment erosion for a tropical cyclone whose intensity was varied as a consequence of the predicted influence of climate change on tropical cyclones (refer to Sections 2.4 and 3.3.2). The sediment erosion was determined by analysing the bed level changes from the sediment transport gradient.

5.2.2 Model bathymetry

As mentioned in Section 4.7, Baird [2003] had conducted a survey of the beach profile at Belle Mare beach. This survey extends offshore by some 830m past the Low Water Mark. The location of the surveyed beach profile is shown in Figure 5-6.



Figure 5-6: Location of surveyed alignment along Belle Mare beach.
(Reproduced from Baird [2003])

Figure 5-7 shows the beach profile obtained from the survey which was digitized and imported into XBEACH. The beach slope is approximately 1 in 10.

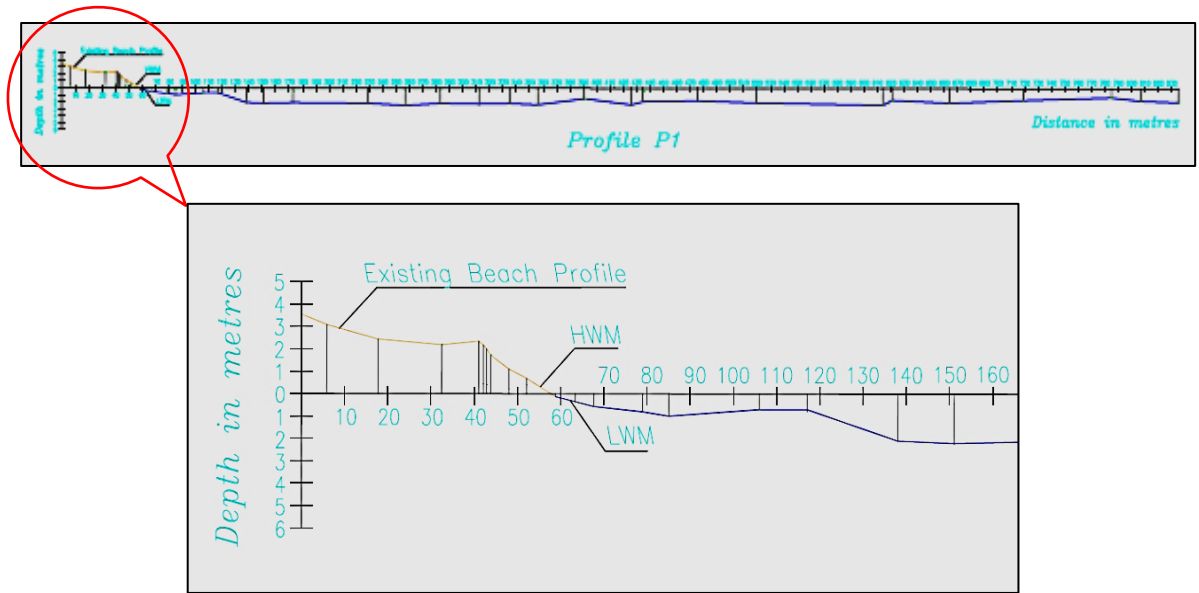


Figure 5-7: Beach Profile along Belle Mare beach shown in different scales.

(Reproduced from Baird, 2003)

5.2.3 Model setup

A 1D model was constructed using the digitized beach profile and it comprised a grid spacing 5m, 20m and 50m nearshore. Owing to the lack of field measurements, this dissertation is aimed at quantifying the relative coastal erosion with respect to the incremental intensification of a tropical cyclone. Several set-up parameters are required for the simulation; some parameters were obtained from the report by Baird [2003] whilst default values were used where data were not available. The values for these parameters are indicated in Table 5-2. The XBEACH set-up file for Scenario 1 for Belle Mare is shown in Appendix B.

Baird [2003] had analysed the grain size distribution at Belle Mare and generally described the sand as being well-graded with a median sediment size of approximately 1.75mm. A JONSWAP spectrum was used to represent the wave field. The recorded tide levels were included and the reefs were defined as a hard layer.

No coastal defence structure was modelled.

Table 5-2: XBEACH input parameters used for sediment transport

No.	Model parameters	Component	Unit	Value
1.	Near-shore bathymetry	Gridsize & depth	m	This data was extracted and digitized from Baird [2003]. Refer to Section 5.3.2.
2.	Time management	Start time of simulation	sec	0
		Time interval output	sec	100
		Stop time simulation	sec	198,000
3.	Action balance	-	-	The Lax Wendroff numerical scheme was chosen to minimize numerical dissipation
4.	Wave model dissipation	Option breaker model	-	2
		Breaker parameter	-	0.8
		Max H/d allowed	-	2
		Wave dissipation coefficient	-	1
		Fraction of wave height to add to water depth	-	0.3
		Bed friction factor (on wave action equation only)	-	0.05
5.	Roller model	Breaker slope coefficient	-	0.1
6.	Wave boundary conditions. The JONSWAP parametric spectrum was used and the relevant data was obtained from MIKE 21 SW output for each time step. A typical JONSWAP input file contains:	Significant wave height, H_{m0}	m	Varies with time
7.		Peak frequency of the wave spectrum, f_p	sec ⁻¹	Varies with time
8.		Main wave angle, $mainang$	°	Varies with time
9.		Peak enhancement factor in the JONSWAP expression, $gamma_{jswp}$	-	2.5
10.		Directional spreading coefficient	-	7
11.		Highest frequency used to create JONSWAP spectrum, f_{nyq}	-	1

Table 5-2 continues

Table 5.2: XBEACH input parameters used for sediment transport (contd)

No.	Model parameters	Component	Unit	Value
12.	Flow parameters	Chezy coefficient, C	-	55
		Eddy Diffusivity	-	0.1
13.	Flow boundary conditions parameters	Left and right lateral boundaries	-	Zero-gradient across boundary
		Seaward and bayside boundaries	-	Set as “1D absorbing-generating boundary” meaning all incoming and outgoing waves propagate normal to the boundary.
14.	Time varying tide levels			This information was obtained from the Mauritius Meteorological Services at the time of the cyclone under consideration, i.e. Davina
15.	Multiple sediment fractions and hard layers	Hard structures	-	The extent of the reefs was specified.
		Sediment diameter, D50	m	0.00175
		Sediment diameter, D90	m	0.003
16.	Morphology parameters	Morphological factor	-	1
		Critical avalanching slope under water (wetslp)	-	0.3
		Critical avalanching slope above water (dryslp)	-	1

5.3 Summary

In this chapter, the input parameters required by the MIKE 21 and XBEACH models were presented. The calibration and validation for MIKE 21 SW module proved to be acceptable when compared with the recorded wave data. Owing to the lack of readily available beach profiles in Mauritius (before and after storms) and hydraulic parameters, XBEACH was used to assess the relative sand erosion resulting from the various intensity scenarios due to the predicted impact of climate change on tropical cyclones. The results are presented in Chapter 6.

CHAPTER 6

RESULTS AND DISCUSSION

This chapter interprets, analyses and critically discusses the results produced by the MIKE 21 SW and XBEACH models for the beach erosion at Belle Mare beach in Mauritius. These results are also compared with the data produced by Baird [2003]. The possible shortcomings of the simulation outputs, in relation with the existing data, are also discussed.

6.1 Introduction

Four scenarios were modelled for cyclone Davina (1999) which are as follows:

1. Scenario 1: Cyclone Davina was modelled using the recorded pressure and wind data. This scenario was used as the baseline (CD) which was then increased incrementally for scenarios 2 to 4.
2. Scenario 2: CD + 5% increase
3. Scenario 3: CD + 10% increase
4. Scenario 4: CD + 15% increase

The results for Scenario 1 were compared with the information produced by Baird [2003]. Also, the results for scenarios 2 to 4 were evaluated quantitatively against the baseline (i.e. Scenario 1). The results for these morphological changes are presented in sections 6.2 and 6.3.

No coastal structures were analysed and therefore their effectiveness have not been assessed.

6.2 MIKE 21 SW

Each scenario was run in the MIKE 21 Cyclone Wind Generator for the duration of the cyclone Davina, i.e. from the 02 March 1999 to the 19 March 1999. This produced the wind/pressure fields which were used as driving forces in MIKE 21 SW. Figure 6-1 shows the wind-generated waves for tropical cyclone Davina, as generated by MIKE 21 SW, from time steps 30 (09 March 1999, 03:00am) to 33 (09 March 1999, 07:30pm). From this figure, it can be seen that cyclone Davina was closest to Mauritius on the 09 of March 1999. Similar results were obtained for scenarios 2 to 4.

Figure 6-2 shows a visual depiction of the overall trajectory for cyclone Davina which was extracted from the Australian Severe Weather and used in MIKE 21 Cyclone Wind Generator to produce the wind/pressure fields.

The significant wave height, the mean wave period and the mean wave direction were extracted for the entire inner grid (refer to Figure 5-2) surrounding Mauritius for each modelled scenario. The significant wave height extracted from MIKE 21 SW at latitude 20.09°S and longitude 57.47°E (outside the lagoon at Belle Mare) for each scenario is shown in Figure 6-3.

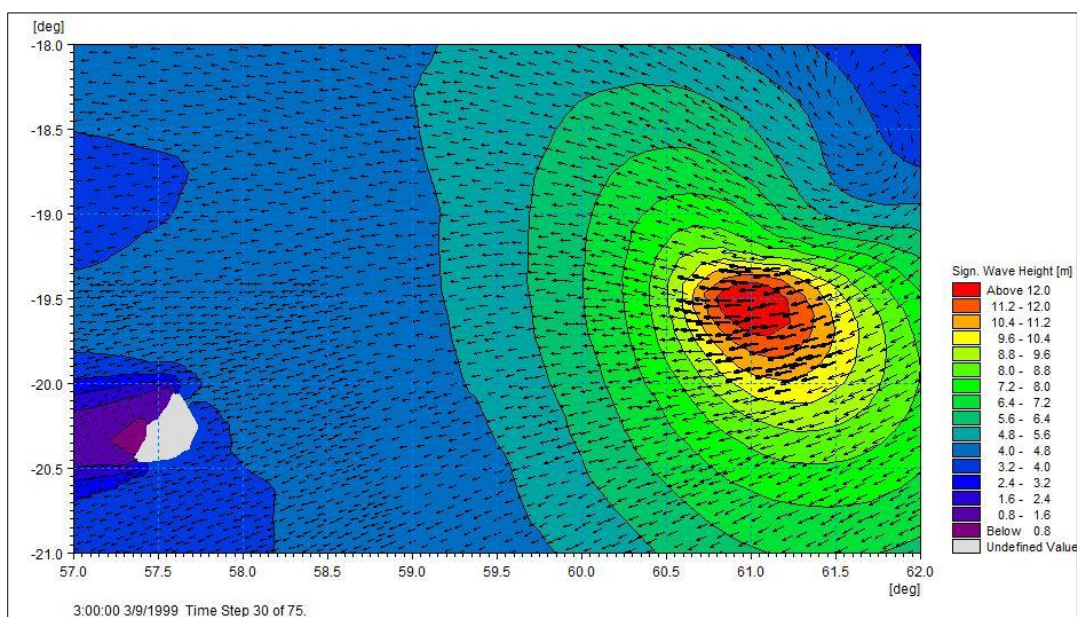


Figure 6-1(a): 09 Mar 99 at 03:00am (Time step 30 of 75).
The arrows show the wave vectors.

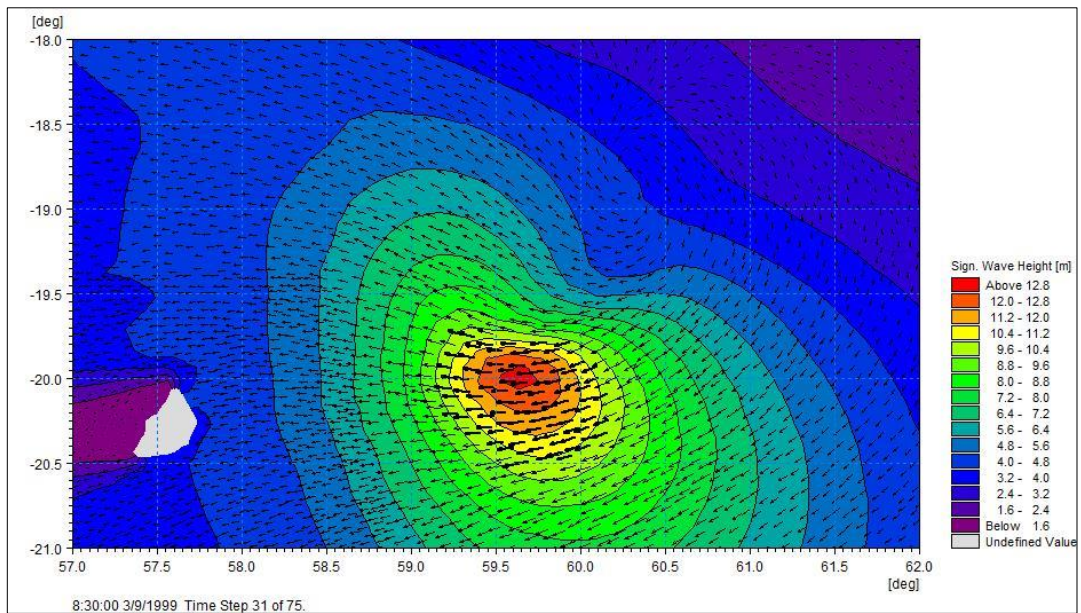


Figure 6-1(b): 09 Mar 99 at 08:30am (Time step 31 of 75)
The arrows show the wave vectors.

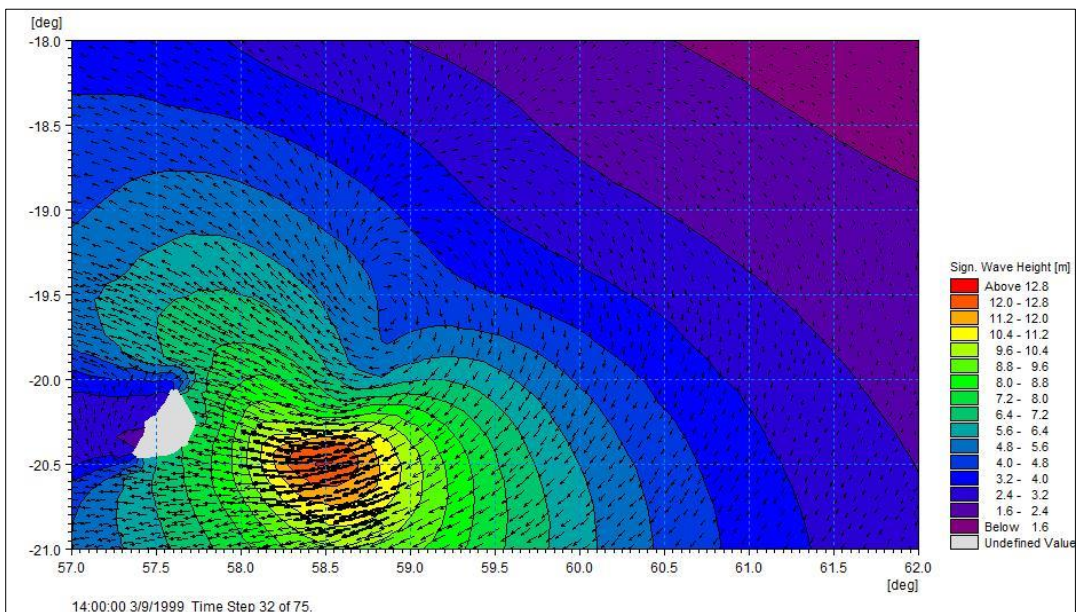


Figure 6-1(c): 09 Mar 99 at 02:00pm (Time step 32 of 75)
The arrows show the wave vectors.

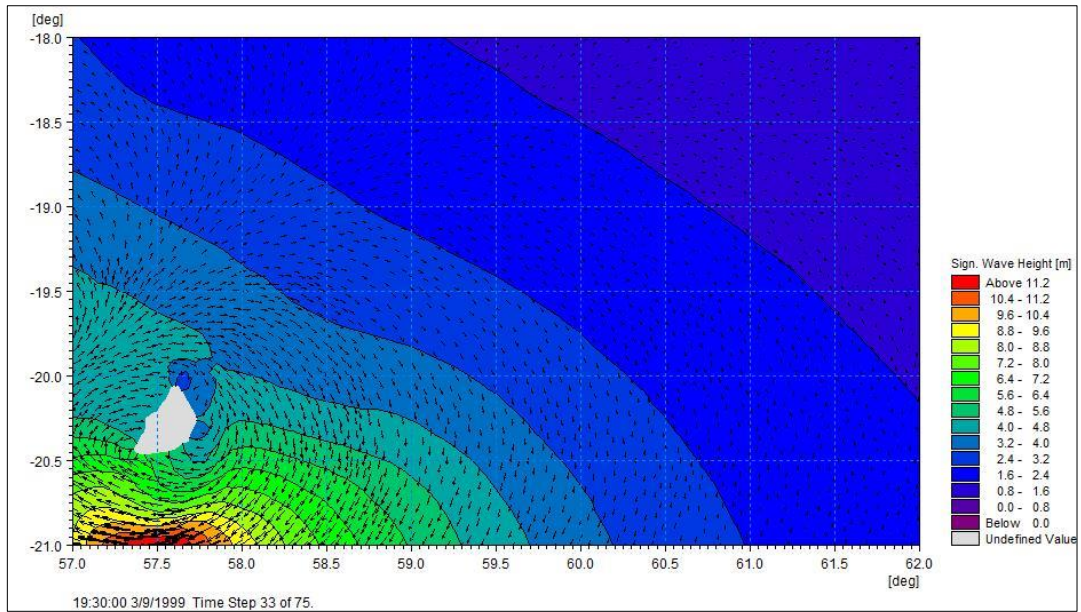


Figure 6-1(d): 09 Mar 99 at 07:30pm (Time step 33 of 75)

Figure 6-1 (a) to (d): Cyclone Davina (1999) trajectory on 09 March 2014 with Significant wave height for Scenario 1.

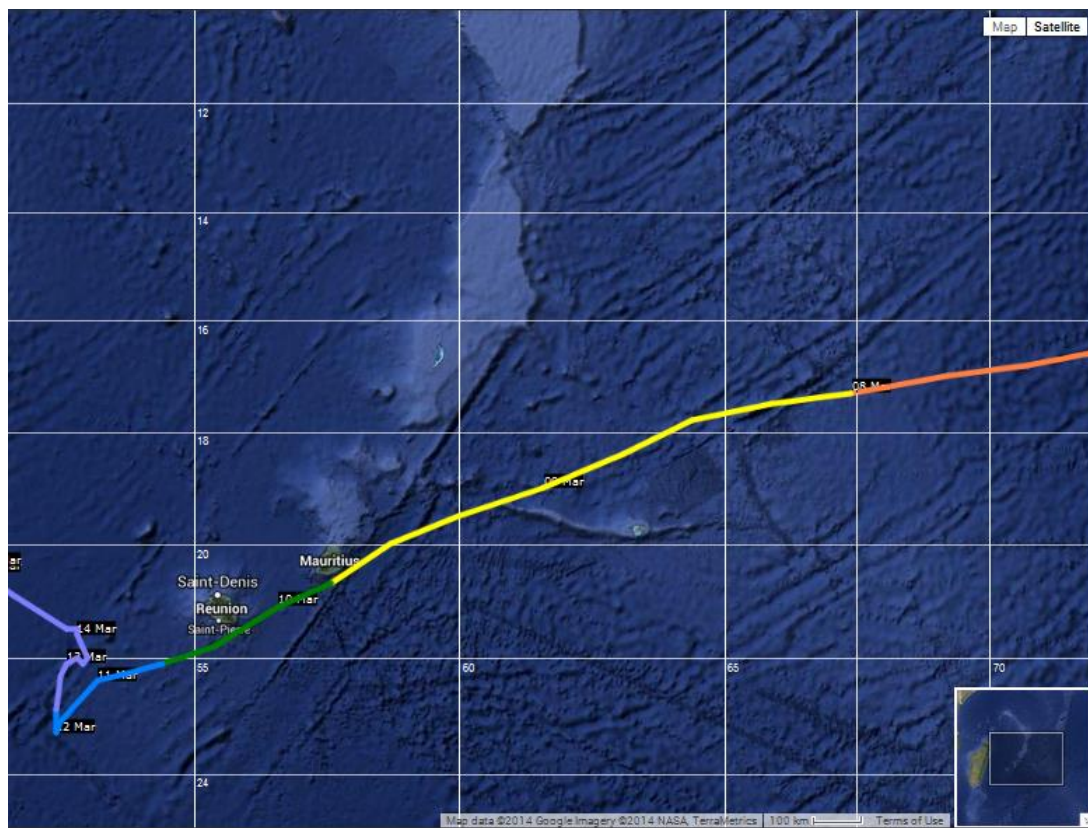


Figure 6-2: Trajectory of cyclone Davina (1999) from the Australian Severe Weather website

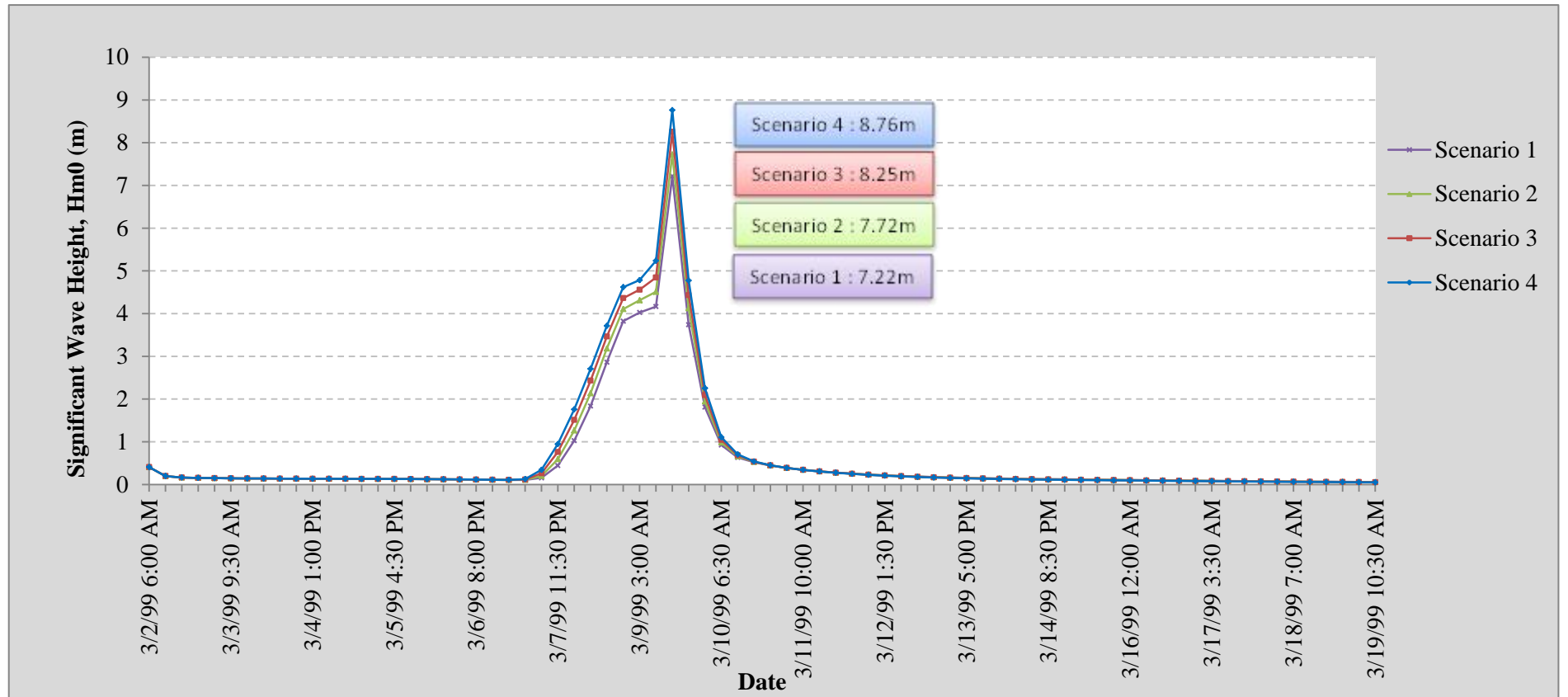


Figure 6-3: Significant wave heights for scenario 1 to 4 at latitude 20.09°S and longitude 57.47°E at Belle Mare for cyclone Davina (1999) using MIKE 21 SW (outside lagoon at depth of 56m).

The results for the significant wave height offshore (at depth 56m) show that the effects of cyclone Davina were mostly felt by Mauritius between the 07th and the 11th of March 1999. As suspected, an increase in the intensity of the cyclone yields an increase in the significant wave height. From the results, an incremental increase of 5%, 10% and 15% in the pressure and wind speed for the cyclone intensity corresponds to a wave height increase of 7%, 14% and 21% respectively. This means that for every 5% increase in the pressure and wind intensities, the wave height increases by $\pm 7\%$.

As expected, the wave rose diagrams, as shown in Figure 6-4, have a similar wave direction for each scenario, with varying significant wave height.

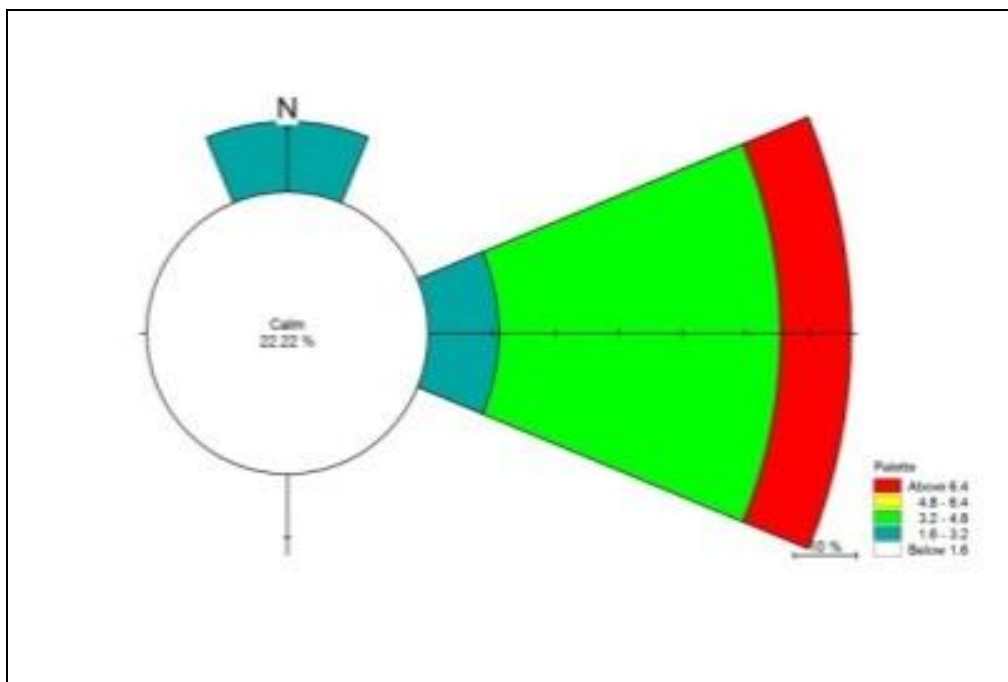


Figure 6-4 (a): Scenario 1 (in-situ condition)

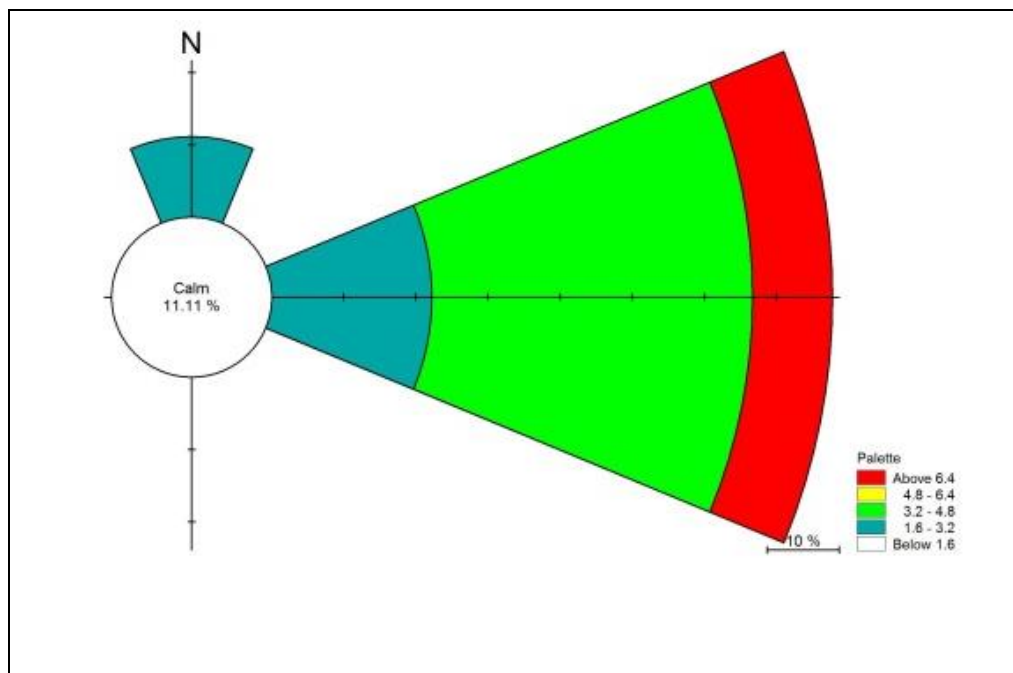


Figure 6-4 (b): Scenario 2 (+5% increase in intensity)

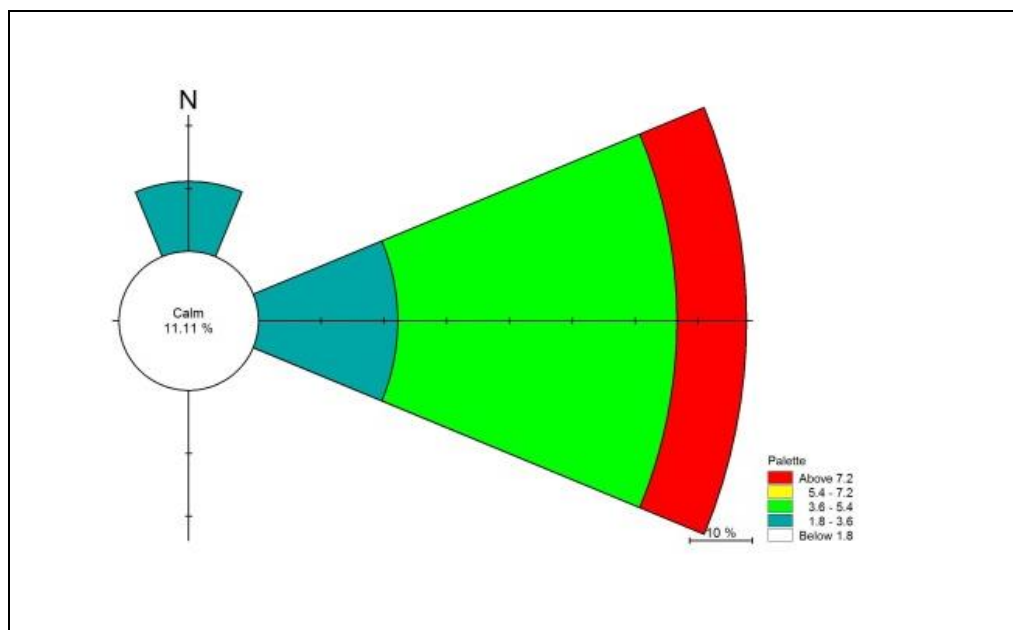


Figure 6-4 (c): Scenario 3 (+10% increase in intensity)

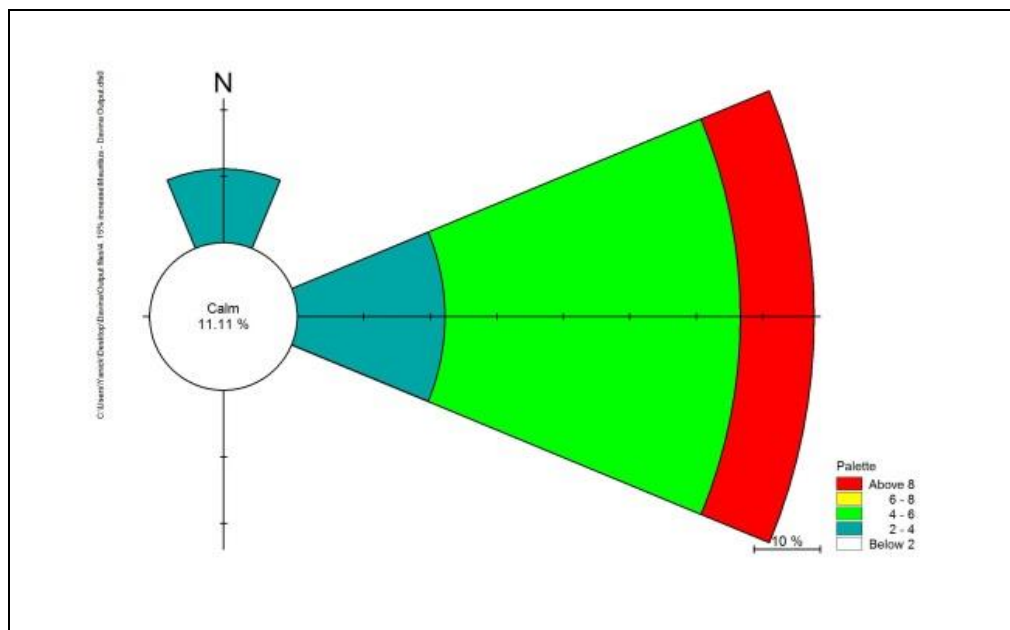


Figure 6-4 (d): Scenario 4 (+15% increase in intensity)

Figure 6-4 (a) to (d) : Wave rose diagrams for the cyclone wind fields (in metres) for scenario 1 to 4 for cyclone Davina (1999) at latitude 20.09°S and longitude 57.47°E (offshore of Belle Mare beach at a depth of 56m).

6.3 XBEACH

6.3.1 Predicted Erosion

XBEACH measures the sediment transport by interpreting the bed level changes over the domain. The surveyed beach profile extracted from Baird [2003], referred to as bed level, was used as datum in XBEACH to model each scenario. Figure 6-5 shows the comparison of the 1D XBEACH post-storm beach profiles at Belle Mare results and the bed level (dotted line) for the forecast scenarios.

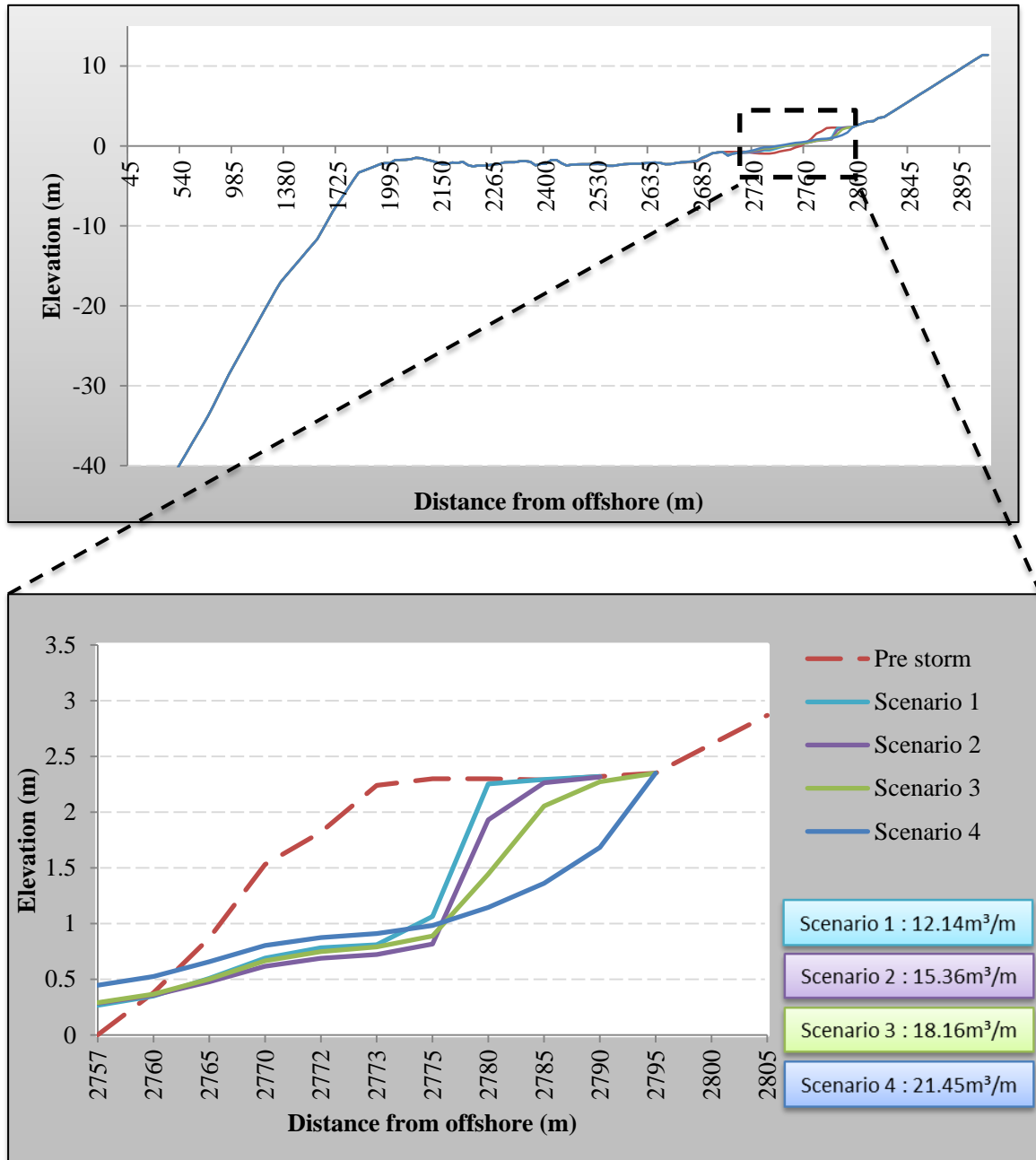


Figure 6-5: Measured beach profiles and surveyed bathymetry at Belle Mare before and after Cyclone Davina shown in different scales.

The XBEACH model predicted an erosion of 12.14m³/m for cyclone Davina (Scenario 1) at Belle Mare. Since no calibration and/or validation of the XBEACH model was possible, this result is compared with the output from COSMOS (refer to Section 4.11). In his report, Baird [2003] classified Davina as a cyclone with a return period of 5 years for which he predicted an erosion between 11.5m³/m to 17m³/m. The result from XBEACH compares relatively well with the prediction by Baird [2003], albeit it is in the lower spectrum of the range. A moderate level of confidence is gained for estimating the potential erosion due to the predicted intensification of a tropical cyclone, i.e. scenarios 2 to 4 for cyclone Davina. Table 6-1 shows that for every 5% increase in cyclone intensity, an expected $\pm 25\%$ increase in erosion is projected.

Table 6-1: XBEACH predicted erosion (m³/m) for scenarios 1 to 4 for cyclone Davina at Belle Mare beach.

Scenario	Description	Output Results			
		Hm0 (m) from MIKE 21 SW	% increase	Erosion (m ³ /m) from XBEACH	% increase
1	Cyclone Davina, CD	7.22	-	12.14	-
2	CD +5% intensity	7.72	$\pm 7\%$	15.36	$\pm 27\%$
3	CD +10% intensity	8.26	$\pm 14\%$	18.16	$\pm 50\%$
4	CD +15% intensity	8.76	$\pm 21\%$	21.45	$\pm 77\%$

Scenario 1 used as baseline

6.3.2 Wave energy dissipation

A key finding of this dissertation is the wave decay due to the shallow lagoon and the presence of reefs as the waves travel shoreward. A comparison between the offshore wave height (from MIKE 21) and the wave height inside the lagoon (from XBEACH) is presented in Table 6-2. The attenuation in the wave height appears to be in the order of 84%. Baird [2003] had found the percentage wave decay to be $\pm 90\%$ (refer to Section 4.9).

Table 6-2: Comparison between the significant wave heights offshore (MIKE 21) and inside the lagoon (XBEACH) for cyclone Davina.

Scenario	Description	Output Results			% attenuation
		MIKE 21 SW	XBEACH		
		*Hm0 (m) outside reef	Hrms (m) inside reef	**Hm0 (m) inside reef	
1	Cyclone Davina, CD	7.22	0.84	1.13	±84%
2	CD +5% intensity	7.72	0.97	1.30	±83%
3	CD +10% intensity	8.26	1.08	1.45	±82%
4	CD +15% intensity	8.76	1.15	1.56	±82%

* Refer to Figure 6-3 & ** Hm0 = 1.4xHrms

The results presented in Table 6-2 generally show an increasing wave height inside the lagoon associated with an increasing intensity. This increase inside the lagoon is much smaller compared with the wave outside the lagoon due to the depth limitation. Also, from the results, there seems to be a drop in the wave energy dissipation as the intensity of the cyclone increases (refer to percentage attenuation). Nonetheless, this finding confirms the fact that as waves propagate into shallower water they reach a point where the water depth cannot support the local wave height. In their experiments, Hardy et al. [1990] and Riedel et al. [1986] discovered that the depth limited wave height over a horizontal seabed and/or over reefs has a wave height to water depth ratio (H/d) of 0.55 in contrast with 0.78 as presented by the U.S. Army Corps of Engineers [2006].

Based on the average lagoon depth of 2.26m at Belle mare and the H/D ratio of 0.55, the limited wave height is ±1.24m. This finding further substantiates the reliability of XBEACH in modelling complex coastal mechanisms when compared with the wave heights produced by XBEACH inside the lagoon as shown in Table 6-2.

This wave decay, as a result of the shallow lagoon and the reefs, ultimately plays a significant role in mitigating the volume of sand eroded from the upper beach. It is therefore imperative that the reef around Mauritius be preserved. Figure 6-6 illustrates the wave decay for Scenario 1 to 4. The effect of sea level change was not modelled and this may affect the beach erosion significantly.

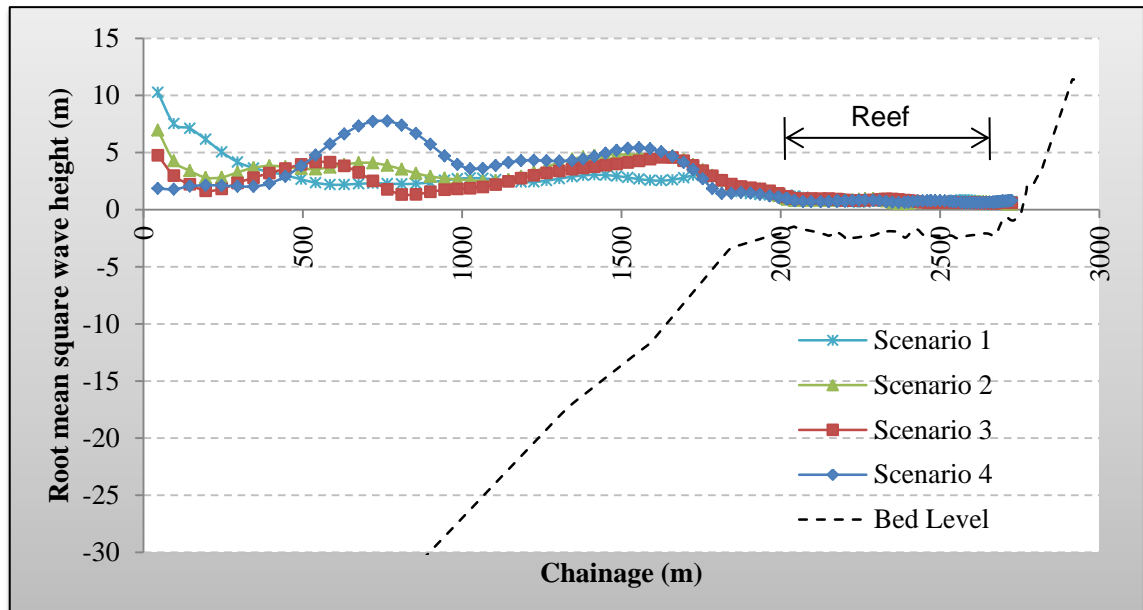


Figure 6-6: XBEACH wave decay for cyclone Davina at time step “0000-01-01 03:00:00” at Belle Mare.

The storm surge associated with Scenario 1 was found to be 0.17m which is $\pm 6\%$ more than the predicted value by Baird [2003]. The surge increased to 0.31m for Scenario 4. This increase in surge height associated with an increasing storm intensity correlates well with the wave theory. The wave run-up, which is associated with erosion, increased incrementally from scenario 1 to 4. Indeed, the waves travelled further up the shoreline with an increase in the intensity of the storm, and hence removing more material and redistributing it to the foreshore and nearshore. Table 6-3 shows the run-up values extracted from XBEACH. Figure 6-7 shows the illustrations of the wave run-up for Scenarios 1 to 4.

Table 6-3: XBEACH output results for surge (m) and wave run-up (m) for cyclone Davina.

Scenario	Description	XBEACH Output Results		
		Hm0 (m) inside reef	Surge (m)	Run-up (m)
1	Cyclone Davina, CD	1.13	0.17	1.58
2	CD +5% intensity	1.30	0.21	1.75
3	CD +10% intensity	1.45	0.29	1.92
4	CD +15% intensity	1.56	0.31	2.05

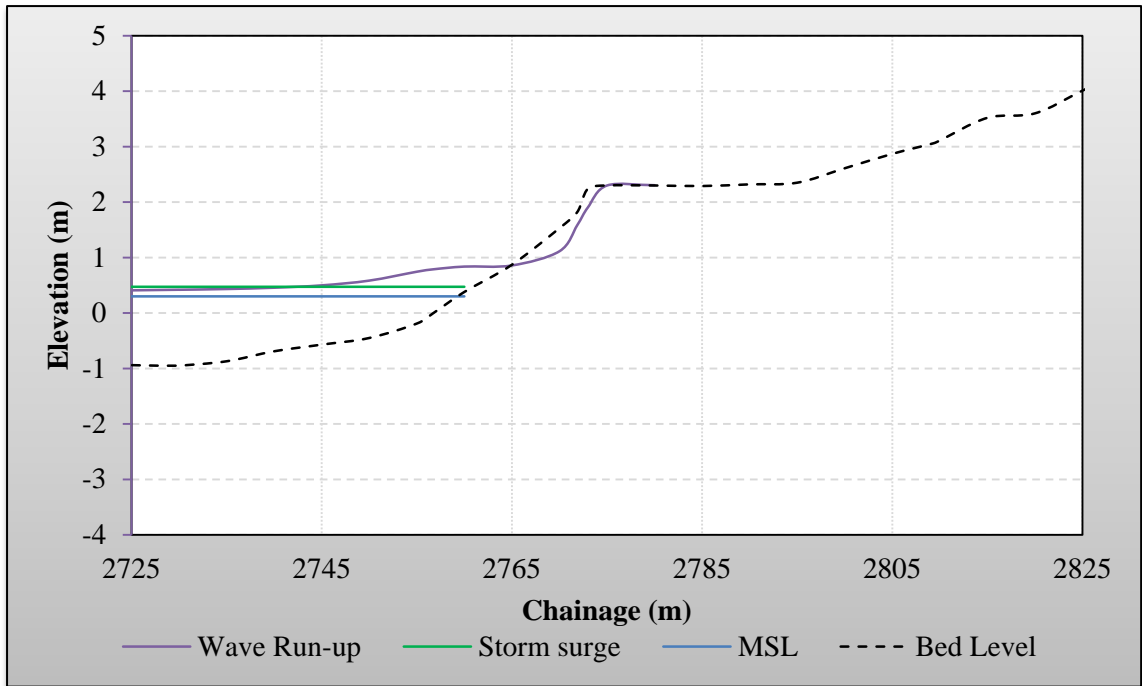


Figure 6-7(a): Scenario 1 :- Wave Run-up: 1.58m, Storm surge: 0.17m, MSL: 0.3m

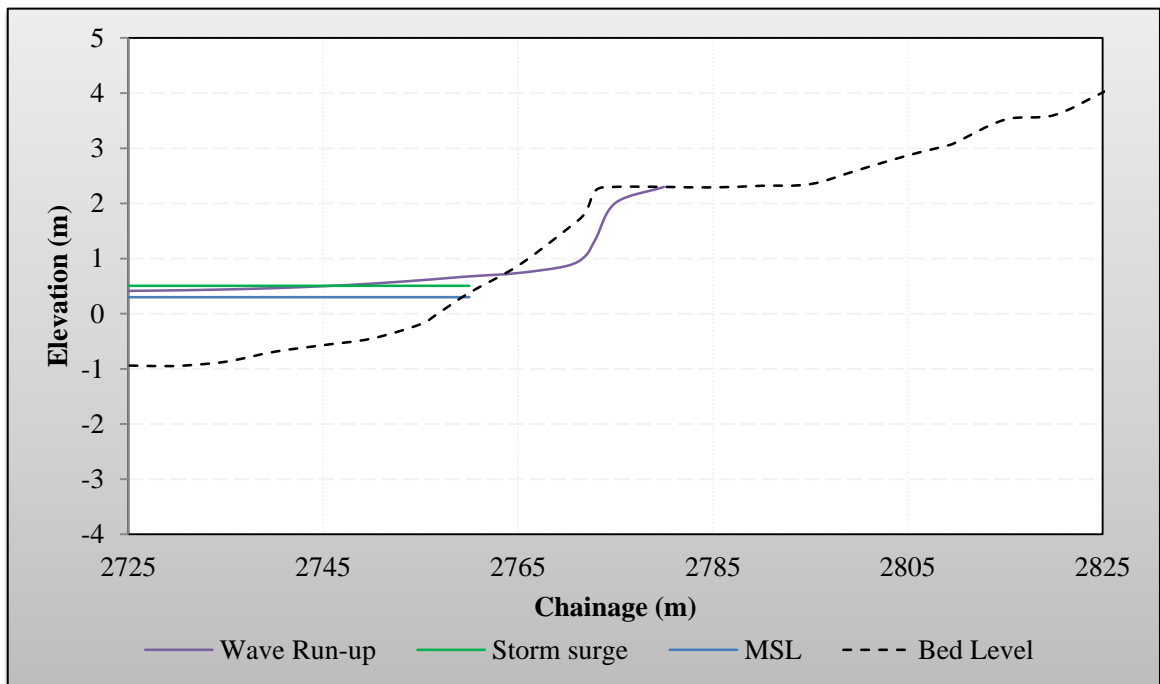


Figure 6-7(b): Scenario 2 :- Wave Run-up: 1.75m, Storm surge: 0.21m, MSL: 0.3m

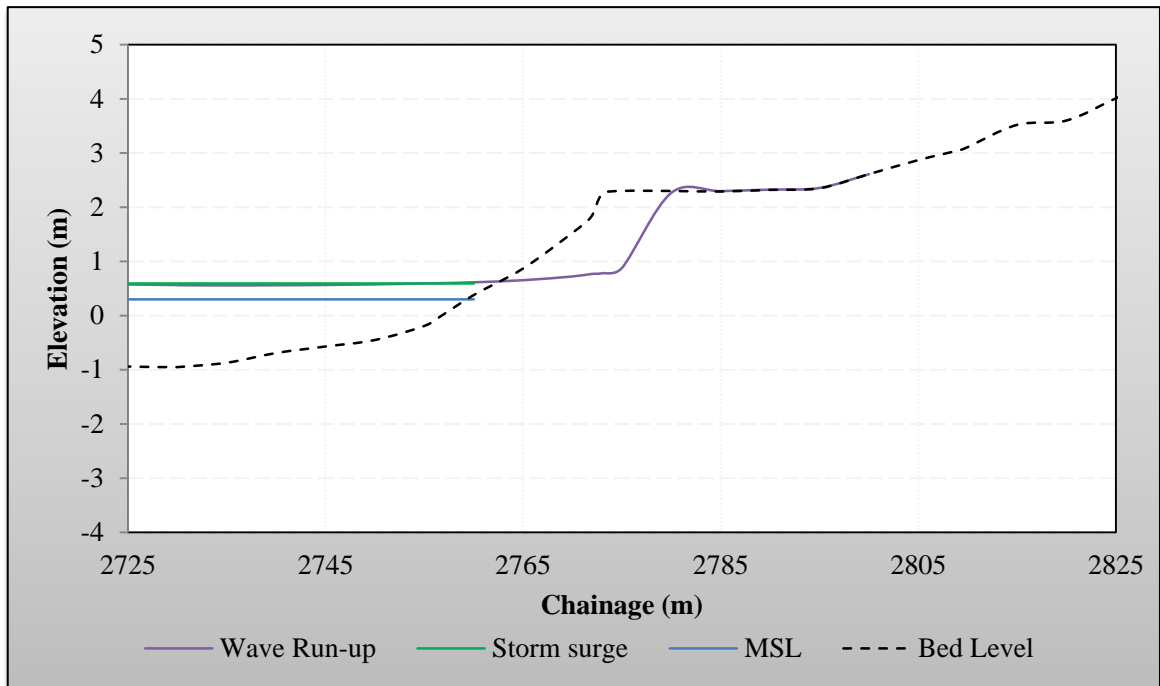


Figure 6-7(c): Scenario 3 :- Wave Run-up: 1.92m, Storm surge: 0.29m, MSL: 0.3m

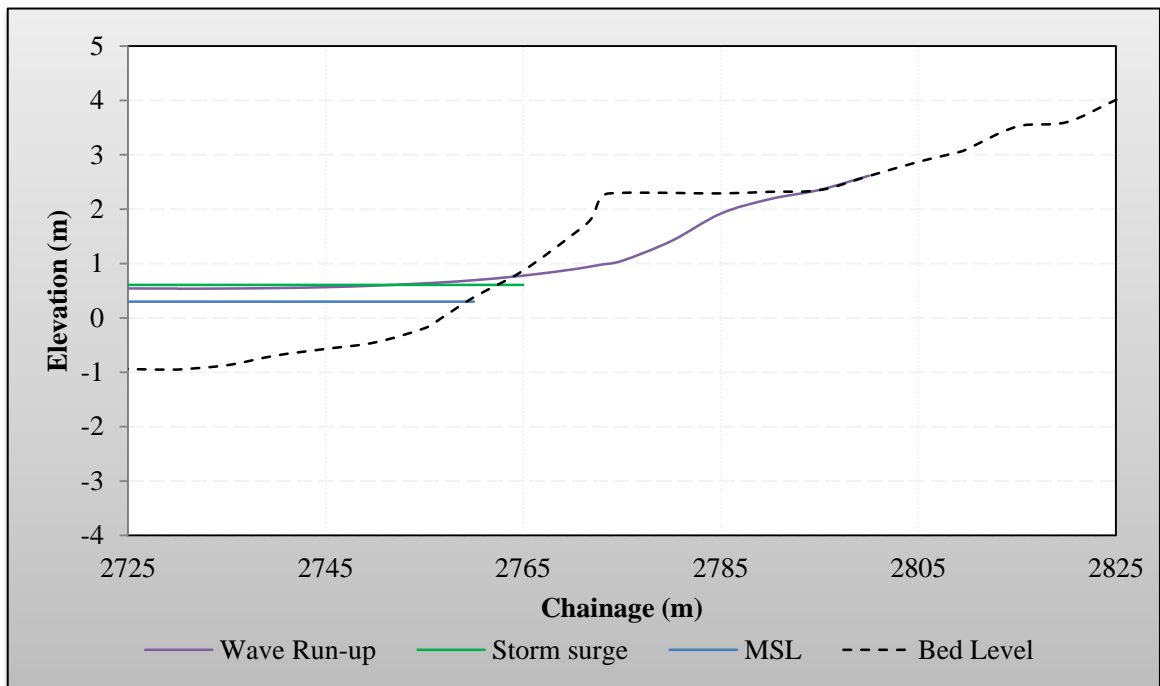


Figure 6-7(d): Scenario 4 :- Wave Run-up: 2.05m, Storm surge: 0.31m, MSL: 0.3m

Figure 6-7 (a to d): Wave run-up and extent of erosion for Scenarios 1 to 4 from XBEACH for cyclone Davina at Belle Mare.

6.4 Discussion of results

Four scenarios have been set up to assess the coastal vulnerability at a case study site in response to the predicted influence of climate change on tropical cyclones. The results from MIKE 21 SW showed that a significant wave height (H_{m0}) of 7.22m (Scenario 1) for offshore wave is obtained for a cyclone with a return period of ± 5 years. This represents a percentage variance of some 39% when compared with the results from Baird [2003] who reported an offshore significant wave height of 11.90m for a similar cyclone (refer to Table 4-1). However, during the calibration and validation process, the results produced by MIKE 21 SW for H_{m0} showed a maximum percentage variance of $\pm 14\%$ in comparison with the recorded data (see Section 5.1.4). This gives a high level of confidence for the use and adequacy of this model in assessing the coastal vulnerability.

The first scenario, which was based on the historical data for tropical cyclone Davina, formed the baseline of this dissertation. Scenario 1 was increased incrementally by 5%, 10% and 15% based on the predicted effect of climate change on tropical cyclone. The corresponding changes in the offshore H_{m0} were found to increase by 7%, 14% and 21% respectively. This meant that every increase of 5% in intensity yielded an increase of $\pm 7\%$ in the wave height. Figure 6-8 shows that a linear relationship between the cyclone intensity and the associated H_{m0} exists.

As the storm waves approach the shoreline, various types of wave transformation occur as a result of the shallow water which invariably affects the coastal morphology. This bed level change and sediment transport were assessed using XBEACH. XBEACH requires numerous input parameters to perform the simulations. For this study, no calibration and/or validation of the XBEACH model were done due to the unavailability of beach profiles before and after a storm. XBEACH was instead used to assess the relative sediment erosion due to the intensification of a tropical cyclone. A linear relationship was observed between the volume of eroded sediment and the cyclone intensity and this is also shown in Figure 6-8. This linear relationship followed a much steeper gradient compared with the relationship between the H_{m0} and cyclone intensity. This implies that a small increase in the wave height can have a significant impact on the erosion of the coast.

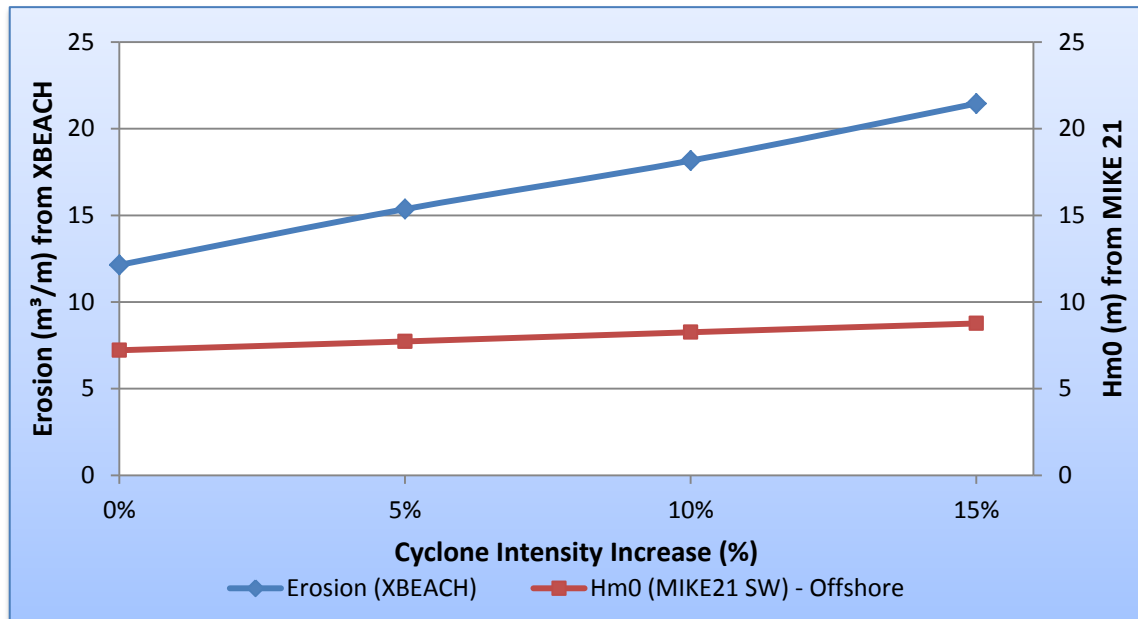


Figure 6-8: Relation between erosion (m³/m) and Hm0 (m) for various cyclone intensities (%) for cyclone Davina.

The model result for Scenario 1 indicated that XBEACH produces predictions that are consistent with the results from Baird [2003]. Scenario 1 produced an erosion of 12.14m³/m for cyclone Davina at Belle Mare whilst Baird [2003] predicted an erosion ranging between 11.5m³/m and 17m³/m (refer to Table 4-3) for a similar cyclone. The XBEACH results are towards the lower end of Baird's estimates, which may imply that XBEACH underestimates the erosion process. It can also be argued that the findings by Baird [2003] may have been an overestimation, since the Hm0 obtained during the calibration of MIKE 21 was similar to the measured wave height. A conclusive outcome to this issue requires additional measured data.

The results from MIKE 21 (offshore) and XBEACH (inside the lagoon) showed that there is a definite attenuation in the wave height as the waves travels over the shallow water of the fringing reef for all four scenarios. The decay in the wave height was found to be as high as 85% and this compared well with the 90% wave attenuation reported by Baird [2003]. A maximum wave height of ±1.75m can be expected inside the lagoon if an H/D of 0.78 is used as a breaking criterion in the model. Also, the storm surge and wave run-up were seen to increase with an increase in the intensity of the storm. This is a key finding which will enable coastal planners in designing adequate mitigating measures.

In general, the results produced by MIKE 21 and XBEACH were in agreement with the WAVAD and COSMOS models adopted by Baird [2003] and reaffirm the impact of a cyclone with a 5-year return period, such as Davina, on the coastline of Mauritius.

CHAPTER 7

SHORELINE DEFENCE

When assessing the coastal vulnerability and/or maintenance, a coastal management plan must consider all the processes that affect the coastline, and not only isolated events. The impacts of cyclones on the East coast of Mauritius are not as detrimental as the impacts caused by the continuous actions of the SE Trade Winds and the Southern sea swells [Baird, 2003]. Therefore, a holistic approach is required for the implementation of a suitable coastal protection measure which would also mitigate the effect a short-term event such as a tropical cyclone.

However, this chapter assesses the need and the merits for a suitable coastal defence to control the amount of erosion predicted at Belle Mare due to storms only, based on a theoretical approach. As mentioned in Section 2.11, no coastal protection structure was modelled as part of this dissertation. The report by Baird [2003] indicated that limited engineering analyses were done by the Government of Mauritius prior to the implementation of the existing coastal protection structures around Mauritius.

7.1 Assessment of various coastal defences for Belle Mare

The reef at Belle Mare, which extends some 900m with the average water depth of approximately 2.26m, is a typical representation of the coastal characteristics surrounding Mauritius (i.e. reef-lagoon-beach systems) and this contributes considerably to the energy dissipation of the storm waves. As a result, the beach at Belle Mare is moderately affected by the actions of the tropical cyclones. Baird [2003] stated that the recent erosion scarping at Belle Mare is due to severe tropical cyclones several decades ago. There is no existing protection measure at Belle Mare. XBEACH predicted a wave run-up of 2.05m for a 15% increase in intensity for a cyclone with a 5-year return period. Belle Mare beach has a slope of 10% which implies that a beach flooding of $\pm 20\text{m}$ is expected.

7.1.1 Alternative 1: “Do-Nothing”

The impacts of tropical cyclones on Belle Mare beach are said to be reversible [Baird, 2003]. The general wave climate driven by the SE Trade Winds helps with the natural replacement of the eroded sand. No development has taken place in the coastal zone and hence, there is no need for the protection of any foundation. Therefore, Belle Mare beach can be classified as stable.

7.1.2 Alternative 2: Vegetated dunes

Baird [2003] stated that the scarping of the beach was due to a severe tropical cyclone some 20 years ago. This can be mitigated by the construction of a vegetated dune using native coastal vegetation. The dune would lessen the wave run-up during severe storm conditions whilst the vegetation will stabilize the dunes.

7.1.3 Alternative 3: GSCs with vegetated dunes

The steep scarping observed along the top of the shoreline indicates that Belle Mare beach is subject to significant flooding. The construction of vegetated dunes only may result in the repeated erosion of the sediments during severe cyclones, especially if the vegetation is not well maintained. Therefore, the implementation of GSCs should be considered as these are less susceptible of being displaced due to their robustness. These can then be covered in sand and vegetation to give an aesthetical appearance. GSCs are very practical and flexible measures as minimal maintenance is required and can be easily cut opened if found unsuitable.

7.1.4 Alternative 4: Beach nourishment

Beach nourishment can be used as a reactive or proactive measure in the case of erosion. Beach nourishment acts as a wave energy absorber and also increases the beach width. The volume of sand required to replenish the eroded beach due to cyclones may be small compared to the annual loss of sediment as a result of the SE Trade Winds along the east coast of Mauritius. Beach nourishment is not a popular practise in Mauritius and is regarded as an expensive process. However, this has been adopted by various hotels for obvious commercial benefits instead of relying on the natural recovery process which may take a long time.

7.1.5 Alternative 5: Hard measures

The provision of “hard” measures such as revetments and/or seawalls must only be considered when all “soft” measures have proven unsuccessful in mitigating erosion. Belle Mare beach, as well as other popular beaches in Mauritius, rely on its pristine and attractive sandy coasts for recreational activities by local residents and the tourism industry. Where “hard” measures are necessitated, these must be assessed as being environmentally, socially, aesthetically, economically and financially acceptable. The status of Belle Mare beach is not considered critical for the implementation of structural protection measures.

7.2 Selection of coastal defence alternative

Belle Mare is well protected from the impact of tropical cyclone by its reef-lagoon-beach system. XBEACH showed that a major transformation of the storm waves as these travelled over the reefs. For Scenario 4 (i.e. 15% increase in the intensity of a tropical cyclone having a 5-year return period), XBEACH predicted an erosion of 21.45m³/m and a wave run-up of 2.05m. Although these values are significant, Baird [2003] reported that the beach recovery can be achieved through natural process. Also, Belle Mare relies on its pristine beach for a prosperous socio-economic development. Considering the above, a “hard” measure is not advisable for mitigating the erosion resulting from tropical cyclones. The implementation of vegetated dunes is more suitable for Belle Mare beach as very little capital and/or knowledge is required. GSCs can be used with vegetated dunes to offer a more robust countermeasure if repeated erosion occurs. Due to the lack of local expertise and capital investment, beach nourishment can be looked at as a last resort. It is imperative that an integrated coastal management plan be commissioned to address any development and/or maintenance in the coastal zone and severe cases can be treated individually.

CHAPTER 8

CONCLUSION

The purpose of the research was to investigate the vulnerability of Mauritius to the effect of climate change on tropical cyclones and to recommend an appropriate mitigation strategy for coastal defence. A literature review was conducted on the parameters that affect the formation of cyclones (cyclo-genesis) and the predicted effect of climate change on cyclo-genesis. It was discovered that the impacts of climate change on cyclo-genesis is still a subject of controversies which is mainly attributable to the lack of reliable data on cyclones. Nevertheless, the general agreement between the researchers suggests that a global increase in the intensity of tropical cyclones is expected as a result of climate change. Based on the various predicted rate of increase, a sensitivity of the beach erosion for four (4) scenarios, at a selected location, was set up.

These models enable the user to estimate the amount of erosion that can be expected from tropical cyclones. However, if the models under or over-estimates the erosion by a considerably large amount, then the implementation of the adopted coastal defence will be inefficient.

As part of the dissertation, a case study, namely Belle Mare beach in Mauritius, was investigated. However, numerous obstacles were encountered to accurately predict the rate of erosion. Obstacles in the form of lack of information for the parameters which are essential in accurately estimating the erosion must be eliminated. These include the historical cyclone wave record, regular survey of beach profiles, bathymetry data, wave transformation over the reefs, the characteristic of the sediments, etc. around Mauritius. This can influence the research outcome significantly; hence the selection of an average value for such parameters was adopted, derived from previous similar studies. Other parameters were confirmed through the calibration and validation of the models when compared with the historic wave data, as in the case of MIKE 21 SW.

The case study revealed that the rate of erosion predicted by the XBEACH model for cyclone Davina (Scenario 1) was well within the range which was predicted by a previous study and this provided a high level of confidence in the suitability of XBEACH for this dissertation. The simulations that were performed for the incremental increases by 5% (Scenario 2), 10% (Scenario 3) and 15% (Scenario 4) in the intensity of cyclone Davina at Belle Mare beach revealed a linear increase of 7% in the rate of erosion for each incremental increase. A vital finding during the cyclone wave modelling was wave decay by 80% observed across the reef at

Belle Mare. This was confirmed by the theoretical formula for the depth limiting wave height for an H/d of 0.55. This indicated that the reef around Mauritius plays an important role in the energy dissipation of the storm waves and therefore it is imperative that these be preserved.

Various coastal protection defence measures were assessed for Belle Mare and the implementation of vegetated dune was recommended. The performance of these vegetated dunes must be monitored regular. In the event these dunes are vulnerable to frequent erosion, GSCs were identified as the next suitable protection measure. Both of these “soft” measures do not affect the socio-economic activities that Belle Mare beach offer.

To summarize, it can be said that the models seem to produce plausible results despite the lack of pertinent parameters. To predict the coastal erosion with a higher degree of confidence and to implement a suitable mitigating measure, it is crucial to reduce the uncertainty of the data. In addition, a proper coastal management plan is required to address the coastal vulnerability in a holistic manner.

The impacts of tropical cyclones on the environment and its socio-economic influences were highlighted. Mitigating shoreline defences were presented which consisted of the “soft” and “hard” protection measures. Hard protection measures involved the construction of man-made structures whilst soft protection measures required the implementation of natural materials. However, the adequacy of an appropriate mitigating defence measure requires a detailed analysis of the coastal wave transformations and processes to predict the impacts of tropical cyclones on the shoreline. Therefore, the literature review identified the models that were used for predicting the wave transformations and sediment transport namely MIKE 21 and XBEACH.

There is still room for improvement for the Ministry of Environment (Republic of Mauritius), in order to achieve a better representation in the modelling of coastal processes.

8.1 Recommendations for future work

The following suggestions are proposed to improve the data and the prediction of models:

- Frequent survey of beach profiles should be conducted to quantify the erosion caused by tropical cyclone.
- The availability of extended cyclone wave data by deploying more wave recording buoys. These are essential data needed by models to accurately predict the erosion from tropical cyclone for the design of suitable protection measure.
- Measure storm surge, beach retreat, wave run-up during cyclonic activities.
- Measurement of the shore characteristics required by the models i.e. grain size, bed friction, etc.
- Promote natural protection measures. Where existing coastal structures are present, their efficiencies must be assessed through modelling.
- Preservation of the endangered reef by restricting nautical activities where the reefs are most damaged and the treatment of effluent before being discharged in the sea.

CHAPTER 9

REFERENCES

Akperov, M. G. Mokhov, I. I. 2013. “Estimates of the sensitivity of cyclonic activity in the troposphere of extratropical latitudes to changes in the temperature regime”. *Atmospheric and Oceanic Physics*, **49**, No. 2, 113 – 120.

ASCLME, 2012. National Marine Ecosystem Diagnostic Analysis. Contribution to the Agulhas and Somali Current Large Marine Ecosystems Project (supported by UNDP with GEF Grant financing).

Baird, 2003. Baird & Associates Coastal Engineers Ltd, in association with Reef Watch Consultancy Ltd. “Mauritius: Study on coastal erosion in Mauritius. Final Technical Report, No. ENV/RM/5/1/1, 2003”. Available from the Ministry of Environment, Republic of Mauritius.

Bengtsson, L. Hodges, K. I. Roeckner, E. 2005. “Storm tracks and climate change”. *Journal of Climate*, **19**, 3518 – 3543.

Bengtsson, L. Botzet, M. Esch, M. 1996. “Will greenhouse gas-induced warming over the next 50 years lead to higher frequency and greater intensity of hurricanes?”. *Tellus* 48A, 57 – 73.

Bengtsson, L. Hodges, K. I. Esch, M. Keenlyside, N. Kornbluh, L. Luo, J-J. Yamagata, T. 2007. “How may tropical cyclones change in a warmer climate?”. *Tellus*, 59A, 539 – 561, doi: 10.1111/j.1600-0870.2007.00251x.

Bosboom, J. Stive, J.F.M. 2012. “Coastal Dynamics 1, Lecture notes, CIE4305”. Delft University of Technology.

Caron, L-P. Jones, C.G. 2007. “Analysing present, past and future tropical cyclones activity as inferred from an ensemble of Coupled Global Climate Models”. *Tellus*, 60A, 80 – 96, doi: 10.1111/j.1600-0870.2007.00291.x.

Corbella, S. Stretch, D. D. 2012a. “Predicting coastal erosion trends using non-stationary statistics and process-based models”. *Coastal Engineering*, **70**, 40 – 49, doi:10.1016/j.coastaleng.2012.06.004

Corbella, S. Stretch, D. D. 2012b. “Coastal defences on the KwaZulu-Natal coast of South Africa: a review with particular reference to geotextiles”. *Journal of the South African institution of Civil Engineering*, **54**, (2), 55 – 64

Corbella, S. Stretch, D. D. 2012c. “Geotextile sand filled containers as coastal defence: South African experience, Geotextiles and Geomembranes”, 35, 120 - 130, doi:10.1016/j.geotextmem.2012.09.004.

DeMaria, M. Kaplan, J. 1993. “Sea surface temperature and the maximum intensity of Atlantic tropical cyclones”. *Journal of Climate*, **7**, 1324 – 1334.

Elsner, J. B. Jagger, T. H. 2009. “Hurricanes and climate change (aegean Conferences)”. Published by Springer, ISBN: 10:0387094091.

Emanuel, K. A. 1987. “The dependence of hurricane intensity on climate”. *Nature*, 326, 483 – 485.

Emanuel, K. 2005. “Increasing destructiveness of tropical cyclones over the past 30 years”. *Nature*, **436**, doi: 10.1038/nature03906.

Emanuel, K. 2006. “Climate and tropical cyclone activity: Anew model downscaling approach”. *Journal of Climate*, **19**, 4797 – 4802, doi: 10.1175/JCLI3908.1.

Evans, J. L. 1993. “Sensitivity of tropical cyclone intensity to sea surface temperature”. *American Meteorological Society*, 1133 – 1140, doi: [http://dx.doi.org/10.1175/1520-0442\(1993\)006<1133:SOTCIT>2.0.CO;2](http://dx.doi.org/10.1175/1520-0442(1993)006<1133:SOTCIT>2.0.CO;2).

Ewing, L. 2010. “ Sea level rise: Major implications to coastal engineering and coastal management”. In: Kim, Y. C. *Handbook for Coastal and Ocean Engineering*. World Scientific Publishing, Singapore.

Goda Y. 2008. “Overview on the applications of random wave concept in coastal engineering. *Proceedings of the Japan Academy. Series B, Physical and Biological Sciences* 2008. 84(9): 374-385, doi:10.2183/pjab/84.374.

Gray, W.M. 1968. “Global view of the origin of tropical disturbances and storms”. *Monthly Weather Review*, **96**, No. 10.

Gray, W.M. 1975. "Tropical cyclone genesis". Department of Atmospheric Science, paper No. 234.

Gray, W.M. 1998. "The formation of tropical cyclones". *Meteorology and Atmospheric Physics*, **67**, 37-69.

Gettelman, A. Collins, W. D. Fetzer, E. J. Eldering, A. Irion, F. W. Duffy, P. B. Bala, G. 2006. "Climatology of upper-tropospheric relative humidity from the atmospheric infrared sounder and implications for climate". *Journal of Climate*, **19**, 6104 – 6121.

Hardy, T.A. Young, I.R. Nelson, R.C. Gourlay, M.R. 1990. "Wave attenuation on an offshore coral reef. Proceedings 22nd International Coastal Engineering Conference, Delft, 26 July 1990, **1**, pp. 330-344.

Held, I. M. 1978. "The tropospheric lapse rate and climatic sensitivity: Experiments with a two-level atmospheric model". *American Meteorological Society*, 2038 – 2098, doi: [http://dx.doi.org/10.1175/1520-0469\(1978\)035%3C2083:TTLAC%3E2.0.CO;2](http://dx.doi.org/10.1175/1520-0469(1978)035%3C2083:TTLAC%3E2.0.CO;2).

Held, I. M. Shell, K. M. 2012. "Using humidity as a state variable in climate feedback analysis". *Journal of Climate*, **25**, 2578 – 2582, doi: 10.1175/JCLI-D-11-00721.1.

Henderson-Sellers, A. Zhang, H. Berz, G. Emanuel, K. Gray, W. Landsea, C. Holland, G. Lighthill, J. Shieh, S-L. Webster, P. McGuffie, K. 1998. "Tropical cyclones and global climate change: A Post-IPCC Assessment". *Bulletin of the American Meteorological Society*, **79**, (1).

IPCC. Climate Change 2013: "The physical science basis". Available from <http://www.ipcc.ch/> [accessed 15 April 2014].

GEBCO: General Bathymetric Chart of the Oceans. IOC, IHO and BODC, 2008. Centenary Edition of the GEBCO Digital Atlas, published on CD-ROM on behalf of the Intergovernmental Oceanographic Commission and the International Hydrographic Organization as part of the General Bathymetric Chart of the Oceans, British Oceanographic Data Centre, Liverpool, U.K. Available from <http://www.gebco.net/> [accessed 27 June 2013].

JICA: Japan International Cooperation Agency. 2013. "The project for capacity development on coastal protection and rehabilitation in the Republic of Mauritius". Progress Report.

Kishtawal, C. M. Jaiswal, N. Singh, R. Niyogi, D. 2012. "Tropical cyclone intensification trends during satellite era". *Geophysical Research Letters*, **39**, LI0810, doi: 10.1029/2012GL051700.

Knutson, T. R. Tuleya, R. E. 2004. "Impact of CO₂-induced warming on simulated hurricane intensity and precipitation: Sensitivity to the choice of climate model and convective parameterization". *Journal of Climate*. **17**, (18).

Knutson, T. R. McBride, J. L. Chan, J. Emanuel, K. Holland, G. Landsea, C. Held, I. Kossin, J. P. Srivastava, A. K. Sugi, M. 2010. "Tropical cyclones and climate change". *Nature Geoscience*. Doi: 10.1038/NGE0779.

Kuleshov, Y. Qi, L. Fawcett, R. Jones, D. 2008. "On tropical cyclone intensity in the Southern Hemisphere: Trends and the ENSO connection". *Geophysical Research Letters*, **5**, LI4S08, doi: 10.1029/2007GL032983.

Li, T. Kwon, M. Zhao, M. Kug, J-S. Luo, J-J. Yu, W. 2010. "Global warming shifts Pacific tropical cyclone location". *Geophysical Research Letters*, **37**, L21804, doi: 10.1029/2010GL045124.

Lowe, R.J. Falter, J.L. Bandet, M.D. Pawlak, G. Atkinson, M.J. Monismith, S.G. Koseff, J.R. 2005. "Spectral wave dissipation over a barrier reef". *Journal of Geophysical Research*, Vol. 110, C04001, doi: 10.1029/2004JC002711.

Nott, J. Jagger, T. H. 2013. "Deriving robust return periods for tropical cyclone inundations from sediments". *Geophysical Research Letters*, **40**, 370 - 373, doi: 10.1029/2012GL054455.

Oouchi, K. Yoshimura, J. Yoshimura, H. Kusunoki, S. Noda, A. 2006. "Tropical cyclone climatology in a global-warming climate as simulated in a 20km-mesh global atmospheric model: frequency and wind intensity analyses". *Journal of the Meteorological Society of Japan*, **84**, 259 – 276.

Paltridge, G. Arking, A. Pook, M. 2009. "Trends in middle- and upper level tropospheric humidity from NCEP reanalysis data". Springer, doi: 10.1007/s00704-009-0117-x.

Prinos, P. Galiatsatou, P. 2010. "Coastal Flooding: Analysis and Assessment of Risk". In: Kim, Y. C. *Handbook for Coastal and Ocean Engineering*. World Scientific Publishing, Singapore.

Riedel, H. P. Byrne, A. P. 1986. Random Breaking Waves Horizontal Seabed. Coastal Engineering Proceedings, [S.I.], no.20, January 2011. ISSN 2156-1028. Available at: <<https://journals.tdl.org/icce/index.php/icce/article/view/4069/3751>>. Date accessed: 21 August 2014. doi: <http://dx.doi.org/10.9753/icce.v20>.

Rind, D. Perlwitz, J. Lonergan, P. Lerner, J. 2005. "AO/NAO response to climate change: Relative importance of low- and high-latitude temperature changes". Journal of Geophysical Research, **110**, D12108, doi: 10.1029/2004JD005686.

Roelvink, D. Van Dongeren, A. Benavente, J. Balouin, Y. Ciavola, P. Taborda, R. Furmanczyk, K. Haerens, P. Trifonova, E. Williams, J. 2009. "Micore: Dune erosion and overwash model validation with data from nine European field sites". Proceedings of 6th International Conference on Coastal Dynamics, 166 – 167.

Sherwood, S. C. Ingram, W. Tsushima, Y. Satoh, M. Roberts, M. Vidale, P. L. O’Gorman, P. A. 2010. "Relative humidity changes in a warmer climate". Journal of Geophysical Research, **115**, D09104, doi: 10.1029/2009JD012585.

Southgate, H.N. Nairn, R. B. 1993. "Deterministic Profile Modeling of Nearshore Processes. Part I. Waves and Currents". Coastal Engineering. **19**, 27 – 56.

Thatcher, L. Zhaoxia, P. "How vertical wind shear affects tropical cyclone intensity change: An Overview. Recent Hurricane Research – Climate, Dynamics, and Societal Impacts, Prof. Anthony Lupo (Ed.), ISBN: 978-953-307-238-8", In Tech, Available from: <http://www.intechopen.com/books/recent-hurricane-research-climate-dynamics-and-societal-impacts/how-vertical-wind-shear-affects-tropical-cyclone-intensity-change-an-overview>

Thompson, E. Cardone, V. 1996. "Practical modelling of hurricane surface and wind fields". Journal of Waterway, Port, Coastal, and Ocean Engineering, July/August 1996.

Tory, K. J. Dare, R. A. Davidson, N. E. McBride, J. L. Chand, S. S. 2013. "The importance of low-deformation vorticity in tropical cyclone formation". Atmospheric Chemistry and Physics, **13**, 2115 – 2132, doi: 10.5194/acp-13-2115-2013.

U.S. Army Corps of Engineers.: Coastal Engineering Manual, EM1110-2-1100, Part II: (Chapter 4), 1 – 5. 2003.

- Vecchi, G. A. Soden, B. J. 2007. "Increased tropical Atlantic wind shear in model projections of global warming". *Geophysical Research Letters*, **34**, L08702, doi: 10.1029/2006GL028905.
- Vitart, F. Doblus-reyes, F. 2007. "Impact of greenhouse gas concentrations on tropical storms in coupled seasonal forecasts". *Tellus*, 59A, 417-427, doi: 10.1111/j.1600-0870.2007.00237.x.
- Walsh, K. Pittock, A.B. 1998. "Potential changes in tropical storms, hurricanes, and extreme rainfall events as a result of climate change". *Climatic Change* 39, 199-213.
- Webster, P. J. Holland, G. J. Curry, J. A. Chang, H. R. 2005. "Changes in tropical cyclone number, duration, and intensity in a warming environment". *Science magazine*, **309**.
- Wood, V. T. White, L. W. 2013. "A Parametric Wind–Pressure Relationship for Rankine versus Non-Rankine Cyclostrophic Vortices. *Journal of Atmospheric and Oceanic Technology*, **30**, 2850–2867. doi: <http://dx.doi.org/10.1175/JTECH-D-13-00041.1>
- Wu, L. Su, H. Fovell, R. G. Wang, B. Shen, J. T. Kahn, B. H. Hristova-Veleva, S. M. Lambriksen, B. H. Fetzer, E. J. Jiang, j. H. 2012. "Relationship of environmental relative humidity with North Atlantic tropical cyclone intensity and intensification rate". *Geophysical Research Letters*, **39**, doi: 10.1029/2012GL053546.
- Yamada, Y. Oouchi, K. Satoh, M. Tomita, H. Yanase, W. 2010. "Projection of changes in tropical cyclone activity and cloud height due to greenhouse warming: Global cloud-system-resolving approach". *Geophysical Research Letters*, **37**, L07709, doi: 10.1029/2010GL042518.
- Young, I.R. Sobey, R.J. 1981. "The numerical prediction of tropical cyclone wind-waves". James Cook University of North Queensland, Townville, Dept. of Civil & Systems Eng., Research Bulletin No. CS20
- Yu, J. Wang, Y. 2009. "Response of tropical cyclone potential intensity over the north Indian Ocean to global warming". *Geophysical Research Letters*, **36**, L03709, doi: 10.1029/2008GL036742.
- Yu, J. Wang, Y. Hamilton, K. 2010. "Response of tropical cyclone potential intensity to a global warming scenario in the IPCC AR4 CGCMs". *Journal of Climate*, **23**, 1354 – 1373, doi: <http://dx.doi.org/10.1175/2009JCLI2843.1>.

APPENDIX A

CYCLONE DATA FROM THE AUSTRALIAN SEVERE WEATHER BETWEEN 1997 AND 2011

Period: Dec 1997 to April 1998

No.	Name	Start Date	End Date	Min. Pressure	Max. Wind speed (kt)	Max. Wind speed (m/s)	Max. Wind speed (km/hr)	Category
1	Sid	26-Dec-97	7-Jan-98	985	50	25.72	92.60	2
2	Selwyn	26-Dec-97	2-Jan-98	966	70	36.01	129.64	3
3	199813	18-Jan-98	23-Jan-98	-	31	15.95	57.41	-
4	Les	23-Jan-98	2-Feb-98	980	55	28.29	101.86	2
5	Tiffany	24-Jan-98	31-Jan-98	930	100	51.44	185.20	4
6	Anacelle	8-Feb-98	14-Feb-98	-	101	51.96	187.05	4
7	199821	9-Feb-98	19-Feb-98	-	31	15.95	57.41	-
8	Victor-Cindy	10-Feb-98	19-Feb-98	965	70	36.01	129.64	3
9	Beltane	16-Feb-98	18-Feb-98	-	35	18.01	64.82	1
10	199824	16-Feb-98	19-Feb-98	-	40	20.58	74.08	1
11	Donaline	6-Mar-98	10-Mar-98	-	48	24.69	88.90	2
12	Elsie	12-Mar-98	17-Mar-98	-	79	40.64	146.31	3
13	Fiona	17-Mar-98	29-Mar-98	-	35	18.01	64.82	1
14	Gemma	7-Apr-98	15-Apr-98	-	62	31.90	114.82	2
15	199833	7-Apr-98	7-Apr-98	-	26	13.38	48.15	-
16	199834	19-Apr-98	22-Apr-98	-	35	18.01	64.82	1
17	199835	19-Apr-98	19-Apr-98	-	35	18.01	64.82	1

Period: Jul 1998 to April 1999

No.	Name	Start Date	End Date	Min. Pressure	Max. Wind speed (kt)	Max. Wind speed (m/s)	Max. Wind speed (km/hr)	Category
1	199901	20-Jul-98	25-Jul-98	998	30	15.43	55.56	-
2	199902	29-Sep-98	2 Oct 1998	1002	35	18.01	64.82	1
3	Zelia	7-Oct-98	10-Oct-98	985	55	28.29	101.86	2
4	Alison	8-Nov-98	13-Nov-98	975	60	30.87	111.12	2
5	Billy	1-Dec-98	6-Dec-98	975	60	30.87	111.12	2
6	Thelma	3-Dec-98	15-Dec-98	925	120	61.73	222.24	5
7	Cathy	16-Dec-98	30-Dec-98	990	45	23.15	83.34	1
8	Alda	14-Jan-99	19-Jan-99	975	52	26.75	96.30	2
9	Damien-Birenda	20-Jan-99	7-Feb-99	955	78	40.13	144.46	3
10	199916	22-Feb-99	27-Feb-99	993	30	15.43	55.56	-
11	Chikita	24-Jan-99	5-Feb-99	990	37	19.03	68.52	1
12	199918	31-Jan-99	14-Feb-99	995	40	20.58	74.08	1
13	199921	11-Feb-99	17-Feb-99	994	33	16.98	61.12	-
14	199923	21-Feb-99	4-Mar-99	1000	25	12.86	46.30	-
15	Davina	1-Mar-99	19-Mar-99	930	90	46.30	166.68	4
16	199926	28-Feb-99	27-Mar-99	999	33	16.98	61.12	-
17	Elaine	14-Mar-99	20-Mar-99	960	75	38.58	138.90	3
18	199929	11-Mar-99	21-Mar-99	995	30	15.43	55.56	-
19	Vance	16-Mar-99	24-Mar-99	915	110	56.59	203.72	5
20	Frederic-Evrina	21-Mar-99	10-Apr-99	915	110	56.59	203.72	5
21	Gwenda	1-Apr-99	7-Apr-99	915	110	56.59	203.72	5
22	Hamish	8-Apr-99	24-Apr-99	985	55	28.29	101.86	2
23	Trop-depression-01	3-Sep-98	6-Sep-99	1005	25	12.86	46.30	-

Period: Jul 1998 to April 1999 (Contd)

No.	Name	Start Date	End Date	Min. Pressure	Max. Wind speed (kt)	Max. Wind speed (m/s)	Max. Wind speed (km/hr)	Category
24	Trop-low-01	7-Dec-98	13-Dec-98	1000	25	12.86	46.30	-
25	Trop-low-02	26-Dec-98	2-Jan-99	996	30	15.43	55.56	-
26	Trop-depression-02	4-Jan-99	6-Jan-99	996	30	15.43	55.56	-
27	Trop-low-03	19-Mar-99	22-Mar-99	996	25	12.86	46.30	-
28	Trop-low-04	13-Apr-99	26-Apr-99	999	35	18.01	64.82	1

Period: Dec 1999 to April 2000

No.	Name	Start Date	End Date	Min. Pressure	Max. Wind speed (kt)	Max. Wind speed (m/s)	Max. Wind speed (km/hr)	Category
1	Ilsa	10-Dec-99	17-Dec-99	985	55	28.29	101.86	2
2	John	9-Dec-99	16-Dec-99	915	110	56.59	203.72	5
3	Astride	24-Dec-99	3-Jan-00	985	50	25.72	92.60	2
4	Babiola	3-Jan-00	12-Jan-00	954	80	41.16	148.16	3
5	200006	18-Jan-00	23-Jan-00	992	35	18.01	64.82	1
6	Connie	25-Jan-00	2-Feb-00	928	100	51.44	185.20	4
7	Kirrily	25-Jan-00	1-Feb-00	965	65	33.44	120.38	2
8	Damienne	31-Jan-00	2-Feb-00	992	40	20.58	74.08	1
9	leon-Eline	3-Feb-00	23-Feb-00	928	100	51.44	185.20	4
10	Marcia	15-Feb-00	21-Feb-00	992	45	23.15	83.34	1
11	Felicia	19-Feb-00	24-Feb-00	974	60	30.87	111.12	2
12	Steve	25-Feb-00	12-Mar-00	975	60	30.87	111.12	2
13	Gloria	28-Feb-00	8-Mar-00	988	45	23.15	83.34	1

Period: Dec 1999 to April 2000 (Contd)

No.	Name	Start Date	End Date	Min. Pressure	Max. Wind speed (kt)	Max. Wind speed (m/s)	Max. Wind speed (km/hr)	Category
14	Norman	28-Feb-00	5-Mar-00	920	110	56.59	203.72	5
15	200017	1-Mar-00	7-Mar-00	998	30	15.43	55.56	-
16	Olga	15-Mar-00	21-Mar-00	980	55	28.29	101.86	2
17	Hudah	24-Mar-00	9-Apr-00	905	120	61.73	222.24	5
18	Paul	13-Apr-00	22-Apr-00	920	110	56.59	203.72	5
19	Innocente	12-Apr-00	19-Apr-00	994	35	18.01	64.82	1
20	Rosita	15-Apr-00	21-Apr-00	930	105	54.02	194.46	4
21	Trop-Disturbance-o1	12-Jan-00	26-Jan-00	998	25	12.86	46.30	-
22	Trop-Depression-o8	2-Mar-00	3-Mar-00	1002	25	12.86	46.30	-
23	Hybrid-Low-03	7-Apr-00	17-Apr-00	-	57	29.32	105.56	2

Period: Aug 2000 to April 2001

No.	Name	Start Date	End Date	Min. Pressure	Max. Wind speed (kt)	Max. Wind speed (m/s)	Max. Wind speed (km/hr)	Category
1	200101	1-Aug-00	3-Aug-00	999	30	15.43	55.56	-
2	200102	11-Nov-00	20-Nov-00	998	30	15.43	55.56	-
3	Sam	2-Dec-00	10-Dec-00	925	105	54.02	194.46	4
4	Ando	31-Dec-00	10-Jan-01	930	100	51.44	185.20	4
5	Bindu	4-Jan-01	17-Jan-01	955	80	41.16	148.16	3
6	Charly	17-Jan-01	26-Jan-01	925	105	54.02	194.46	4
7	Terri	28-Jan-01	31-Jan-01	975	60	30.87	111.12	2
8	Winsome	8-Feb-01	11-Feb-01	980	40	20.58	74.08	1
9	Vincent	5-Feb-01	15-Feb-01	980	55	28.29	101.86	2

Period: Aug 2000 to April 2001 (Contd)

No.	Name	Start Date	End Date	Min. Pressure	Max. Wind speed (kt)	Max. Wind speed (m/s)	Max. Wind speed (km/hr)	Category
10	Dera	5-Mar-01	13-Mar-01	960	75	38.58	138.90	3
11	200116	2-Apr-01	5-Apr-01	997	30	15.43	55.56	-
12	Walter	1-Apr-01	8-Apr-01	950	80	41.16	148.16	3
13	Evariste	1-Apr-01	8-Apr-01	976	60	30.87	111.12	2
14	Alistair	16-Apr-01	22-Apr-01	975	60	30.87	111.12	2
15	200121	20-Jun-01	23-Jun-01	1000	40	20.58	74.08	1
16	Trop-Low-01	28-Nov-00	30-Nov-00	1001	30	15.43	55.56	-
17	Trop-Depression-03	22-Jan-01	24-Jan-01	997	30	15.43	55.56	-
18	Trop-Low-03	7-Jan-01	10-Jan-01	999	30	15.43	55.56	-
19	Trop-Depression-04	31-Jan-01	3-Feb-01	996	30	15.43	55.56	-
20	Trop-Low-04	16-Mar-01	17-Mar-01	1002	30	15.43	55.56	-
21	Trop-Low-05	4-Apr-01	5-Apr-01	1004	30	15.43	55.56	-

Period: Oct 2001 to Jun 2002

No.	Name	Start Date	End Date	Min. Pressure	Max. Wind speed (kt)	Max. Wind speed (m/s)	Max. Wind speed (km/hr)	Category
1	200201	4-Oct-01	8-Oct-01	998	30	15.43	55.56	-
2	Alex-Andre	24-Oct-01	1-Nov-01	980	55	28.29	101.86	2
3	200203	15-Nov-01	24-Nov-01	1002	0	0.00	0.00	-
4	200204	15-Nov-01	23-Nov-01	998	30	15.43	55.56	-
5	Bessi-Bako	25-Nov-01	6-Dec-01	966	65	33.44	120.38	3
6	Cyprien	30-Dec-01	3-Jan-02	980	55	28.29	101.86	2
7	Dina	17-Jan-02	26-Jan-02	910	115	59.16	212.98	5

Period: Oct 2001 to Jun 2002 (Contd)

No.	Name	Start Date	End Date	Min. Pressure	Max. Wind speed (kt)	Max. Wind speed (m/s)	Max. Wind speed (km/hr)	Category
8	Eddy	22-Jan-02	28-Jan-02	965	70	36.01	129.64	3
9	Francesca	30-Jan-02	19-Feb-02	925	100	51.44	185.20	4
10	Chris	2-Feb-02	6-Feb-02	915	110	56.59	203.72	5
11	Guillaume	14-Feb-02	22-Feb-02	920	105	54.02	194.46	4
12	Hary	5-Mar-02	15-Mar-02	905	120	61.73	222.24	5
13	Ikala	22-Mar-02	31-Mar-02	940	90	46.30	166.68	4
14	Dianne-Jery	5-Apr-01	15-Apr-02	954	80	41.16	148.16	3
15	Bonnie	9-Apr-02	15-Apr-02	985	50	25.72	92.60	2
16	Kesiny	30-Apr-02	11-May-02	965	70	36.01	129.64	2
17	Errol	8-May-02	16-May-02	995	35	18.01	64.82	1
18	Trop-Low-01	7-Nov-01	13-Nov-01	998	30	15.43	55.56	-
19	Trop-Disturbance-01	5-Feb-02	6-Feb-02	1005	25	12.86	46.30	-
20	Trop-Low-03	9-Feb-02	13-Feb-02	998	30	15.43	55.56	-
21	Trop-Low-04	16-Feb-02	23-Feb-02	995	0	0.00	0.00	-
22	Trop-Disturbance-02	11-Jun-02	15-Jun-02	1000	25	12.86	46.30	-

Period: Sep 2002 to May 2003

No.	Name	Start Date	End Date	Min. Pressure	Max. Wind speed (kt)	Max. Wind speed (m/s)	Max. Wind speed (km/hr)	Category
1	200301	5-Sep-02	8-Sep-02	1000	30	15.43	55.56	-
2	Atang	4-Nov-02	13-Nov-02	997	30	15.43	55.56	-
3	Boura	15-Nov-02	23-Nov-02	968	65	33.44	120.38	3
4	Crystal	22-Dec-02	30-Dec-02	956	75	38.58	138.90	3

Period: Sep 2002 to May 2003

No.	Name	Start Date	End Date	Min. Pressure	Max. Wind speed (kt)	Max. Wind speed (m/s)	Max. Wind speed (km/hr)	Category
5	200307	25-Dec-02	4-Jan-02	996	30	15.43	55.56	-
6	Delfina	30-Dec-02	1-Jan-03	984	50	25.72	92.60	2
7	Bom200208	4-Jan-03	16-Jan-03	995	30	15.43	55.56	-
8	Ebula	7-Jan-03	13-Jan-03	975	60	30.87	111.12	2
9	Fari	23-Jan-03	1-Feb-03	984	50	25.72	92.60	2
10	Bom200201	19-Jan-03	24-Jan-03	995	30	15.43	55.56	-
11	Fiona	4-Feb-03	13-Feb-03	930	105	54.02	194.46	4
12	Gerry	8-Feb-03	17-Feb-03	940	90	46.30	166.68	4
13	Hape	9-Feb-03	16-Feb-03	965	70	36.01	129.64	3
14	Isha	11-Feb-03	14-Feb-03	995	35	18.01	64.82	1
15	Japhet	25-Feb-03	3-Mar-03	927	100	51.44	185.20	4
16	Graham	26-Feb-03	1-Mar-03	985	45	23.15	83.34	1
17	Harriet	2-Mar-03	11-Mar-03	980	55	28.29	101.86	2
18	Kalunde	4-Mar-03	16-Mar-03	905	115	59.16	212.98	5
19	Craig	7-Mar-03	12-Mar-03	980	55	28.29	101.86	2
20	Inigo	1-Apr-03	8-Apr-03	900	120	61.73	222.24	5
21	Luma	6-Apr-03	12-Apr-03	985	65	33.44	120.38	3
22	Manou	2-May-03	10-May-03	952	80	41.16	148.16	3
23	Trop-Disturbance-01	6-Jan-03	12-Jan-03	1000	25	12.86	46.30	-
24	Trop-Low-01	4-Feb-03	6-Feb-03	998	0	0.00	0.00	-
25	Trop-Low-02	8-May-03	11-May-03	1003	0	0.00	0.00	-

Period: Sep 2003 to May 2004

No.	Name	Start Date	End Date	Min. Pressure	Max. Wind speed (kt)	Max. Wind speed (m/s)	Max. Wind speed (km/hr)	Category
1	Abaimba	29-Sep-03	4-Oct-03	990	45	23.15	83.34	1
2	Beni	9-Nov-03	22-Nov-03	935	100	51.44	185.20	4
3	Cela	5-Dec-03	21-Dec-03	968	65	33.44	120.38	3
4	Jana	7-Dec-03	12-Dec-03	960	75	38.58	138.90	3
5	Debbie	17-Dec-03	21-Dec-03	970	65	33.44	120.38	3
6	Darius	29-Dec-03	4-Jan-04	976	55	28.29	101.86	2
7	Ken	1-Jan-04	6-Jan-04	992	40	20.58	74.08	1
8	Elita	26-Jan-04	12-Feb-04	974	60	30.87	111.12	2
9	Frank	27-Jan-04	7-Feb-04	925	105	54.02	194.46	4
10	Linda	28-Jan-04	1-Feb-04	978	55	28.29	101.86	2
11	Monty	26-Feb-04	2-Mar-04	935	95	48.87	175.94	4
12	Evan	29-Feb-04	2-Mar-04	994	40	20.58	74.08	1
13	Gafilo	2-Mar-04	15-Mar-04	895	125	64.31	231.50	5
14	Nicky-Helma	8-Mar-04	13-Mar-04	972	60	30.87	111.12	2
15	Fay	14-Mar-04	28-Mar-04	910	115	59.16	212.98	5
16	Oscar-Itseng	20-Mar-04	28-Mar-04	935	95	48.87	175.94	4
17	200421	13-Mar-04	28-Mar-04	1002	26	13.38	48.15	-
18	Juba	5-May-04	28-May-04	980	55	28.29	101.86	2
19	Trop-Low-01	8-Feb-04	12-Feb-04	994	30	15.43	55.56	-

Period: Sep 2004 to Apr 2005

No.	Name	Start Date	End Date	Min. Pressure	Max. Wind speed (kt)	Max. Wind speed (m/s)	Max. Wind speed (km/hr)	Category
1	Phoebe	31-Aug-04	4-Sep-04	984	50	25.72	92.60	2
2	200502	25-Oct-04	29-Oct-04	996	30	15.43	55.56	-
3	Arola	7-Nov-04	13-Nov-04	976	60	30.87	111.12	2
4	Bento	20-Nov-04	30-Nov-04	905	120	61.73	222.24	5
5	200505	2-Dec-04	7-Dec-04	998	30	15.43	55.56	-
6	Chambo	23-Dec-04	2-Jan-05	945	85	43.73	157.42	3
7	Raymond	31-Dec-04	3-Jan-05	990	45	23.15	83.34	1
8	Sally	7-Jan-05	10-Jan-05	988	45	23.15	83.34	1
9	200510	13-Jan-05	19-Jan-05	998	30	15.43	55.56	-
10	Daren	17-Jan-05	22-Jan-05	940	40	20.58	74.08	1
11	Ernest	17-Jan-05	25-Jan-05	988	90	46.30	166.68	4
12	Tim	23-Jan-05	26-Jan-05	995	45	23.15	83.34	1
13	Felapi	26-Jan-05	2-Feb-05	973	35	18.01	64.82	1
14	Gerard	28-Jan-05	5-Feb-05	990	60	30.87	111.12	2
15	Vivienne	5-Feb-05	10-Feb-05	925	45	23.15	83.34	1
16	Ingrid	5-Mar-05	19-Mar-05	960	120	61.73	222.24	5
17	Willy	9-Mar-05	17-Mar-05	980	80	41.16	148.16	3
18	Hennie	21-Mar-05	29-Mar-05	1000	55	28.29	101.86	2
19	Isang	29-Mar-05	7-Apr-05	998	60	30.87	111.12	2
20	Adeline-Juliet	1-Apr-05	14-Apr-05	997	120	61.73	222.24	5
21	Trop-Disturbance-01	11-Dec-04	11-Dec-04	1000	25	12.86	46.30	-
22	Trop-Disturbance-02	4-Jan-05	5-Jan-05	998	30	15.43	55.56	-
23	Trop-Depression-04	4-Feb-05	8-Feb-05	997	35	18.01	64.82	1

Period: Sep 2004 to Apr 2005 (Contd)

No.	Name	Start Date	End Date	Min. Pressure	Max. Wind speed (kt)	Max. Wind speed (m/s)	Max. Wind speed (km/hr)	Category
24	Trop-Disturbance-03	8-Feb-05	17-Feb-05	1000	25	12.86	46.30	-
25	Trop-Depression-05	24-Feb-05	28-Feb-05	998	30	15.43	55.56	-

Period: Oct 2005 to Mar 2006

No.	Name	Start Date	End Date	Min. Pressure	Max. Wind speed (kt)	Max. Wind speed (m/s)	Max. Wind speed (km/hr)	Category
1	200601	21-Oct-05	15-Oct-05	997	30	15.43	55.56	-
2	200602	5-Nov-05	8-Nov-05	995	30	15.43	55.56	-
3	Bertie-Alvin	18-Nov-05	28-Nov-05	930	100	51.44	185.20	4
4	200604	21-Dec-05	29-Dec-05	998	30	15.43	55.56	-
5	Clare	7-Jan-06	10-Jan-06	960	75	38.58	138.90	3
6	Daryl	17-Jan-06	23-Jan-06	965	65	33.44	120.38	3
7	Boloetse	24-Jan-06	6-Feb-06	946	90	46.30	166.68	4
8	200612	19-Feb-06	21-Feb-06	995	40	20.58	74.08	1
9	Carina	23-Feb-06	3-Mar-06	910	115	59.16	212.98	5
10	Emma	26-Feb-06	28-Feb-06	986	40	20.58	74.08	1
11	Diwa	2-Mar-06	10-Mar-06	980	60	30.87	111.12	2
12	Floyd	19-Mar-06	27-Mar-06	915	105	54.02	194.46	4
13	Glenda	23-Mar-06	31-Mar-06	910	115	59.16	212.98	5
14	Hubert	4-Apr-06	7-Apr-06	970	55	28.29	101.86	2
15	Elia	6-Apr-06	16-Apr-06	987	45	23.15	83.34	1
16	Monica	16-Apr-06	26-Apr-06	905	135	69.45	250.02	5
17	Trop-Disturbance-01	5-Sep-05	6-Sep-05	1001	25	12.86	46.30	-

Period: Oct 2005 to Mar 2006 (Contd)

No.	Name	Start Date	End Date	Min. Pressure	Max. Wind speed (kt)	Max. Wind speed (m/s)	Max. Wind speed (km/hr)	Category
18	Trop-Depression-01	6-Nov-05	8-Nov-05	998	30	15.43	55.56	-
19	Trop-Disturbance-02	3-Jan-06	7-Jan-06	1000	25	12.86	46.30	-
20	Trop-Disturbance-03	4-Mar-06	4-Mar-06	1000	25	12.86	46.30	-
21	Trop-Low-01	28-Feb-06	7-Mar-06	998	30	15.43	55.56	-
22	Trop-Low-02	26-Mar-06	27-Mar-06	996	30	15.43	55.56	-

Period: Oct 2006 to Apr 2007

No.	Name	Start Date	End Date	Min. Pressure	Max. Wind speed (kt)	Max. Wind speed (m/s)	Max. Wind speed (km/hr)	Category
1	Anita	26-Nov-06	3-Dec-06	994	35	18.01	64.82	1
2	Bondo	17-Dec-06	26-Dec-06	915	110	56.59	203.72	5
3	Clovis	29-Dec-06	4-Jan-07	975	60	30.87	111.12	2
4	Isobel	31-Dec-06	3-Jan-07	982	45	23.15	83.34	1
5	Dora	28-Jan-07	12-Feb-07	930	100	51.44	185.20	4
6	Enok	6-Feb-07	11-Feb-07	980	60	30.87	111.12	2
7	Favio	12-Feb-07	23-Feb-07	930	100	51.44	185.20	4
8	Gamede	20-Feb-07	4-Mar-07	935	95	48.87	175.94	4
9	Humba	20-Feb-07	28-Feb-07	960	75	38.58	138.90	3
10	George	26-Feb-07	10-Mar-07	910	105	54.02	194.46	4
11	Jacob	5-Mar-07	12-Mar-07	954	75	38.58	138.90	3
12	Indlala	10-Mar-07	17-Mar-07	935	95	48.87	175.94	4
13	Kara	24-Mar-07	28-Mar-07	942	85	43.73	157.42	3
14	Jaya	29-Mar-07	8-Apr-07	930	105	54.02	194.46	4

Period: Oct 2006 to Apr 2007 (Contd)

No.	Name	Start Date	End Date	Min. Pressure	Max. Wind speed (kt)	Max. Wind speed (m/s)	Max. Wind speed (km/hr)	Category
15	Trop-Disturbance-01	18-Oct-06	23-Oct-06	1002	25	12.86	46.30	-
16	Trop-Disturbance-02	25-Dec-06	28-Dec-06	1000	25	12.86	46.30	-
17	Trop-Disturbance-03	6-Jan-07	8-Jan-07	999	25	12.86	46.30	-
18	Trop-Disturbance-04	13-Mar-07	17-Mar-07	1000	25	12.86	46.30	-
19	Subtrop-Disturbance-01	20-Mar-07	21-Mar-07	-	-			-
20	Subtrop-Depression-01	9-Apr-07	12-Apr-07	998	45	23.15	83.34	1

Period: Jul 2007 to Apr 2008

No.	Name	Start Date	End Date	Min. Pressure	Max. Wind speed (kt)	Max. Wind speed (m/s)	Max. Wind speed (km/hr)	Category
1	200801	27-Jul-07	31-Jul-07	998	30	15.43	55.56	-
2	Lee-Ariel	13-Nov-07	22-Nov-07	980	50	25.72	92.60	2
3	Bongwe	17-Nov-07	24-Nov-07	976	60	30.87	111.12	2
4	Celina	12-Dec-07	21-Dec-07	992	40	20.58	74.08	1
5	Dama	18-Dec-07	21-Dec-07	995	35	18.01	64.82	1
6	Melanie	27-Dec-07	2-Jan-08	964	60	30.87	111.12	2
7	Elnus	30-Dec-07	5-Jan-08	994	35	18.01	64.82	1
8	Helen	3-Jan-08	6-Jan-08	975	50	25.72	92.60	2
9	Fame	24-Jan-08	1-Feb-08	972	60	30.87	111.12	2
10	Gula	26-Jan-08	3-Feb-08	950	85	43.73	157.42	3
11	Hondo	4-Feb-08	25-Feb-08	906	120	61.73	222.24	5
12	200817	4-Feb-08	10-Feb-08	990	30	15.43	55.56	-
13	Ivan	7-Feb-08	22-Feb-08	930	100	51.44	185.20	4

Period: Jul 2007 to Apr 2008 (Contd)

No.	Name	Start Date	End Date	Min. Pressure	Max. Wind speed (kt)	Max. Wind speed (m/s)	Max. Wind speed (km/hr)	Category
14	Nicholas	12-Feb-08	20-Feb-08	944	80	41.16	148.16	3
15	Ophelia	27 fen 2008	7-Mar-08	972	60	30.87	111.12	2
16	Jokwe	4-Mar-08	15-Mar-08	930	105	54.02	194.46	4
17	Kamba	7-Mar-08	12-Mar-08	930	100	51.44	185.20	4
18	Lola	20-Mar-08	26-Mar-08	994	35	18.01	64.82	1
19	Pancho	24-Mar-08	30-Mar-08	938	90	46.30	166.68	4
20	Rosie	20-Apr-08	25-Apr-08	980	50	25.72	92.60	2
21	Durga	22-Apr-08	25-Apr-08	988	40	20.58	74.08	1
22	Trop-Disturbance-01	21-Jul-07	24-Jul-07	-	26	13.38	48.15	-
23	Trop-Disturbance-02	11-Oct-07	14-Oct-07	1005	25	12.86	46.30	-
24	Trop-Low-01	31-Dec-07	2-Jan-08	994	30	15.43	55.56	-

Period: Oct 2008 to Apr 2009

No.	Name	Start Date	End Date	Min. Pressure	Max. Wind speed (kt)	Max. Wind speed (m/s)	Max. Wind speed (km/hr)	Category
1	Asma	16-Oct-08	23-Oct-08	985	45	23.15	83.34	1
2	Anika	19-Nov-08	21-Nov-08	990	50	25.72	92.60	2
3	Bernard	19-Nov-08	21-Nov-08	994	35	18.01	64.82	1
4	Cinda	15-Dec-08	21-Dec-08	985	50	25.72	92.60	2
5	Billy	17-Dec-08	29-Dec-08	948	95	48.87	175.94	4
6	Dongo	8-Jan-09	18-Jan-09	946	55	28.29	101.86	2
7	Eric	17-Jan-09	21-Jan-09	994	35	18.01	64.82	1
8	Fanele	18-Jan-09	27-Jan-09	927	100	51.44	185.20	4

Period: Oct 2008 to Apr 2009 (Contd)

No.	Name	Start Date	End Date	Min. Pressure	Max. Wind speed (kt)	Max. Wind speed (m/s)	Max. Wind speed (km/hr)	Category
9	Dominic	25-Jan-09	27-Jan-09	980	50	25.72	92.60	2
10	Gael	1-Feb-09	12-Feb-09	934	95	48.87	175.94	4
11	Freddy	3-Feb-09	15-Feb-09	983	50	25.72	92.60	2
12	Hina	21-Feb-09	26-Feb-09	980	55	28.29	101.86	2
13	Gabrielle	1-Mar-09	5-Mar-09	998	40	20.58	74.08	1
14	200919	8-Mar-09	10-Mar-09	997	30	15.43	55.56	-
15	Ilsa	17-Mar-09	27-Mar-09	958	90	46.30	166.68	4
16	Izilda	24-Mar-09	29-Mar-09	974	60	30.87	111.12	2
17	Jade	3-Apr-09	14-Apr-09	957	60	30.87	111.12	2
18	Kirrily	26-Apr-09	20-Apr-09	998	35	18.01	64.82	1
19	Trop-Low-01	26-Feb-02	28-Feb-02	996	33	16.98	61.12	-

Period: Aug 2009 to May 2010

No.	Name	Start Date	End Date	Min. Pressure	Max. Wind speed (kt)	Max. Wind speed (m/s)	Max. Wind speed (km/hr)	Category
1	Anja	14-Nov-09	29-Nov-09	950	85	43.73	157.42	3
2	Bongani	22-Nov-09	25-Nov-09	997	40	20.58	74.08	1
3	Cleo	6-Dec-09	14-Dec-09	927	105	54.02	194.46	4
4	David	13-Dec-09	27-Dec-09	980	55	28.29	101.86	2
5	Laurence	10-Dec-09	24-Dec-09	927	110	56.59	203.72	5
6	Edzani	2-Jan-10	17-Jan-10	905	120	61.73	222.24	5
7	Magda	19-Jan-10	22-Jan-10	980	60	30.87	111.12	2
8	201011	26-Jan-10	30-Jan-10	995	35	18.01	64.82	1

Period: Aug 2009 to May 2010 (Contd)

No.	Name	Start Date	End Date	Min. Pressure	Max. Wind speed (kt)	Max. Wind speed (m/s)	Max. Wind speed (km/hr)	Category
9	Fami	1-Feb-10	3-Feb-10	994	40	20.58	74.08	1
10	Gelane	15-Feb-10	21-Feb-10	930	110	56.59	203.72	5
11	Hubert	9-Mar-10	11-Mar-10	987	55	28.29	101.86	2
12	Imani	21-Mar-10	26-Mar-10	965	70	36.01	129.64	3
13	Paul	26-Mar-10	1-Apr-10	982	55	28.29	101.86	2
14	Robyn	2-Apr-10	11-Apr-10	976	65	33.44	120.38	3
15	Sean	21-Apr-10	28-Apr-10	987	55	28.29	101.86	2
16	Joel	25-May-10	29-May-10	996	60	30.87	111.12	2
17	Trop-Disturbance-01	17-Aug-09	20-Aug-09	-	0	0.00	0.00	-
18	Trop-Disturbance-02	7-Nov-09	10-Nov-09	1000	25	12.86	46.30	-
19	Trop-Disturbance-03	15-Jan-10	15-Jan-10	1005	25	12.86	46.30	-
20	Trop-Low-01	2-Jan-10	4-Jan-10	991	25	12.86	46.30	-

Period: Oct 2010 to Apr 2011

No.	Name	Start Date	End Date	Min. Pressure	Max. Wind speed (kt)	Max. Wind speed (m/s)	Max. Wind speed (km/hr)	Category
1	201101	25-Oct-10	29-Oct-10	997	30	15.43	55.56	-
2	Anggrek	30-Oct-10	4-Nov-10	986	50	25.72	92.60	2
3	Abele	28-Nov-10	4-Dec-10	973	70	36.01	129.64	3
4	Vince	11-Jan-11	23-Jan-11	986	40	20.58	74.08	1
5	Bianca	21-Jan-11	30-Jan-11	945	90	46.30	166.68	4
6	Yasi	26-Jan-11	5-Feb-11	922	115	59.16	212.98	5
7	Bingiza	9-Feb-11	2-Mar-11	953	90	46.30	166.68	4

Period: Oct 2010 to Apr 2011 (Contd)

No.	Name	Start Date	End Date	Min. Pressure	Max. Wind speed (kt)	Max. Wind speed (m/s)	Max. Wind speed (km/hr)	Category
8	201114	10-Feb-11	16-Feb-11	1000	30	15.43	55.56	-
9	Carlos	15-Feb-11	1-Mar-11	968	65	33.44	120.38	3
10	Dianne	15-Feb-11	23-Feb-11	962	70	36.01	129.64	3
11	Cherono	14-Mar-11	25-Mar-11	-	40	20.58	74.08	1
12	201120	30-Mar-11	4-Apr-11	994	30	15.43	55.56	-
13	Errol	14-Apr-11	18-Apr-11	986	55	28.29	101.86	2
14	Trop-Low-01	3-Dec-10	3-Jan-11	993	30	15.43	55.56	-
15	Trop-Disturbance-02	31-Dec-10	3-Jan-11	996	30	15.43	55.56	-
16	Trop-Disturbance-03	14-Jan-11	16-Jan-11	-	0	0.00	0.00	-
17	Trop-Disturbance-05	30-Jan-11	31-Jan-11	998	25	12.86	46.30	-
18	Trop-Disturbance-06	15-Feb-11	18-Feb-11	1000	25	12.86	46.30	-
19	Trop-Low-02	25-Feb-11	28-Feb-11	992	0	0.00	0.00	-
20	Trop-Disturbance-08	29-Mar-11	31-Mar-11	1004	25	12.86	46.30	-
21	Trop-Disturbance-10	12-Apr-11	17-Apr-11	985	50	25.72	92.60	2

APPENDIX B

XBEACH SET-UP FILE FOR BELLE MARE: SCENARIO 1

Params file

XBEACH parameter settings input file

Grid parameters

gridform = xbeach
nx = 165
ny = 0
xori = 0
yori = 0
alfa = 0
posdwn = -1
vardx = 1
depfile = BM_bed(Rev2).dep
xfile = BM_x(Rev2).grd
yfile = BM_y(Rev2).grd
thetamin = -180
thetamax = 180
dtheta = 10
thetanaut = 1

Model time

tstart = 0
tint = 100
tstop = 198000

Wave numerics parameters

scheme = 2
wci = 0

Wave dissipation model

break = 3
gamma
gammamax = 2
alpha
n = 10
delta
fw = 0.05

Roller parameters

roller = 1
beta = 0.100000

Wave boundary condition parameters

instat = jons

Spectral parameter input

bcfile = filelist_Actual.txt

Flow parameters

C = 55
nuh = 0.1
lat

Flow boundary condition parameters

left = 0
right = 0
front = abs_1d
back = abs_1d

Tide boundary conditions

zs0file = Mtius_tide.txt
tideloc = 1

Sediment transport parameters

waveform = 2
form = 2
facsl = 0
BRfac = 0.200000
turb = 2
facua = 0.100000
rfb = 1

Multiple sediment fractions and hard layers

struct = 1
ne_layer = BM_reef(Rev2).dep
D50 = 0.00175
D90 = 0.003

Morphology parameters

morfac = 1
wetslp = 0.3
dryslp = 1

Output variables

outputformat = netcdf

Bathymetry

x-grid (m)	y-grid (m)	Bathymetry (m)	reef
45	0	-66.4	0
95	0	-61.71	0
145	0	-57.02	0
195	0	-52.33	0
245	0	-47.64	0
295	0	-45.43	0
345	0	-44.19	0
395	0	-42.96	0
445	0	-41.72	0
495	0	-40.48	0
540	0	-39.37	0
585	0	-38.26	0
630	0	-37.14	0
675	0	-36.03	0
720	0	-34.92	0
765	0	-33.8	0
810	0	-32.56	0
855	0	-31.24	0
900	0	-29.92	0
945	0	-28.61	0
985	0	-27.44	0
1025	0	-26.27	0
1065	0	-25.09	0
1105	0	-23.92	0
1145	0	-22.75	0
1185	0	-21.58	0
1225	0	-20.41	0
1265	0	-19.24	0
1305	0	-18.07	0
1345	0	-17.01	0
1380	0	-16.25	0
1415	0	-15.48	0
1450	0	-14.72	0
1485	0	-13.96	0
1520	0	-13.19	0
1555	0	-12.43	0
1590	0	-11.67	0
1625	0	-10.54	0
1660	0	-9.38	0
1695	0	-8.22	0
1725	0	-7.22	0
1755	0	-6.23	0

x-grid (m)	y-grid (m)	Bathymetry (m)	reef
1785	0	-5.23	0
1815	0	-4.24	0
1845	0	-3.33	0
1875	0	-3.08	0
1905	0	-2.82	0
1935	0	-2.57	0
1965	0	-2.31	0
1991.01	0	-2.14	0
1995	0	-2.14	0
2015.95	0	-1.76	0
2019.52	0	-1.75	0
2020	0	-1.73	0
2021.58	0	-1.66	0
2042.03	0	-1.48	0
2045	0	-1.53	0
2070	0	-1.72	0
2095	0	-1.86	0
2125	0	-2.05	0
2150	0	-2.28	0
2150.98	0	-2.28	0
2175	0	-2.08	0
2177.76	0	-2.13	0
2179.22	0	-1.99	0
2200	0	-2.4	0
2201.62	0	-2.55	0
2203.57	0	-2.45	0
2225	0	-2.47	0
2245	0	-2.41	0
2265	0	-2.31	0
2290	0	-2.25	0
2310	0	-2.05	0
2330	0	-2.04	0
2330.14	0	-2.04	0
2331.44	0	-1.91	0
2350	0	-1.89	0
2370	0	-1.98	0
2388.75	0	-2.44	0
2400	0	-2.25	0
2400.35	0	-2.24	0
2415	0	-1.77	0
2430	0	-1.75	0
2445	0	-2.16	0

Bathymetry (Contd)

x-grid (m)	y-grid (m)	Bathymetry (m)	reef
2459.6	0	-2.45	0
2470	0	-2.35	0
2470.87	0	-2.31	0
2485	0	-2.28	0
2500	0	-2.29	0
2515	0	-2.27	0
2530	0	-2.26	0
2540	0	-2.31	0
2550	0	-2.48	0
2565	0	-2.49	0
2575	0	-2.37	0
2585	0	-2.29	0
2595	0	-2.25	0
2605	0	-2.22	0
2615	0	-2.21	0
2625	0	-2.17	0
2635	0	-2.09	0
2645	0	-2.08	0
2655	0	-2.13	0
2665	0	-2.28	0
2666.34	0	-2.27	0
2670	0	-2.14	0
2675	0	-2.05	0
2677.44	0	-2.05	0
2678.98	0	-2.03	0
2680	0	-1.96	0
2685	0	-1.58	0
2690	0	-1.27	0
2695	0	-0.93	0
2696.05	0	-0.81	0
2697.34	0	-0.76	0
2700	0	-0.75	100
2705	0	-0.75	100
2710	0	-0.74	100
2712.6	0	-0.71	100
2715	0	-0.77	100
2720	0	-0.88	100
2725	0	-0.94	100
2730	0	-0.95	100
2730.03	0	-0.95	100
2735	0	-0.87	100
2740	0	-0.69	100

x-grid (m)	y-grid (m)	Bathymetry (m)	reef
2745	0	-0.57	100
2750	0	-0.45	100
2755	0	-0.19	100
2756.75	0	0	100
2760	0	0.38	100
2765	0	0.87	100
2770	0	1.53	100
2771.87	0	1.82	100
2772.99	0	2.24	100
2775	0	2.3	100
2780	0	2.3	100
2785	0	2.29	100
2790	0	2.32	100
2795	0	2.35	0
2800	0	2.61	0
2805	0	2.87	0
2809.31	0	3.06	0
2810	0	3.11	0
2815	0	3.52	0
2820	0	3.6	0
2825	0	4.01	0
2830	0	4.42	0
2835	0	4.83	0
2840	0	5.24	0
2845	0	5.65	0
2850	0	6.06	0
2855	0	6.47	0
2860	0	6.88	0
2865	0	7.29	0
2870	0	7.7	0
2875	0	8.11	0
2880	0	8.52	0
2885	0	8.93	0
2890	0	9.34	0
2895	0	9.75	0
2900	0	10.16	0
2905	0	10.57	0
2910	0	10.98	0
2915	0	11.39	0
2920	0	11.8	0

JONSWAP

JONSWAP 1

Hm0 = 1.02563
fp = 0.0625
mainang = 80.5648
gammajsp = 2.5
s = 7
fnyq = 1

JONSWAP 2

Hm0 = 1.83638
fp = 0.0625
mainang = 80.1593
gammajsp = 2.5
s = 7
fnyq = 1

JONSWAP 3

Hm0 = 2.86149
fp = 0.0625
mainang = 79.8563
gammajsp = 2.5
s = 7
fnyq = 1

JONSWAP 4

Hm0 = 3.8235
fp = 0.0625
mainang = 79.2929
gammajsp = 2.5
s = 7
fnyq = 1

JONSWAP 5

Hm0 = 4.02497
fp = 0.064243
mainang = 78.6034
gammajsp = 2.5
s = 7
fnyq = 1

JONSWAP 6

Hm0 = 4.1646
fp = 0.072214
mainang = 81.1827
gammajsp = 2.5
s = 7
fnyq = 1

JONSWAP 7

Hm0 = 7.21716
fp = 0.079145
mainang = 100.551
gammajsp = 2.5
s = 7
fnyq = 1

JONSWAP 8

Hm0 = 3.73918
fp = 0.139839
mainang = 9.63801
gammajsp = 2.5
s = 7
fnyq = 1

JONSWAP 9

Hm0 = 1.81064
fp = 0.182738
mainang = 355.322
gammajsp = 2.5
s = 7
fnyq = 1

JONSWAP 10

Hm0 = 0.925122
fp = 0.183525
mainang = 26.3113
gammajsp = 2.5
s = 7
fnyq = 1